Synthesis and Biological Evaluation of $PreQ_0$ Derivatives

Romain Paumier, MChem (Hons.)

School of Chemistry

Trinity College Dublin, The University of Dublin

A thesis submitted for the degree of *Master of Science* (MSc)

September 2020

Declaration

I declare that this thesis has not been submitted as an exercise for a degree at this or any other university and it is entirely my own work. I agree to deposit this thesis in the University's open access institutional repository or allow the Library to do so on my behalf, subject to Irish Copyright Legislation and Trinity College Library conditions of use and acknowledgement.

Acknowledgements

I would first like to thank the University of Dublin and its School of Chemistry for funding this project and my supervisor, Dr. Mike Southern, for the opportunity to work in his group and for his support throughout my work. His expertise was invaluable for the progress of this project.

I would like to extend my gratitude to our collaborators, Dr. Vincent Kelly, Prof. Stephen Connon and their respective groups for their contributions to the project. Many thanks to Magda Ghanim, Jill Browning and Dr. Claire Fergus for teaching me cell culture and assays with special thanks to Magda, who performed many of the assays for the project. Thank you to the many in the Connon group who taught me new methods and gave me sound synthetic advice: Simon Nicholas Smith, Dr. Michelle Cotter, Dr. Umar Farid, Dr. Romain Claveau, Dr. Bruce Lockett-Walters, Dr. Aaron Gutiérrez Collar, Dr. Sarah Cronin, Ciara McDonnell and Amy Maguire.

Thank you to the members of the Rozas group for their generosity, the insightful conversations (on chemistry or otherwise) and in general for being great scientists to share an office with: Hélène Bikorimana, Adeyemi Rahman, Nikolina Stipaničev, Dr. Jagdeep Grover and Dr. Filippo Prencipe. Thank you to my other friends Daniel Nelis and June Lovitt for the cherishable non-research-related moments and to the Southern group's undergraduate students, Lee Anderson and Cliona Redington, for the cherishable research-related moments.

I would also like to express my gratitude towards all members of the faculty who helped me in one way or another to complete this project, with special mentions to Dr. John O'Brien, Dr. Manuel Ruether and Dr. Gary Hessman for their help acquiring spectroscopic data.

I wish to extend my thanks to my family for their continued support. I am especially grateful to my parents María Dolores Montoya Marín and Philippe Paumier for the unconditional help whenever it was needed.

Thank you to my dear childhood friend, Marc López Pascual, for his constant encouragement and optimism in the face of all adversities.

Finally, my most heartfelt gratitude goes to my partner Ciara Crosby for her limitless empathy and support. Thank you for always being by my side to face the storm.

Table of Contents

Abstract

tRNA-guanine transglycosylase (TGT) is a key enzyme involved in the posttranscriptional modification of tRNA across all kingdoms of life. In eukaryotes and eubacteria, TGT catalyses the incorporation of hypermodified nucleobase queuine into the anticodon of $tRNA^{Asn}$, $tRNA^{Asp}$, $tRNA^{His}$ and $tRNA^{Tyr}$. Queuine hypomodification has been reported in several types of neoplasms where queuine deficiency is correlated with histological signs of malignancy. Recent work from Southern, Kelly and Connon has shown that queuine analogues can be incorporated into tRNA by TGT to affect the development of multiple sclerosis. This project seeks to exploit the catalytic activity of TGT to selectively target queuine-deficient cancer cells by disrupting the translation process with queuine analogues. A library of queuine analogues bearing aliphatic, aromatic and electrophilic side-chains at the 2-position was synthesised *via* amide bond formation and assessed against human epithelial mammary cancer cell line MDA-MB-231.

Abbreviations

A	adenine
A site	aminoacyl site
Ac	acetyl
Ala	alanine
APCI	atmospheric pressure chemical ionization
Arg	arginine
Asn	asparagine
Asp	aspartic acid
ATR	attenuated total reflectance
C	cytosine
Cys	cysteine
DMF	dimethyl formamide
DMPU	*N*,*N*'-dimethylpropyleneurea
DMSO	dimethyl sulphoxide
DNA	deoxyribonucleic acid
E site	exit site
ESI	electrospray ionisation
FTIR	Fourier-transform infrared spectroscopy
G	guanine
Gln	glutamine
Glu	glutamic acid
Gly	glycine
His	histidine
HPLC	high-performance liquid chromatography
HRMS	high-resolution mass spectrometry
HSQC	heteronuclear single quantum correlation
Ile	isoleucine
Leu	leucine
Lys	lysine
Me	methyl
Met	methionine
mRNA	messenger RNA
MS	multiple sclerosis
m.p.	melting point
NADH	nicotinamide adenine dinucleotide (reduced)
^{n}Hep	*n*-heptyl
NMR	nuclear magnetic resonance
P site	peptidyl site
Phe	phenylalanine
$PreQ_0$	7-cyano-7-deazaguanine
$PreQ_1$	7-aminomethyl-7-deazaguanine
Pro	proline
Q	queuosine
q	queuine
RNA	ribonucleic acid
rRNA	ribosomal RNA
r.t.	room temperature
Ser	serine
^{t}Bu	*tert*-butyl
TGT	tRNA-guanine transglycosylase
THF	tetrahydrofuran
Thr	threonine
TLC	thin layer chromatography
tRNA	transfer RNA
Trp	tryptophan
Tyr	tyrosine
U	uracil
Val	valine
δ	chemical shift

1. Introduction

The project presented in this document is concerned with developing novel substrates for tRNA-guanine transglycosylase (TGT), an enzyme that catalyses an unusual reaction in the body. TGT removes the nuclear encoded guanine from position 34 of the tRNAs for asparagine, aspartic acid, histidine and tyrosine and replaces it with the hypermodified nucleobase queuine (q). The function of queuine in tRNA is believed to be linked to translation in cells. We have recently shown that providing false substrates for TGT can have a dramatic effect on the development of multiple sclerosis.[1] The vast majority of tRNA in the body is already modified with queuine. However, this is often not the case in cancer cells. Indeed, the degree of a cell's hypomodification with queuine has been postulated as a marker for a poor disease prognosis.[2] We are seeking to expand the therapeutic potential of this enzyme to explore its potential role as a cancer treatment by interfering with translation in tumorous cells. First, an overview of tRNA, TGT and translation will be provided.

1.1. Transfer RNA and chemical modifications

1.1.1. Transfer RNA and its role in translation

Transfer RNA (tRNA) is a polymeric molecule that plays an essential role in translation. Genetic material in DNA is translated into messenger RNA (mRNA) which is transported from the cell nucleus to the cytosol. The information in the mRNA, encrypted in the triplet codon sequence, is decoded by the ribosome by means of transfer RNA (tRNA) molecules that both read the codon and carry the appropriate amino acids for assembling a polypeptide chain. This polypeptide may then undergo post-translational modifications to become a functional protein.[3]

1.1.2. Translation

Translation involves several components: amino-acyl synthase enzymes, mRNA, tRNA, the ribosome and a multitude of ancillary proteins that regulate translation initiation, the delivery of aminoacyl-charged tRNA, codon selection, the translocation of the ribosome along the mRNA and termination of protein synthesis. Conceptually, the ribosome translation process can be considered to comprise three stages: initiation, elongation and termination.

Ribosomes are macromolecular biomolecules that consist of four ribosomal RNA (rRNA) and 80 proteins that are arranged into a large subunit that mediates peptide bond formation

and a small subunit required for tRNA anticodon-codon recognition.[4] Ribosomes are located in the cytoplasm in prokaryotes and in the cytoplasm or in association with the endoplasmic reticulum in eukaryotes. The role of the ribosome is to translate the mRNA transcribed from a particular gene to its protein counterpart. During initiation, the small subunit of the ribosome binds to the initiation site on the mRNA strand. Transfer RNA, which contains an anticodon complementary to the mRNA codon, then attaches to the initiation site. Codons are sets of three nucleobases that code for a specific amino acid each. Typically, the first codon is the start codon, and is primarily identified as the nucleotide sequence AUG. The bound tRNA will carry the amino acid that corresponds to the codon being translated. The start codon AUG codes for methionine and is normally the first amino acid in a protein's primary structure.[5] **Table 1.1** describes the codons associated with each amino acid.

***Table 1.1**. DNA codon table*

First position	Second Position: U		Second Position: C		Second Position: A		Second Position: G		Third position
U	UUU	Phe	UCU	Ser	UAU	Tyr	UGU	Cys	U
	UUC		UCC		UAC		UGC		C
	UUA	Leu	UCA		UAA	Stop	UGA	Stop	A
	UUG		UCG		UAG		UGG	Trp	G
C	CUU	Leu	CCU	Pro	CAU	His	CGU	Arg	U
	CUC		CCC		CAC		CGC		C
	CUA		CCA		CAA	Gln	CGA		A
	CUG		CCG		CAG		CGG		G
A	AUU	Ile	ACU	Thr	AAU	Asn	AGU	Ser	U
	AUC		ACC		AAC		AGC		C
	AUA		ACA		AAA	Lys	AGA	Arg	A
	AUG	Met	ACG		AAG		AGG		G
G	GUU	Val	GCU	Ala	GAU	Asp	GGU	Gly	U
	GUC		GCC		GAC		GGC		C
	GUA		GCA		GAA	Glu	GGA		A
	GUG		GCG		GAG		GGG		G

After the first tRNA molecule binds to the start codon, the large ribosomal subunit binds to the other components and forms a translation complex, completing the initiation stage.[5]

The translation complex contains three spaces called the A, P and E sites. The first tRNA is initially located in the P (peptidyl) site. At the start of the elongation stage, a second tRNA molecule enters the A (aminoacyl) site and binds to the second codon in the sequence. The amino acid on the first tRNA is then transferred to the A site amino acid and the first tRNA moves to the E (exit) site before leaving the translation complex. The ribosome then moves along the mRNA which causes the second tRNA, still attached to its corresponding codon, to shift from the A site to the P (peptidyl) site. A tRNA corresponding to the next codon then enters the vacant A site and the process of elongation continues, gradually growing the peptide chain. The process is depicted in **Figure 1.1**. Elongation proceeds until a stop codon is encountered, marking the beginning of the termination phase.[5]

When a stop codon is found in the A site after mRNA shifts, a protein called a release factor binds to the site instead of another tRNA molecule causing the polypeptide to be released. The translation complex then dissociates and its components can take part in subsequent translations.[5]

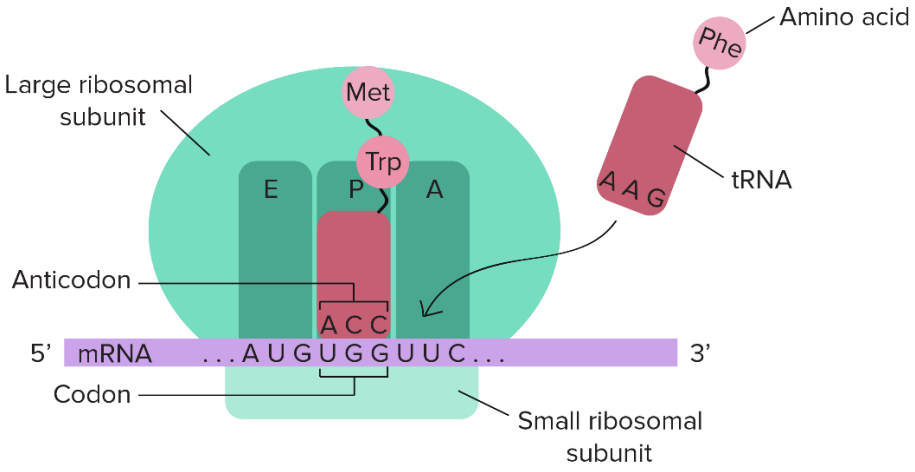

Figure 1.1.[3,6] *A tRNA molecule enters the A site as the ribosome moves across the mRNA strand during elongation.*

1.1.3. Structure of tRNA

Transfer RNA is a macromolecule 73 to 95 nucleotides in length[7] and contains an anticodon and its associated amino acid (**Figure 1.2**). Its secondary structure consists of various loops that fold into an L-shaped conformation that allows it to bind to the ribosomal A, P and E sites. The secondary structure of tRNA is frequently compared to the shape of a cloverleaf, with the D, T, and anticodon loops arranged as leaves around a stem composed of the acceptor stem. An amino acid corresponding to the anticodon is attached to the acceptor stem at the 3' end. The structure is also comprised of a fourth variable loop between the T arm and the anticodon arm.[5]

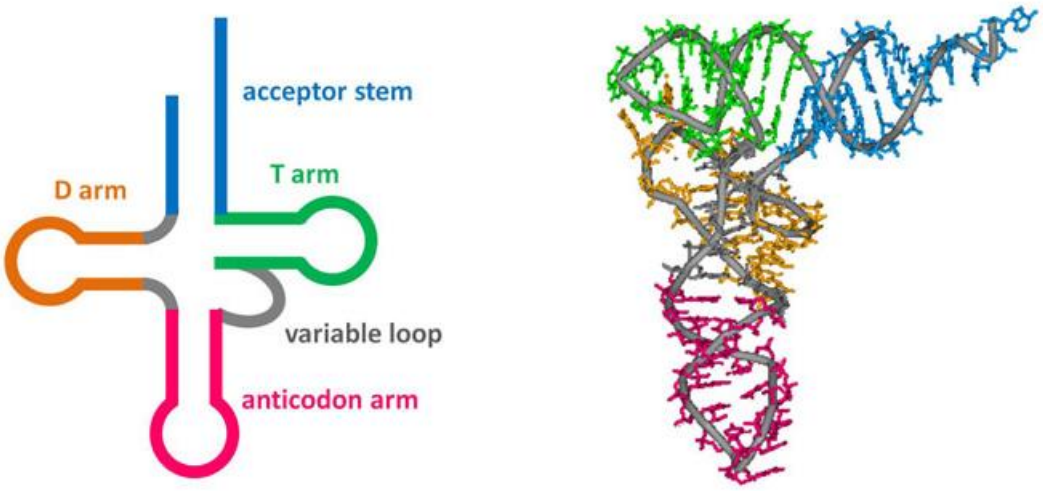

***Figure 1.2**. Secondary and tertiary structures of tRNA (Saccharomyces cerevisiae, $tRNA^{Phe}$).*

The cloverleaf structure is formed by base pairing within the tRNA's arms and acceptor stem. The D, T and anticodon arms end in the non-base-paired D, T and anticodon loops.[8] The loops contain hypermodified nucleotides in a variety of positions which may alter its functionality.[9]

1.1.4. Posttranscriptional modifications of tRNA

A myriad of modifications can be found in the primary structure of tRNA; to date, 112 unique modifications have been characterised.[10] These are the result of chemical transformations performed by enzymes on the nucleotide bases and ribose sugars post-transcriptionally. Complex modifications can arise from these chemical alterations and include oxidative reactions, C-H activation by transition metals, thioalkylation, selenation, amidation and ring

modification among many others.[9] Independent modifications can take place at several sites of a nucleoside to yield a variety of different derivatives; other times the modifications are performed in a precise order to afford a specific structure, as is the case for wybutosine (**1.1**). Hypermodified forms of all four RNA nucleotides are naturally occurring, with a higher proportion of those being derived from uridine.[11] Other examples of hypermodified nucleotides are N^6-isopentenyladenosine (**1.2**), N^4-acetylcytidine (**1.3**) and 4-thiouridine (**1.4**). Their structures are reported in **Figure 1.3**.

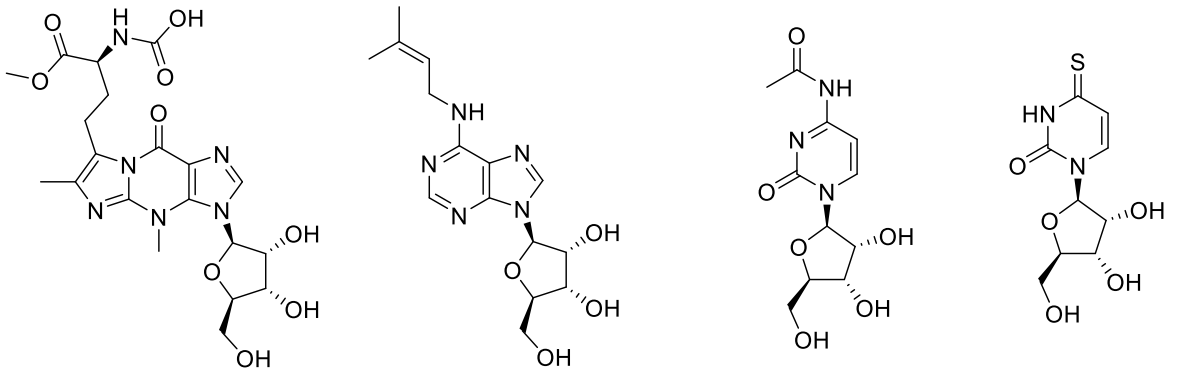

Wybutosine, **1.1** N^6-Isopentenyladenosine, **1.2** N^4-Acetylcytidine, **1.3** 4-Thiouridine, **1.4**

Figure 1.3*. Examples of hypermodified nucleobases.*

Post-transcriptional modifications of RNA allow basic nucleotides to alter their functionality resulting in a variety of chemical properties akin to side-chains of amino acid residues, which may be *e.g.* hydrophobic, ionic or conformationally restricted. The alteration of intramolecular interactions can have a dramatic effect on tertiary structure and conformation. This, in turn, alters RNA interactions with other molecules, in particular proteins.[11]

Of all nucleotides in tRNA, positions 34 and 37 show the greatest diversity of hypermodified nucleotides.[9] These positions are located on the anticodon loop and their hypermodification is hypothesised to allow for non-standard base pairings, also called wobble pairing. As the first two letters of each codon are the primary determinants of specificity, this allows a single tRNA to bind to several codons that could code for the same amino acid. An example can be found in yeast, where one $tRNA^{Arg}$ features another hypermodified nucleoside, inosine, at position 34 on the anticodon and can recognise three arginine codons: CGA, CGU, and CGC.[5]

Position 34 of the tRNA molecule is also known as the wobble position. It corresponds to the third nucleotide in the anticodon and is so called because of the frequent non-standard base pairings that occur between it and the mRNA codons, even in the absence of nucleotide modification. This is made possible by the fact that the wobble position pairs weakly with the mRNA nucleotide compared to the other two in the anticodon; having only two strongly binding nucleotides in tRNA is thought to contribute to faster protein synthesis than if three strong base pairings occurred.[5]

1.2. Queuine

1.2.1. Queuine structure

When eukaryotic and prokaryotic tRNA contains a $G_{34}U_{35}N_{36}$ anticodon, where N represents any nucleotide, the guanine (**1.5**) at the wobble position is usually hypermodified by queuine base (q, **1.6**), resulting in the formation of queuosine (Q, **1.7**). Q is thus found at the wobble position of mature $tRNA^{Asn}$, $tRNA^{Asp}$, $tRNA^{His}$ and $tRNA^{Tyr}$ in most organisms, with some yeast and archaea being notable exceptions.[5,9,12]

The structure of queuine, first characterised by Nishimura in 1983,[12] consists of a 7-deazaguanine core with an aminomethyl side-chain terminated by a cyclopentendiol ring attached to what would be position 7 in guanine. The numbering convention of queuosine, queuine and guanine is shown in **Figure 1.4**. Queuine contains three stereogenic centres arising from its functionality at the 5-position and its systematic name is 2-amino-5-[[[(*1S*,*4S*,*5R*)-4,5-dihydroxycyclopent-2-en-1yl]amino]methyl]-1,7-dihydropyrrolo[2,3-d]pyrimidin-4-one. In mammals, queuine is further decorated by sugars as is the case of $tRNA^{Tyr}$ and $tRNA^{Asp}$—the diol can be functionalised by galactose or mannose, respectively.[13]

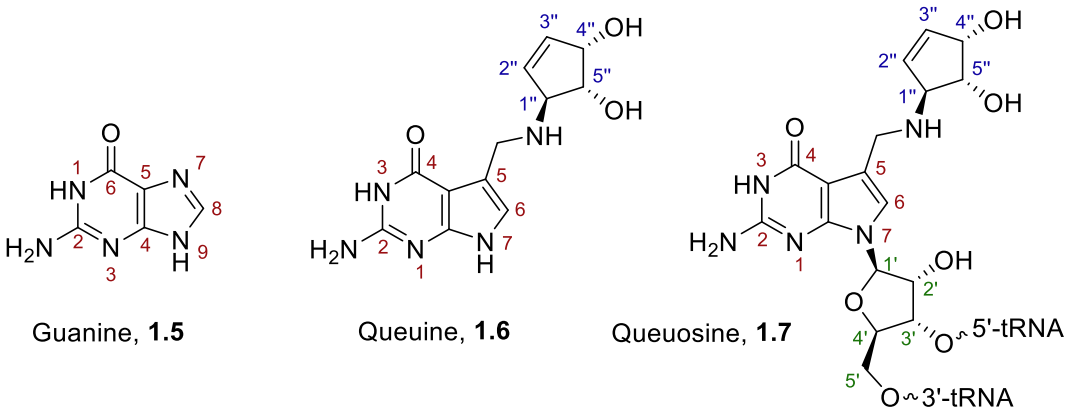

***Figure 1.4**. Chemical structures and numbering convention of queuosine, queuine and guanine.*

1.2.2. Queuosine formation and function

Queuosine formation in tRNA is markedly distinct in bacteria and eukarya. In bacteria, 7-cyano-7-deazaguanine ($preQ_0$, **1.8**) is biosynthesised *via* four enzymatic steps from a guanosine triphosphate nucleoside, which is then converted to 7-aminomethyl-7-deazaguanine ($preQ_1$, **1.9**) by $preQ_0$ reductase. The chemical structures of $preQ_0$ and $preQ_1$ are shown in **Figure 1.5**. The bacterial enzyme tRNA-guanine transglycosylase (TGT) subsequently performs a base exchange reaction, cleaving guanine from the sugar backbone of tRNA before inserting $PreQ_1$ in its stead. Following this, the 7-aminomethyl moiety is functionalised with a cyclopentendiol unit *via* two further enzymatic steps, resulting in a queuine molecule where guanine previously was on the tRNA, irreversibly yielding the final queuosine nucleotide.[9,14,15] With respect to queuine, eukaryotes are capable of neither $preQ_1$ nor queuine biosynthesis. As a result, eukaryotes must instead rely on salvage from diet or gut bacteria before exchanging queuine with guanine at position 34 of the appropriate tRNAs by eukaryotic TGT.[16]

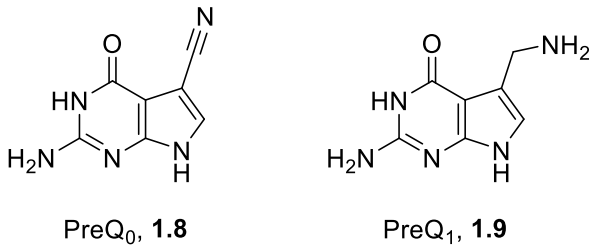

***Figure 1.5**. Chemical structures of queuine precursors $preQ_0$ and $preQ_1$.*

The family of enzymes responsible for the incorporation of 7-deazaguanines into tRNA is known as tRNA-guanine transglycosylases. These enzymes are shared across all biological domains and contain a high degree of sequence homology.[17] The sequence conservation between these ancient enzymes implies that they play an essential part of an organism's physiology.[18] The enzymes contain a zinc-binding domain that is thought to have a structural rather than a catalytic role and spectroscopic studies have suggested that it may play a role in tRNA recognition.[19]

So far, little is known about the function of queuosine or how it affects translation.[20] When compared to G, Q·U (wobble pairing) shows an approximate 3-fold increase in stability whereas Q·C (standard pairing) base-pairing is destabilised in regards to G·C.[21] These subtle differences support the hypothesis that queuosine may facilitate translation in U-ending codons. This suggestion is supported in a study by Tuorto *et. al*[22] where queuine-depleted human cells had reduced translational efficiency at the Q codons with the U-ending codons for Asn, His and Tyr more severely slowed down than the respective C-ending codons. In another study,[23] unmodified $tRNA^{His}$ in *Xenopus oocytes* had a bias for the C-ending codon over the U-ending codon whereas Q-containing $tRNA^{His}$ showed equal decoding of the two codons. These studies suggest that the purpose of queuosine in tRNA could be to bring the affinity of standard and wobble pairings closer.

1.2.3. Queuine and cancer

In rapidly-proliferating tissue such as regenerating liver, embryos or neoplasms, tRNA has been observed to be partially queuine-deficient.[24] Q-hypomodification has been reported in human colon,[25] ovarian,[26] brain[27] and lung[28] cancer as well as leukaemia and lymphomas[29] but is not a universal characteristic of cancer. In tumours where hypomodification is observed, queuine deficiency can be correlated with the histological signs of malignancy, with long-term survival worsening with the decrease of Q-modified tRNA in favour of unmodified tRNA.[26] Reports have also demonstrated that inhibition of queuine modification can promote cellular transformation.[30]

Reasons for this reported Q-hypomodification have not been established but several explanations have been suggested in various studies. Researchers in the field have proposed that it could be due to increased transcription and turnover of tRNA observed in tumour cells.

Alternatively, the hypomodification of tRNA could be the result of loss of function in TGT, a decrease in its expression, or loss of transport of TGT to the mitochondria.[31] Yet another explanation for this observation could be decreased salvage activity of cancer cells.[32]

The presence of Q-hypomodification in some forms of tumour enables the use of treatments that can discriminate between cancerous and healthy cells. Research aiming to exploit this difference will be the focus of this project.

1.3. Synthetic analogues of queuine

1.3.1. Previous work

Early work on tRNA-guanine transglycosylase established that many structures beyond queuine and its precursors may act as substrates for the enzyme. On the first reported study on eukaryotic TGT,[33] Howes & Farkas showed that the enzyme would incorporate free guanine in place of the guanine present at position 34 of $tRNA^{Asn}$, $tRNA^{Asp}$, $tRNA^{His}$ and $tRNA^{Tyr}$ in the absence of queuine. Subsequent studies reported the irreversible incorporation of analogous molecules such as 7-deazaguanine (**1.10**), 2",3"-dihydroqueuine (**1.11**), 6-thioguanine (**1.12**) and 2-thiohypoxanthine (**1.13**) as well as confirming that queuine precursors $preQ_0$ (**1.8**) and $preQ_1$ (**1.9**) were substrates for the enzyme. 8-Azaguanine (**1.14**) was also shown to replace guanine in tRNA although queuine would be incorporated in its place if available, thus making its insertion into tRNA reversible.[15] The structures of compounds **1.10** – **1.14** can be found in **Figure 1.6**.

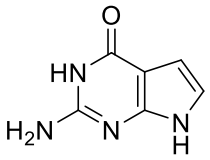

7-Deazaguanine, **1.10**

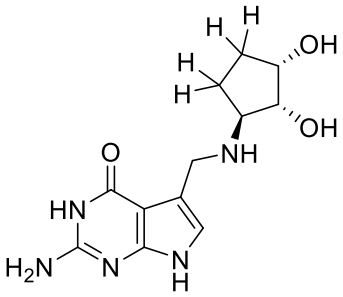

2",3"-Dihydroqueuine **1.11**

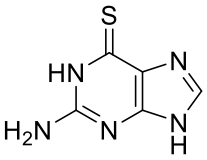

6-Thioguanine, **1.12**

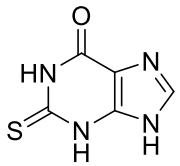

2-Thiohypoxanthine, **1.13**

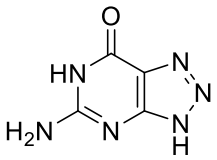

8-Azaguanine, **1.14**

Figure 1.6*. Chemical structures of various TGT substrates.*

These findings suggested that it might be possible to exploit the TGT insertion pathway with analogues of queuine. In 1986, Nishimura *et al.* reported the synthesis of a library of 7-deazapurines.[34] The compounds were tested against the mouse lymphoma L5178Y cell line and some displayed promising growth inhibition at concentrations as low as 1 μM. The highest inhibitory effect was recorded for compounds **1.15** – **1.19**; their structure and inhibition of growth are reported in **Figure 1.7**. Analogues **1.15** – **1.17** are derivatives of $preQ_1$ with either a phenol or iodoacetyl moiety whereas analogues **1.18** and **1.19** bear a sulphur atom in place of oxygen at position 4 and either an unmodified or 2,2-propanediol-protected side-chain at the 5-position with respect to queuine.

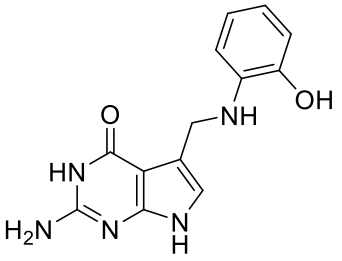

1.15

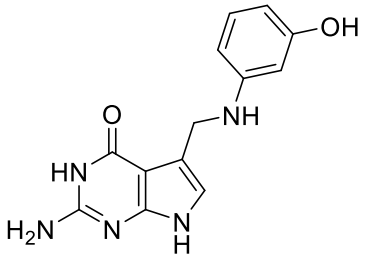

1.16

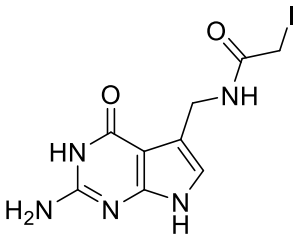

1.17

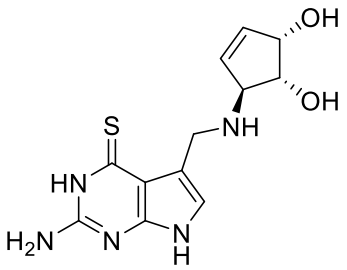

1.18

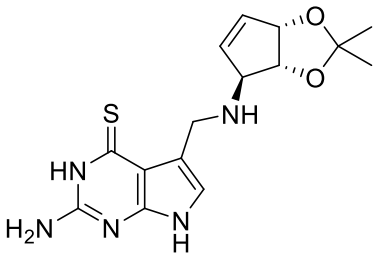

1.19

	Inhibition of growth of L5178Y cells (%)		
Compound	1 µg/mL	10 µg/mL	100 µg/mL
1.15	25	53	90
1.16	12	75	79
1.17	49	87	89
1.18	12	55	88
1.19	46	87	94

***Figure 1.7**. Chemical structures of **1.15** – **1.19** and growth inhibition percentage against the L5178Y cancer cell line.*

Compounds **1.15**, **1.16**, **1.18** and **1.19** were all found to be incorporated into yeast tRNA. Interestingly, **1.17** had the strongest inhibitory effect on L5178Y cells despite not being incorporated into yeast tRNA. The authors do not provide an explanation for this observation but it is possible that this cytotoxic effect could be caused by the reactivity of the iodoacetyl side-chain, a known toxicophore.[35]

Decades later, in a study by Southern, Connon and Kelly,[1] TGT was exploited to treat a murine model of multiple sclerosis (MS). An analogue of queuine, NPPDAG (**1.20**, **Figure 1.8**)

was administered to the murine model and incorporated into hypomodified tRNA by TGT, after which full remission of the multiple sclerosis model was reported. During this work, it was discovered that while TGT was highly specific for $tRNA^{Asn}$, $tRNA^{Asp}$, $tRNA^{His}$ and $tRNA^{Tyr}$ it was less specific with respect to the deazaguanine substrate. Many NPPDAG derivatives were found to be substrates for TGT but, regrettably, did not alter the progression of MS.

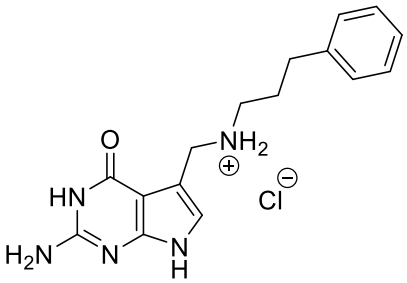

NPPDAG, **1.20**

Figure 1.8*. Chemical structure of NPPDAG, a substrate for TGT. Administration of NPPDAG led to full remission in a murine model of multiple sclerosis.*

Given the Q-hypomodification observed in cancer cells and the promiscuous nature of TGT we wondered whether we could selectively deliver disruptive compounds to the tRNA of cancer cells. Although queuine and selected analogues such as NPPDAG were found to have a significant effect on tRNA, we postulated that a more direct approach to cellular disruption could be developed.

We postulated that the addition of a side-chain at the 2-position would have a greater impact on translation due to its close proximity to the H-bonding sites of the queuine core compared to functionalisation at the 5-position (**Figure 1.9**). Thus, selective disruption of protein synthesis in cancer cells might be achieved. Furthermore, it was also believed that the high demand for protein synthesis in cancer cells could reinforce this effect.

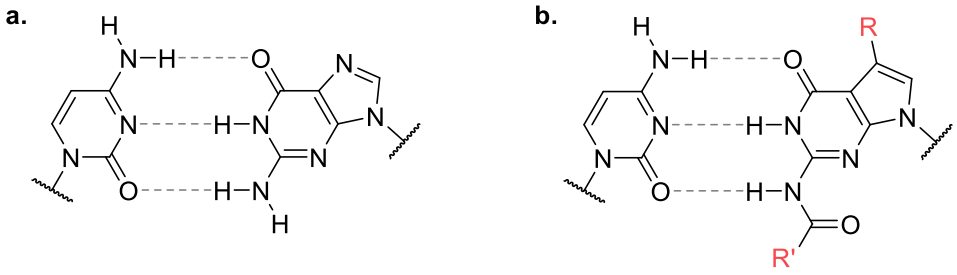

***Figure 1.9**. **a.)** Watson-Crick H-bonding between cytosine and guanine. **b.)** Watson-Crick H-bonding between cytosine and hypothetical 2-functionalised queuine analogue, where R and R' can be any functional group. R' is much closer to the codon-anticodon recognition than the R group at the 5-position.*

As discussed above, previous research established that derivatives with differing R groups at position 5 could be accommodated by TGT. However, no evidence of the acceptance of R' groups at the 2-position could be found in the literature. We hypothesised that the use of a small R group might be prudent if extra steric bulk was being incorporated *via* the R'. As $preQ_0$ was a known substrate we employed this molecule as a framework.

Proof of concept studies by Áine Harney (chemistry) and PhD candidate Mashael Al-Qasem (biochemistry) indicated that $preQ_0$ derivatives with R' sidechains such as Me, ^{t}Bu and ^{n}Hep would act as substrates for TGT. Unfortunately, at the time it was not possible to test these compounds against any cancer cell lines. The method employed by Áine Harney was cumbersome, employing pyridine at reflux and subsequent removal of pyridine by distillation giving compounds that lacked the high purity required for systematic analysis. Future efforts would require devising a better synthetic route and assessing the derivatives against a suitable cancer cell line.

1.3.2. Covalent inhibitors

The pharmaceutical industry has a history of being hesitant in developing covalent inhibitors. The perceived risk for off-target covalent bonding leading to toxicity and side-effects means that many companies have been unwilling to invest funds towards a compound only to realise that it causes life-threatening idiosyncratic reactions in patients after it has been released to the market.[36] However, scientists' perception on the subject is changing due in part to an increase of interest in such compounds and the recent understanding that the modes of action of many approved drugs proceed by the formation of covalent bonds. These include a list of commonly

prescribed pharmaceuticals such as aspirin,[37] omeprazole,[38] penicillin,[39] clopidogrel[40] and ibrutinib.[41] Furthermore, research corroborates that the high potencies and long-lasting effects achievable with covalent drugs could allow for less frequent drug administration. Evidence also suggests that covalent drugs have a reduced risk of resistance which is of major importance in areas such as oncology and infectious disease.[42]

Interestingly, much early work in cancer research relied on alkylating agents. The field of chemotherapy grew rapidly with the discovery of nitrogen mustards as chemotherapeutical agents in the 1940s.[43] These compounds typically consist of two chloroethyl groups attached to a nitrogen atom which can each form covalent bonds with the 7-position of guanine in DNA strands. The multiple alkylating functional groups on nitrogen mustards allow them to create crosslinks within DNA which interfere with transcription and can trigger apoptosis. The high toxicity of some of the older compounds such as chlormethine led to them being phased out in favour of safer drugs, the most widespread currently being cyclophosphamide.[44]

The deliberate design of Michael acceptors as chemotherapeutical agents has been scarce, in part due to their cytotoxicity. However, many anticancer drugs have been found to be metabolised into Michael acceptors which is believed to contribute to their therapeutic efficacy. Some examples are tamoxifen,[45] etoposide[46] and mitomycin C[47]. Michael acceptors are known to alkylate the sulphur atom in cysteine residues as well as other biological nucleophiles.[48]

The toxicity of older alkylating groups arises from their lack of selectivity and the necessity for high activity to ensure reaction when DNA is available. We thought that the repetitive nature of protein synthesis and the repetitive interaction of the unmodified tRNA with the ribosome and the enzymes of protein synthesis (*e.g.* synthases) would mean that milder alkylating agents such as alkyl chlorides or Michael acceptors might be successful in hampering protein synthesis.

1.4. Project aims

Building upon the work previously conducted within the group, the aims of this project were to develop an improved synthetic route, prepare a library of $preQ_0$ derivatives of general structure **1.21** (**Figure 1.10**) and assess these derivatives against a suitable cancer cell line. A library of $preQ_0$ analogues with subsequent viability assays would provide much-needed insight on the structure-activity relationship (SAR) between the analogues and the target biochemical

entities—namely, TGT, tRNA, mRNA and the ribosome. Three classes of compounds bearing a variety of functional groups at position 2 were designed to probe for SAR:

1. Simple aliphatic steric bulk
2. Aromatic steric bulk
3. Mild electrophilic alkylating agents

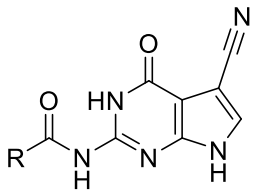

1.21

***Figure 1.10**. Target general structure for the synthesis of a library of preQ$_0$ analogues.*

2. Results and discussion

2.1. Synthesis of the main scaffold

Preliminary work within the Southern group showed that general structure **1.21** can be synthesised in one step from preQ$_0$ (**1.8**) using acylating reagents. Thus, the synthetic strategy involves the acylation of the main scaffold preQ$_0$ (**1.8**) before a derivatisation step to synthesise a library of analogues.

It is possible to acquire preQ$_0$ (**1.8**) through commercial suppliers. However, due to the high cost and the large quantities of the material likely required the material was prepared in-house. Fortunately, the synthesis of PreQ$_0$ (**1.8**) is known[49-52] and the procedure has been extensively explored in Dr. Michelle Cotter's doctoral thesis,[53] where a two-step procedure is carried out (**Scheme 2.1**).

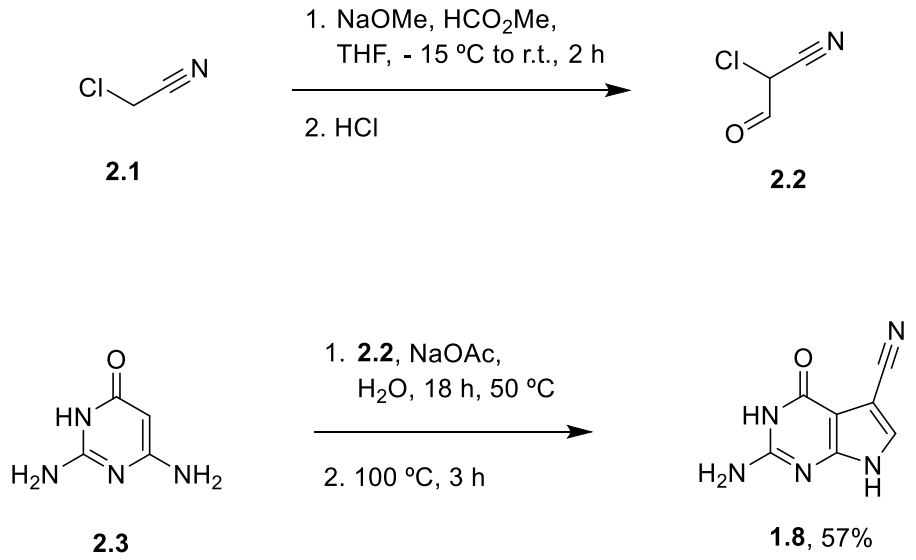

***Scheme 2.1**. The two-step synthesis of preQ$_0$ (**1.8**).*

The synthesis of preQ$_0$ started with the condensation of chloroacetonitrile (**2.1**) with methyl formate in the presence of sodium methoxide to yield 2-chloro-3-oxopropanenitrile (**2.2**). The reaction mixture was quenched with concentrated hydrochloric acid and a characteristic colour

change from yellow to a deep cherry red was observed. **2.2** has been observed to decompose under storage and reports[49-52] of its synthesis in the literature consistently mention that the compound is submitted to subsequent reactions without further purification or characterisation. Thus, the product of the reaction was immediately reacted with 2,4-diamino-6-hydroxypyrimidine (**2.3**) to yield $preQ_0$ (**1.8**).

Removal of the water solvent from product **1.8** required extensive efforts and was critical to the success of subsequent reactions. After successive cycles of azeotropic distillation employing toluene and methanol, the resulting white paste of $preQ_0$ and water had to undergo three cycles of drying in a vacuum desiccator in the presence of phosphorus pentoxide overnight and grinding with mortar and pestle. The subsequent derivatisation step required anhydrous conditions so the white powder was heated to 100 °C under high vacuum for 4 h to ensure a completely anhydrous material. Typically, the mass of a sample would decrease by around 10% during this process indicating an unusual affinity for water.

Analysis of the product was complicated by its relative insolubility in most common organic solvents. However, $preQ_0$ (**1.8**) is somewhat soluble in hot dimethyl sulphoxide (DMSO) which allowed its identity and purity to be confirmed by ^{1}H NMR analysis.

2.2. Acylation of the 7-cyano-7-deazaguanine core

2.2.1. Previous conditions

Previous strategies towards the synthesis of $preQ_0$ analogues focused on functionalising the 2-position with acyl chlorides to yield the corresponding amide. Previous $preQ_0$ analogues were prepared by reacting $preQ_0$ with four equivalents of the acyl chloride in pyridine at 90 °C. In this reaction, pyridine acts both as a solvent and a base to neutralise the hydrogen chloride by-product. The use of four equivalents of acyl chloride yields the bis-acylated product which is then converted to the desired product by hydrolysis with sodium hydroxide (**Scheme 2.2**). However, pyridine needed to be distilled in order to isolate the product. This caused purity issues as pyridine traces could not be eliminated from the product.

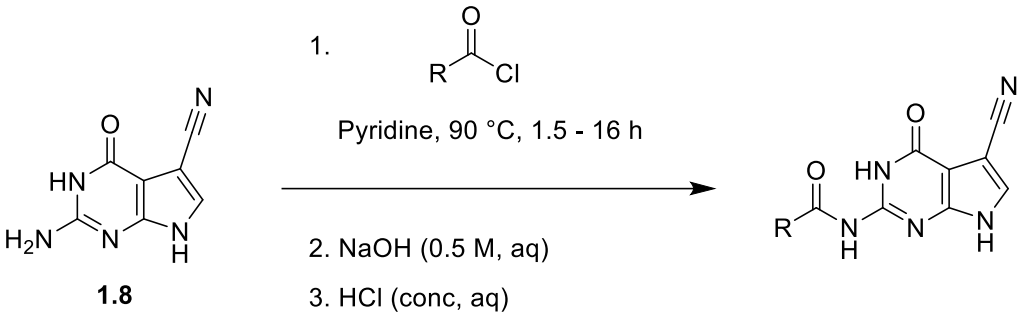

***Scheme 2.2**. Previous synthesis of preQ$_0$ analogues employing pyridine.*

In addition to the less than ideal purity achieved by this procedure, subsequent work recognised a number of issues with this method. The solubility of **1.8** in pyridine is very low below room temperature and reactions would not proceed. Furthermore, the chloroalkane and α,β-unsaturated carbonyl acyl chloride reagents needed for the synthesis of the alkylating analogues would likely be prone to degradation at high temperatures.

It was decided to explore other solvents. DMSO solubilises preQ$_0$ but was disregarded because of its reactivity towards acyl chlorides.[54] Similar solvents, dimethyl formamide (DMF) and *N*,*N*'-dimethylpropyleneurea (DMPU), were also considered. Ultimately, DMPU was chosen over DMF as it offered superior solubilisation at room temperature and triethylamine was chosen to fill the role of base. Interestingly, the solubility of **1.8** in DMPU in the presence of triethylamine was much improved over pyridine, even at 0 °C.

2.2.2. New synthetic approach

Despite attempts at mono acylation we were never able to singly acylate preQ$_0$ cleanly. Rather, we were forced to bis-acylate and then perform a selective hydrolysis. Initial optimisation was performed with acetyl chloride. A suspension of preQ$_0$ and 4 equivalents of triethylamine in DMPU was cooled to 0 °C before the dropwise addition of four equivalents of acetyl chloride. The mixture was then stirred at 0 °C for 16 h. During this time a suspension formed. The reaction was monitored by ^{1}H NMR and stopped when the starting material was fully consumed. Subsequently, a volume of 0.1 M aqueous potassium hydroxide equal to the volume of solvent used was added to the mixture and stirred at room temperature for 30 min, which solubilised the suspension. After 30 min, TLC analysis showed the disappearance of a compound and the appearance of a new compound, hence the solution was acidified to pH 2 with concentrated

hydrochloric acid causing a tan precipitate to form, which was collected by vacuum filtration. ^{1}H NMR indicated formation of the expected product, albeit contaminated with other unknown species. Purification by extraction and flash column chromatography were attempted but were unsuccessful due to the insolubility of the product in most common organic solvents. Eventually this insolubility was exploited: the amorphous power was washed with dichloromethane, methanol and water, affording a light free-flowing powder. Analysis of the substance revealed this to be the desired product, **2.4**. Regrettably, a yield of only 10% was obtained (**Scheme 2.3**).

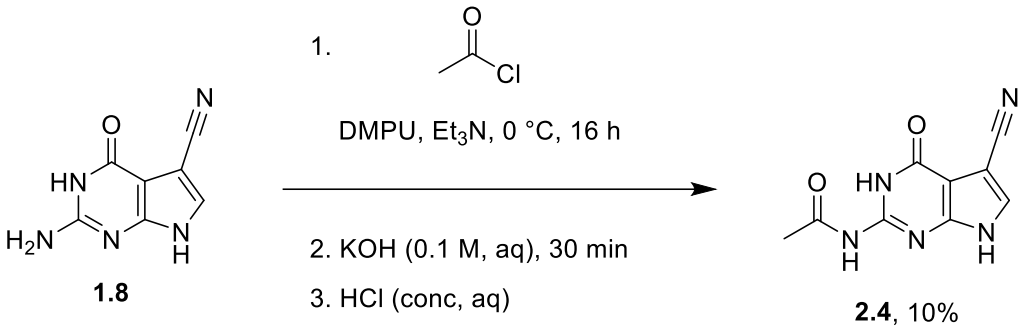

***Scheme 2.3**. Low-yielding synthesis of **2.4**.*

2.2.3. Optimisation of reaction conditions

It became evident that a more efficient methodology would have to be developed for the reaction. Two key aspects of the reaction were designated for further investigation: the hydrolysis and the purification.

It was suspected that one of the reasons for the low yield of **2.4** was that conversion from the bis-acetylated intermediate, **2.5**, into **2.4** during hydrolysis did not reach completion. The reaction and hydrolysis for the reaction are believed to proceed *via* the mechanism suggested in **Scheme 2.4**. Acetyl chloride is expected to acylate preferentially at the more labile 7-position. The addition of excess acetyl chloride forces the acylation of both *N*-7 and *N*-2, forming species **2.5**. We exploited the fact that the *N*-7 amide is more labile to selectively cleave the position with an appropriate concentration of potassium hydroxide.

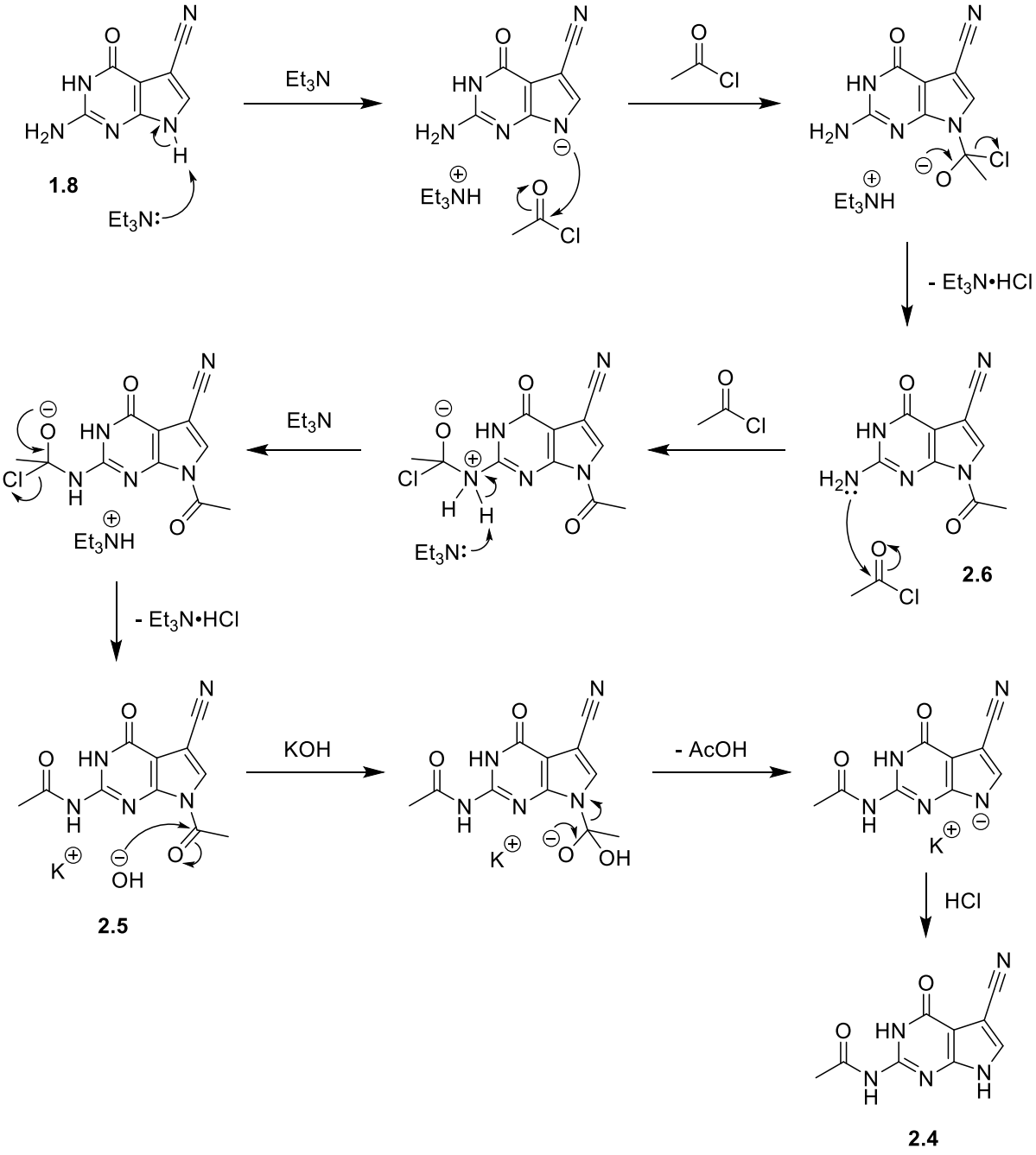

***Scheme 2.4**. Suggested mechanism for the synthesis of **2.4** using excess acetyl chloride. Potassium hydroxide selectively cleaves the amide at position 7 during the work-up.*

In order to assess the role of hydrolysis in reaction yield we performed the standard initial reaction. Keeping the reaction mixture at 0 °C was deemed unnecessary and the reaction was performed at room temperature instead. When NMR analysis indicated full consumption of the starting material, the reaction mixture was split into 6 portions. The first set of 3 was stirred at room temperature for 30 min with 0.5 M, 1 M and 2 M potassium hydroxide, respectively. The

second set was treated with the same KOH concentrations but for 20 h. In each case, the volume of potassium hydroxide solution was equal to the volume of solvent in the sample. After the allotted time, each was acidified to pH 2 and the resulting precipitate was collected by vacuum filtration, washed with methanol and analysed by NMR. **Table 2.1** below shows the ratios of **1.8, 2.4** and **2.5** found in each sample.

***Table 2.1**. Ratios of equivalents of species **1.8, 2.4** and **2.5** found in the products of each work-up*

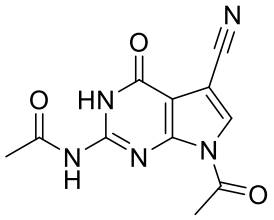

2.5

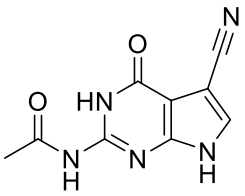

2.4

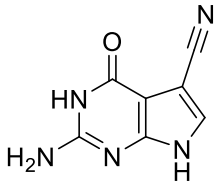

1.8

	2.5	**2.4**	**1.8**
0.5 M, 30 min	5	1	0
0.5 M, 20 h	1	20	0
1 M, 30 min	0	1	0
1 M, 20 h	0	1	0
2 M, 30 min	0	3	4
2 M, 20 h	0	0	1

Deacetylation at a 0.5 M concentration proved to be proceeding very slowly; even after 20 h, **2.5** still had not fully converted to **2.4**. On the other hand, a concentration of 2 M KOH led to rapid hydrolysis of both amide bonds, yielding a majority of completely deacylated $preQ_0$ (**1.8**) after only 30 min. 1 M proved to be the ideal concentration for this reaction: hydrolysis of position 7 occurred selectively both after 30 min and 20 h and yielded desired product **2.4** exclusively. All subsequent reactions employed the same procedure.

Unfortunately, low levels of DMPU contamination were observed by NMR in each sample. One sample was triturated vigorously in methanol for 30 min. The solids were then collected by filtration and analysed with ^{1}H NMR spectroscopy. Most of the DMPU had been removed but solvent bysignals were still visible in the spectrum. Repetition of the process removed DMPU below levels detectable by NMR.

It was concluded that the appropriate hydrolysis conditions and purification method would be 1 M potassium hydroxide for 30 min followed by trituration in methanol for 30 min, filtering and repeating the trituration until satisfactory purity was achieved. As long as no starting material was present in the final mixture, methanol washing would be a viable way to purify the compounds. This work-up procedure served as the standard protocol for the synthesis of the remaining analogues.

Since the acylation reaction above proceeded without setbacks at room temperature, it was proposed that heating could significantly reduce reaction time as long as the acyl chlorides were not reactive enough to undergo degradation. Another test reaction was set up as above, this time while heating the reaction mixture to 100 °C. Reaction completion was attained after 2 h and the mixture was worked up following the methods presented above. **2.4** was isolated as a light brown amorphous solid in a 63% yield. This is also a noticeable improvement over the first attempt in this project (10%) (**Scheme 2.5**).

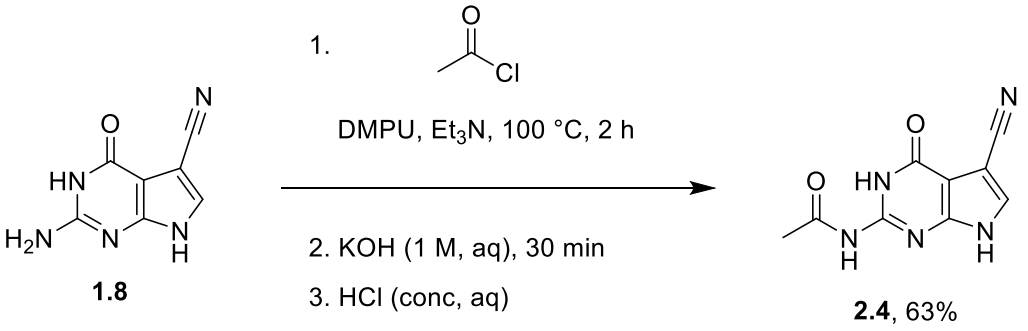

Scheme 2.5*. Improved synthesis of* ***2.4****.*

It is important to acknowledge that a possible product for the reaction is the 7-acetylated isomer of **2.4**, **2.6**. Fortunately, the two isomers are distinguishable by ^{1}H NMR. The spectrum of the final product in the reaction above is depicted in **Figure 2.1**.

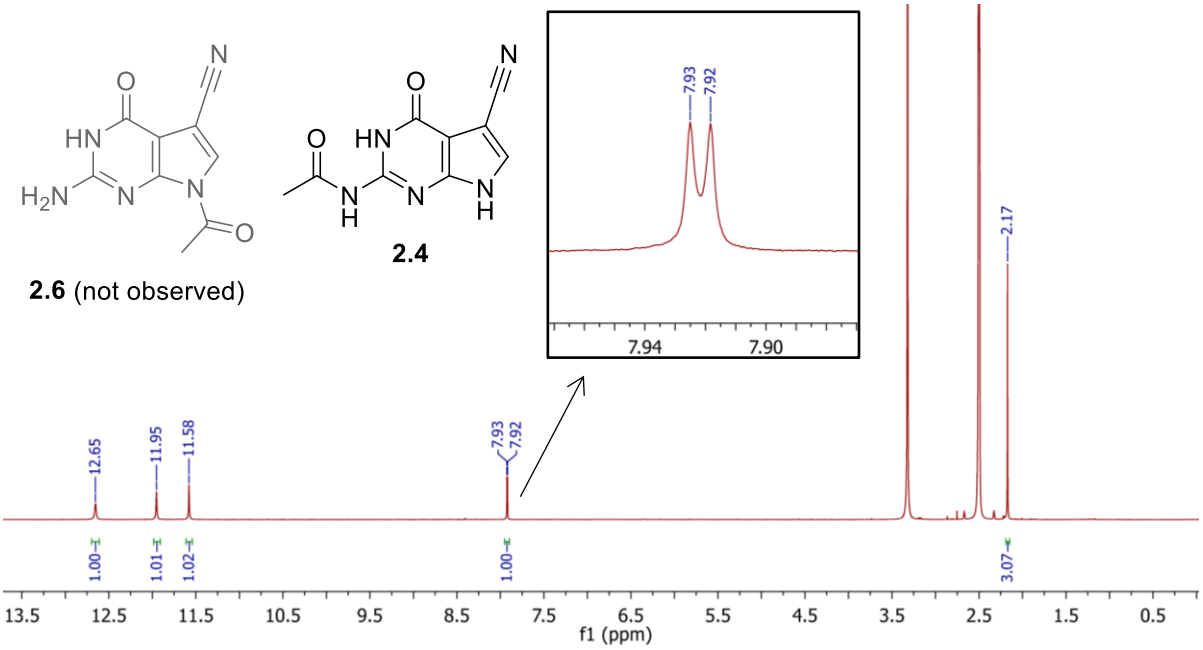

***Figure 2.1**. [1]H NMR spectrum of the product from **Scheme 2.5**. Resonances for **2.4** are accounted for while **2.6** is not observed.*

The methyl group is clearly visible at δ 2.17 ppm with integration 3. At δ 7.93 ppm, a doublet corresponding to the C-H at position 6 can be seen. The multiplicity of the peak indicates that the aryl proton is coupling with the vicinal N-H of position 7, thus supporting that the product is not **2.6**. Three singlets of integration 1 corresponding to the N-Hs can be observed at δ 11.58, 11.95 and 12.65 ppm, although experimentally these resonances have been known to shift based on sample concentration. This phenomenon is common for protons involved in hydrogen bonding.[55] These three N-H resonances confirm the position of the acetyl group on position 2 as acetylation at positions 3 or 7 would have yielded two signals for N-H of integrations 1 and 2.

2.3. Synthesis of a library of preQ$_0$ analogues

2.3.1. Target compounds

The next step in the project consisted in creating a small library of preQ$_0$ analogues. The amides were chosen to have three distinct characteristics: aliphatic steric bulk, aromatic steric bulk and mild alkylating agents. The target structures are shown in **Figure 2.2**.

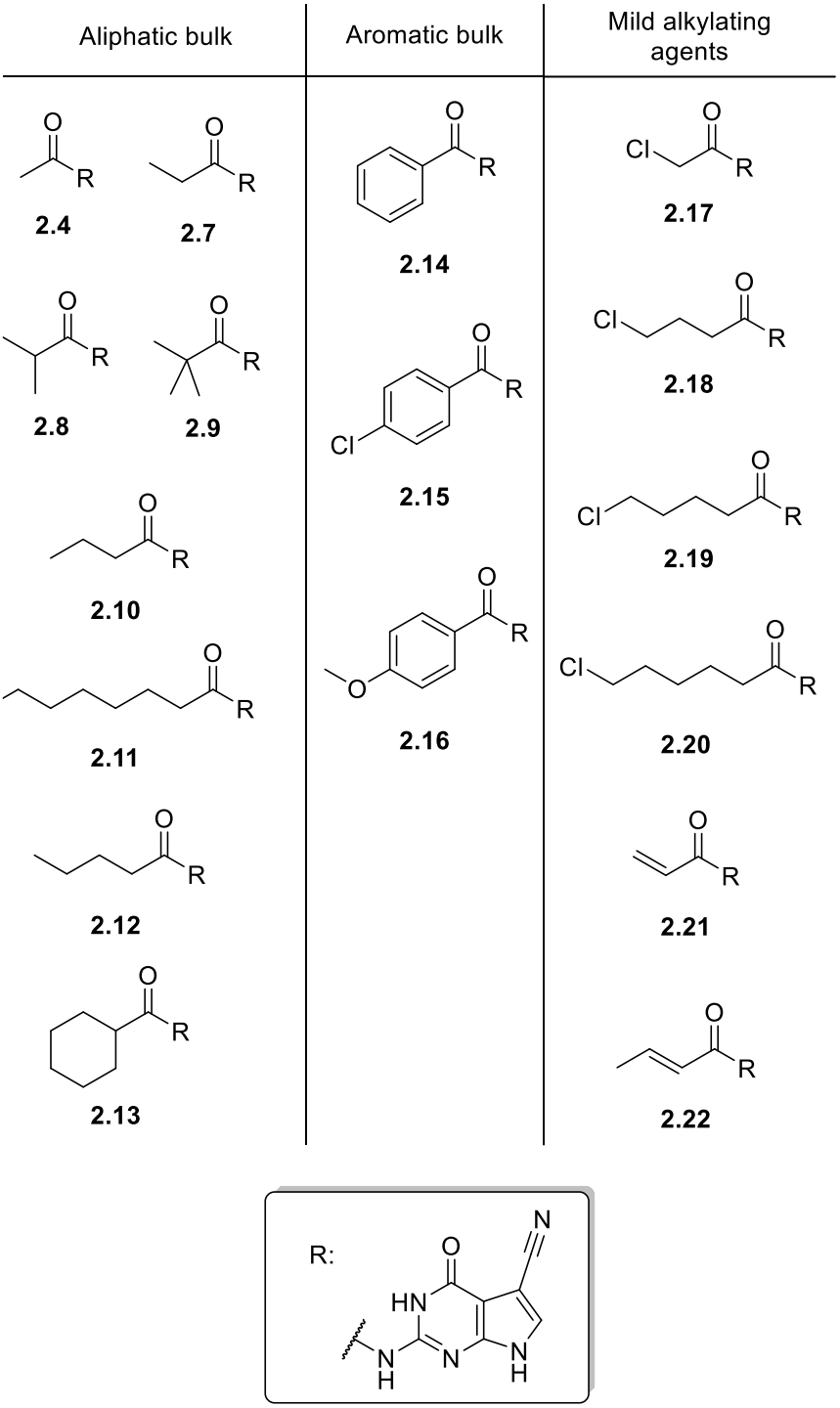

***Figure 2.2**. Proposed library of preQ$_0$ analogues. The collection is divided into aliphatic steric bulk, aromatic steric bulk and mild alkylating agents.*

We deemed that the aliphatic amides would offer the least synthetic challenge so these were the first prepared.

2.3.2. Synthesis of $preQ_0$ analogues with aliphatic substituents

Vials containing $preQ_0$, triethylamine and DMPU were each treated with the appropriate acyl chloride before being heated to 100 °C for 2 h. The mixtures were allowed to cool to room temperature before the addition of 1 M potassium hydroxide and were left to stir for 30 min. After acidification to pH 2, the resulting precipitates were collected under vacuum, triturated in methanol for 30 min and filtered again. The purification step was repeated as required until DMPU was undetectable by NMR (**Scheme 2.6**).

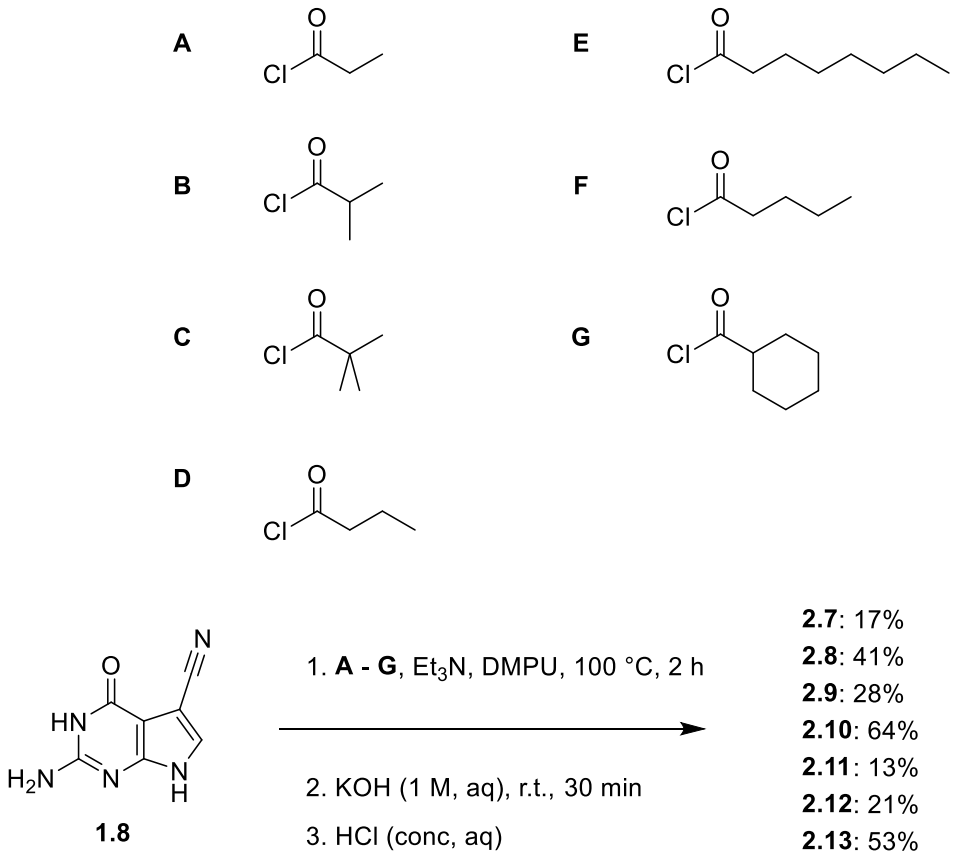

***Scheme 2.6**. The synthesis of compounds **2.7** – **2.13**.*

This gave compounds **2.7** – **2.13** in yields of 13 – 64%. The identities of **2.7** – **2.13** were confirmed by ^{1}H NMR, ^{13}C NMR, ^{13}C HSQC, FTIR and HRMS.

2.3.3. Synthesis of $preQ_0$ analogues with aromatic substituents

Having prepared the aliphatic targets, our attention turned to the aromatic systems (**Scheme 2.7**). Unexpectedly, employing the same conditions as previously with benzoyl chloride yielded a brown oil. Inspection of the material by ^{1}H NMR detected integrations, multiplicities and shifts that could correspond to the desired product, **2.14**. However, many resonances in the δ 7.2 – 8.1 ppm range could not be accounted for and resulted in a complex collection of signals, suggesting a mixture of compounds. One such impurity was identified as benzoic acid by comparison to a reference spectrum. Attempts towards purifying the mixture with additional methanol washes proved unsuccessful. The oil was found to be somewhat soluble in a mixture of dichloromethane and methanol so purification *via* flash column chromatography was performed using 3% methanol in dichloromethane. Unfortunately, the various species in the mixture co-eluted over the same range of fractions.

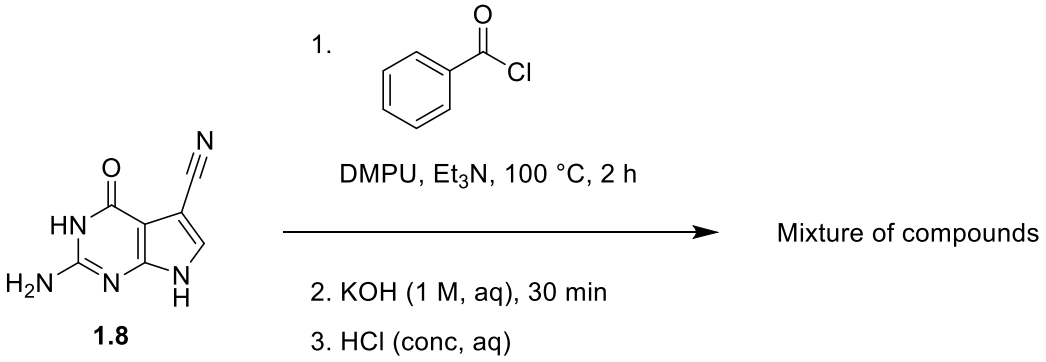

***Scheme 2.7**. The attempted synthesis of **2.14**.*

In order to circumvent this issue a different procedure was developed to isolate **2.14**. Benzoyl chloride was added to a new reaction vessel containing $preQ_0$, triethylamine and DMPU and the suspension was heated to 100 °C for 1 h until ^{1}H NMR analysis indicated the full consumption of the starting material. Then, 1 M potassium hydroxide was added to the mixture and left to stir at room temperature for 30 min. The suspension was transferred to a separating funnel and washed with dichloromethane. The intent was to remove as much of the unidentified organic impurity as possible while retaining the potassium salt of the desired product in the aqueous phase. The aqueous phase was isolated and acidified to pH 2, causing a yellow precipitate to form. The precipitate was collected *via* vacuum filtration and washed with methanol. Upon analysis of the sample by ^{1}H NMR, **2.14** was successfully identified along the presence of a

structurally similar compound. It was thought that this impurity could be the bis-acylated intermediate, so the powder was stirred in 1 M potassium hydroxide for 30 more minutes. Surprisingly, the relative amounts of impurity to product increased. We proposed that the product was undergoing nitrile hydrolysis, hypothesis that was further supported by the presence of five peaks at δ 8.43, 8.61, 11.37, 11.86 and 12.46 ppm in the ^{1}H NMR spectrum which could correspond to the 5 N-H signals (**Figure 2.3**).

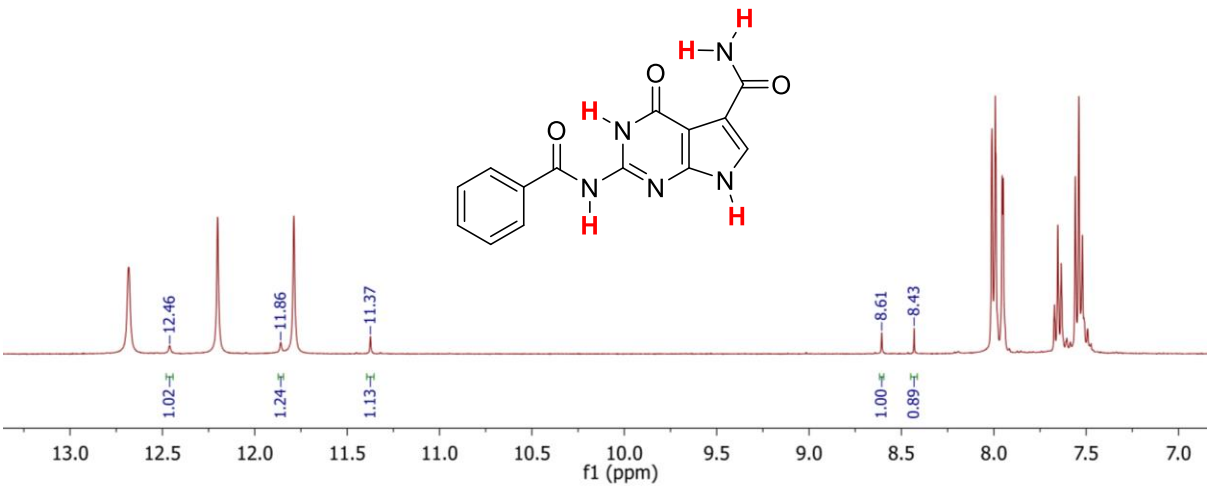

***Figure 2.3**. Suggested structure of impurity giving rise to additional peaks. The other signals observed are consistent with the identity of the major product being **2.14**.*

A procedure that did not use hydroxide to deacylate position 7 was attempted. After heating the standard reaction mixture at 100 °C for 1 h, water was added and the suspension was transferred to a separating funnel. In contrast to the previous experiment, this time the species of interest was the bis-acylated intermediate, which would be expected to be found in the organic layer due to the improved solubility the second phenyl group would confer to the molecule. The suspension was extracted with dichloromethane and the combined organics were concentrated under reduced pressure. Analysis of the sample by ^{1}H NMR confirmed the presence of the expected compound. The residue was treated with 1 N methanolic ammonia and stirred at room temperature. After 16 h, spectral analysis confirmed complete conversion to **2.14** with no side products. The mixture was acidified to pH 2 and the precipitate was collected by vacuum filtration, triturated in methanol for 30 min and filtered again to give **2.14** as an amorphous white solid in 52% yield (**Scheme 2.8**).

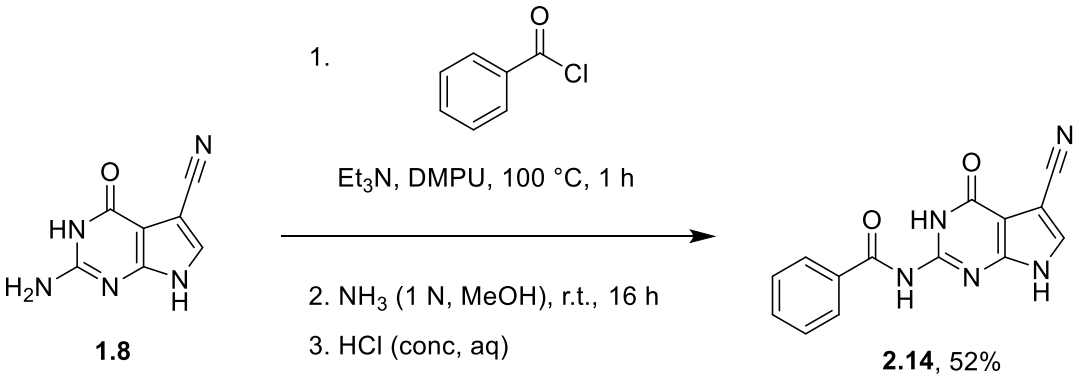

***Scheme 2.8**. Successful synthesis of **2.14** employing aminolysis during the work-up.*

The first synthetic attempt towards **2.15** gave once again a complex mixture of products. Thus, it was decided to employ the same methodology used as the successful synthesis of **2.14**, using extraction in dichloromethane to remove hydrophilic impurities before hydrolysis. After heating the standard reaction mixture at 100 °C for 1 h, water was added and the suspension was transferred to a separating funnel. The crude mixture was extracted with dichloromethane, the combined organics were concentrated under reduced pressure and the residue was treated with 1 M potassium hydroxide. After 30 min, ^{1}H NMR analysis found that the sample still contained a majority of the bis-acylated intermediate so the reaction was left to stir for a further 90 min. The suspension was centrifuged at 3750 rpm for 10 min, which caused a distinct separation of liquid and solid phases. The liquid phase was collected and acidified to pH 2 with concentrated hydrochloric acid, causing a pale yellow precipitate to form. The precipitate was collected *via* vacuum filtration and washed with methanol. Subsequent ^{1}H NMR analysis identified the yellow solid as a 1:5 mixture of **2.15** and 4-chlorobenzoic acid. The compound proved difficult to separate from the hydrolysis byproduct; four cycles of trituration in methanol for 10 min and filtration were required to isolate **2.15** as a mustard powder in 14% yield (**Scheme 2.9**)

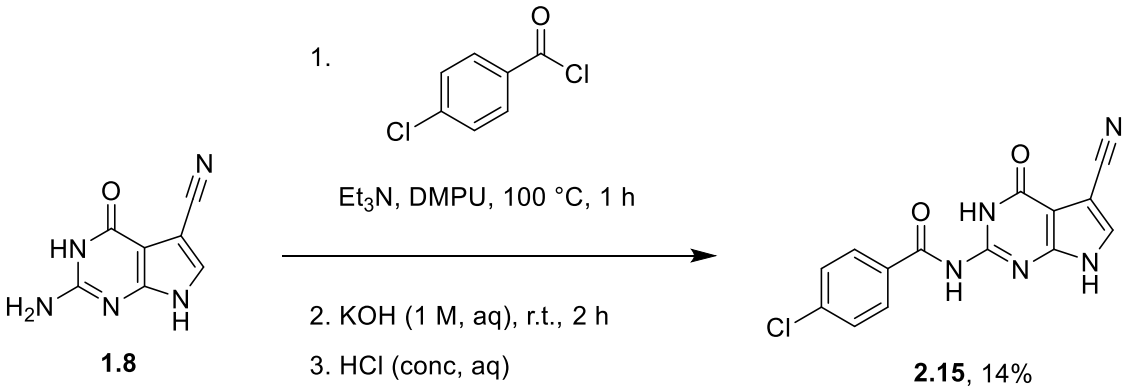

***Scheme 2.9**. Successful synthesis of **2.15**.*

The next synthetic target was **2.16**. A reaction with the standard parameters was performed, successfully isolating **2.16** in 33% yield (**Scheme 2.10**).

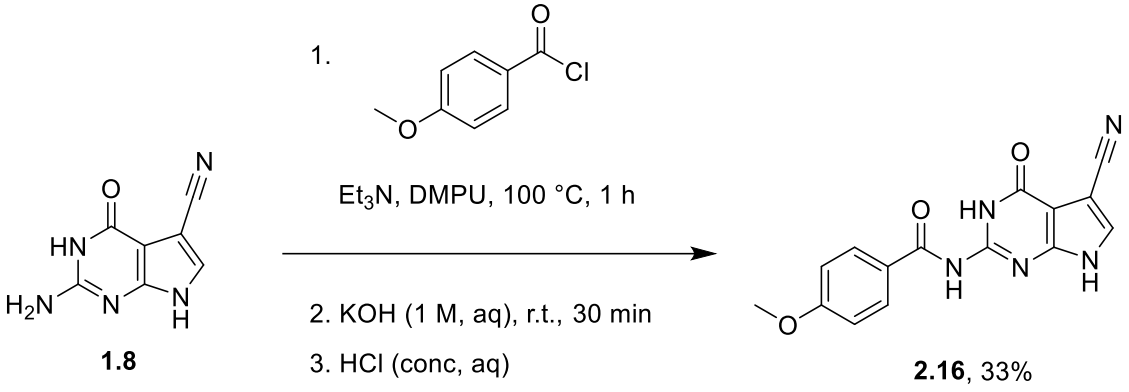

***Scheme 2.10**. Successful synthesis of **2.16**.*

2.3.4. Synthesis of preQ$_0$ analogues with electrophilic substituents

The following step in the project was to synthesise electrophilic analogues **2.17** – **2.22**. Given the reactive nature of the side-chains, we anticipated some issues with their synthesis. However, we found that cooling the initial amide-forming reactions to 0 °C and adopting either the KOH or NH_3 based work-ups as appropriate we were able to isolate all the desired compounds (**Scheme 2.11**). In some cases, the time and concentrations used for the work-ups had to be adjusted to achieve satisfactory purity and yield.

Reagent	Structure	Work-up (**x**)
A	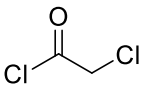	KOH (0.25 M), r.t., 1 h
B	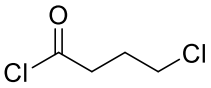	NH_3 (2 N, MeOH), r.t., 2 h
C	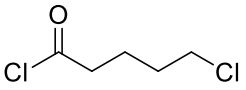	KOH (1 M, aq), r.t., 30 min
D	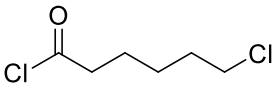	NH_3 (2 N, MeOH), r.t., 4 h
E	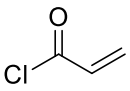	KOH (0.5 M, aq), r.t., 1.5 h
F	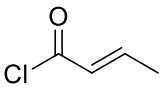	NH3 (1 N, MeOH), r.t., 2 h

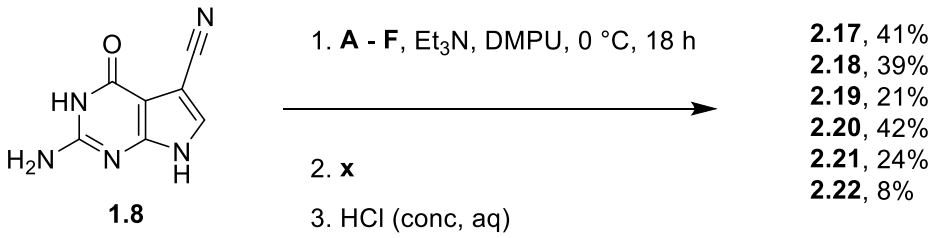

Scheme 2.11*. The successful synthesis of* ***2.17*** *–* ***2.22****. A variety of work-up conditions were employed for each reaction.*

2.4. Biological assays

Following the synthesis of the library of analogues, the compounds were submitted to a series of viability assays to investigate their effect on cancer cell growth. The cells studied were the human epithelial mammary cancer cell line MDA-MB-231 and were grown in queuine-free conditions to induce queuine hypomodification.

An alamarBlue assay was performed on the cell line using **2.4**, **2.7** – **2.22** and $PreQ_0$ (**1.8**) (**Figure 2.4**). The cells were treated for 72 h and the assay was performed twice to confirm the reproducibility of the results.

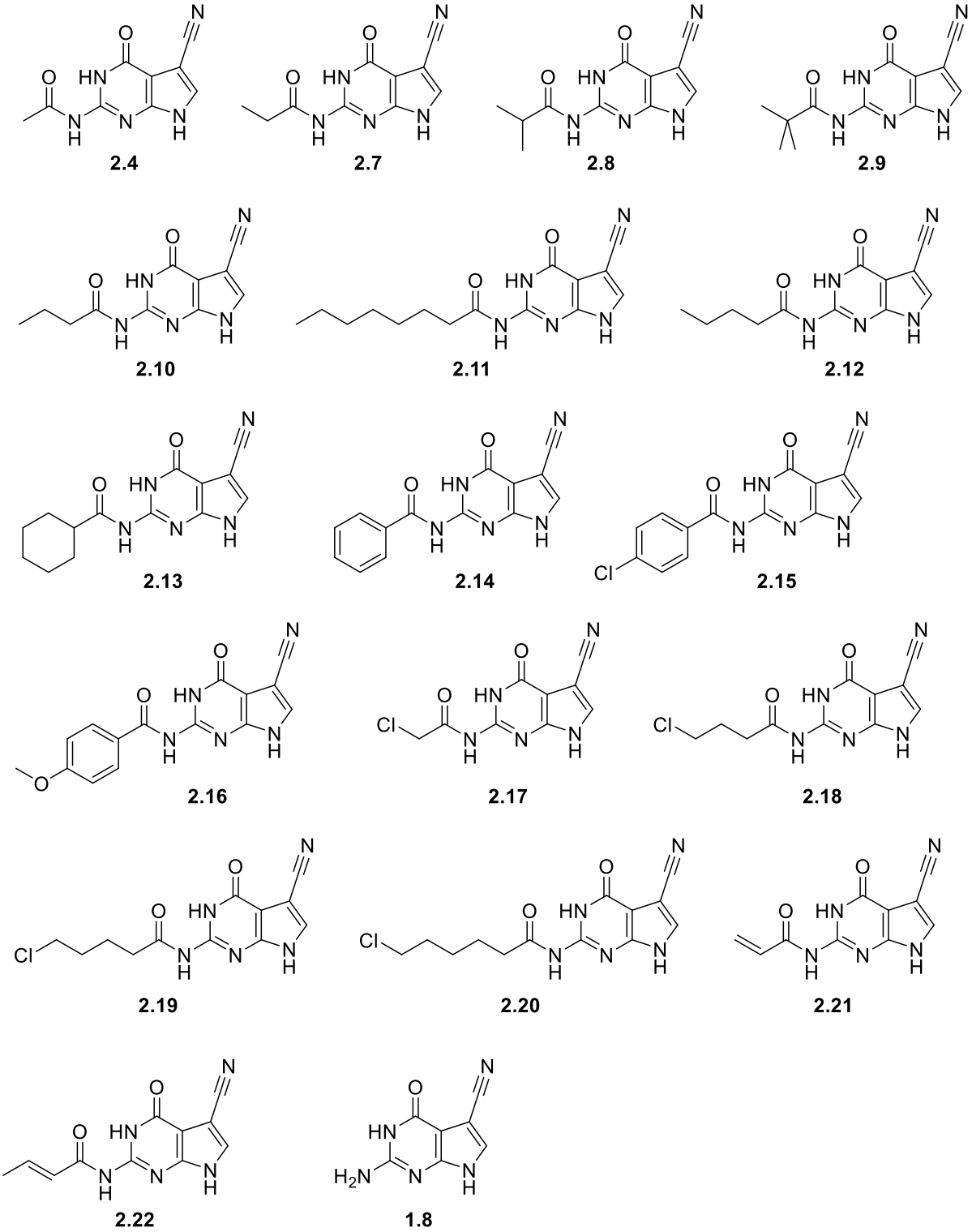

***Figure 2.4**. List of compounds assessed against MDA-MB-231 cancer cells, **2.4, 2.7** – **2.22** and **1.8**.*

The alamarBlue assay uses a non-cytotoxic fluorescent blue dye, resazurin (**2.23**), as indicator of cell viability. The dye is reduced to the pink-coloured resorufin (**2.24**) by the reductive metabolism of cells by a variety of reducing species, one of them being NADH in the presence of NADH dehydrogenase (**Scheme 2.12**).[56] Comparison of emission values at 590 nm between control and treated wells yields quantitative viability data.[57]

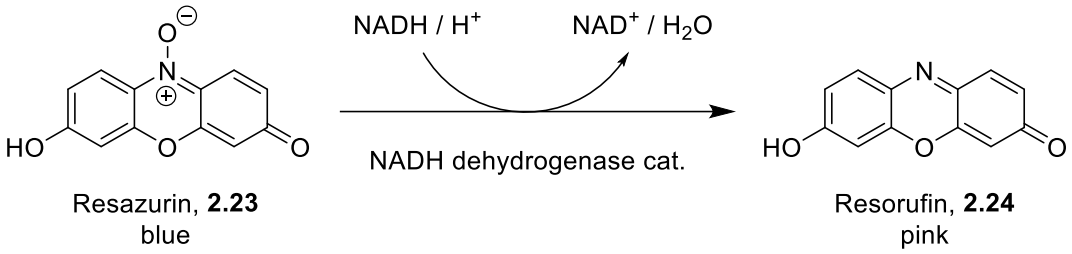

Scheme 2.12. *The reduction of resazurin to resorufin by the reductive metabolism of cells.*

The results for the alamarBlue assays are reported in **Figure 2.5** and **Table 2.2** below. Immediately noticeable is that many of the viability values obtained are above 100%. These perplexing results initially suggest that the compounds used to treat the cells promote the growth of MDA-MB-231 cells. Interestingly, a trend observed for almost all compounds is that viability decreases as concentration of queuine analogues increases.

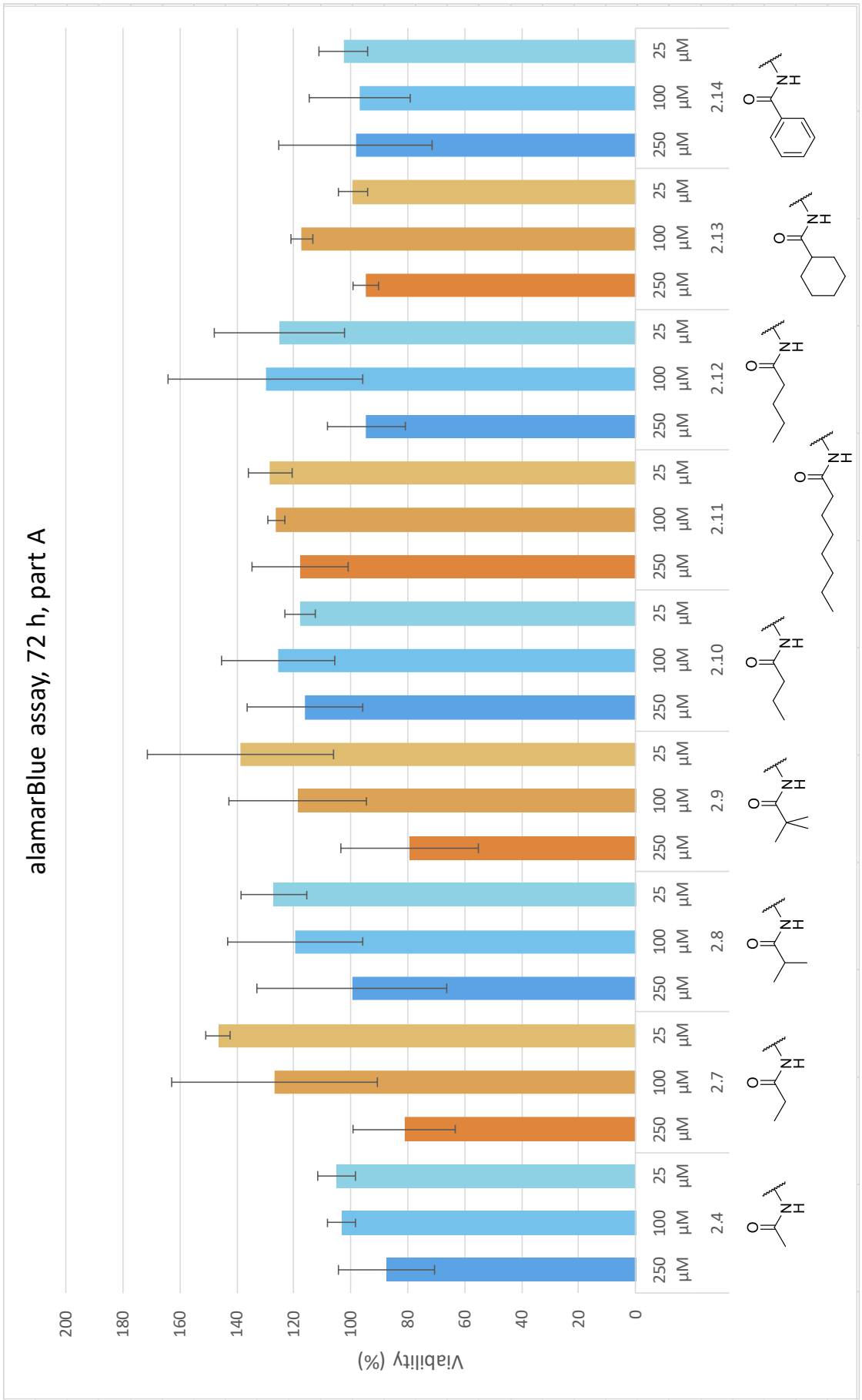
alamarBlue assay, 72 h, part A
Viability (%)
0
20
40
60
80
100
120
140
160
180
200
2.4
2.7
2.8
2.9
2.10
2.11
2.12
2.13
2.14
25 µM
100 µM
250 µM

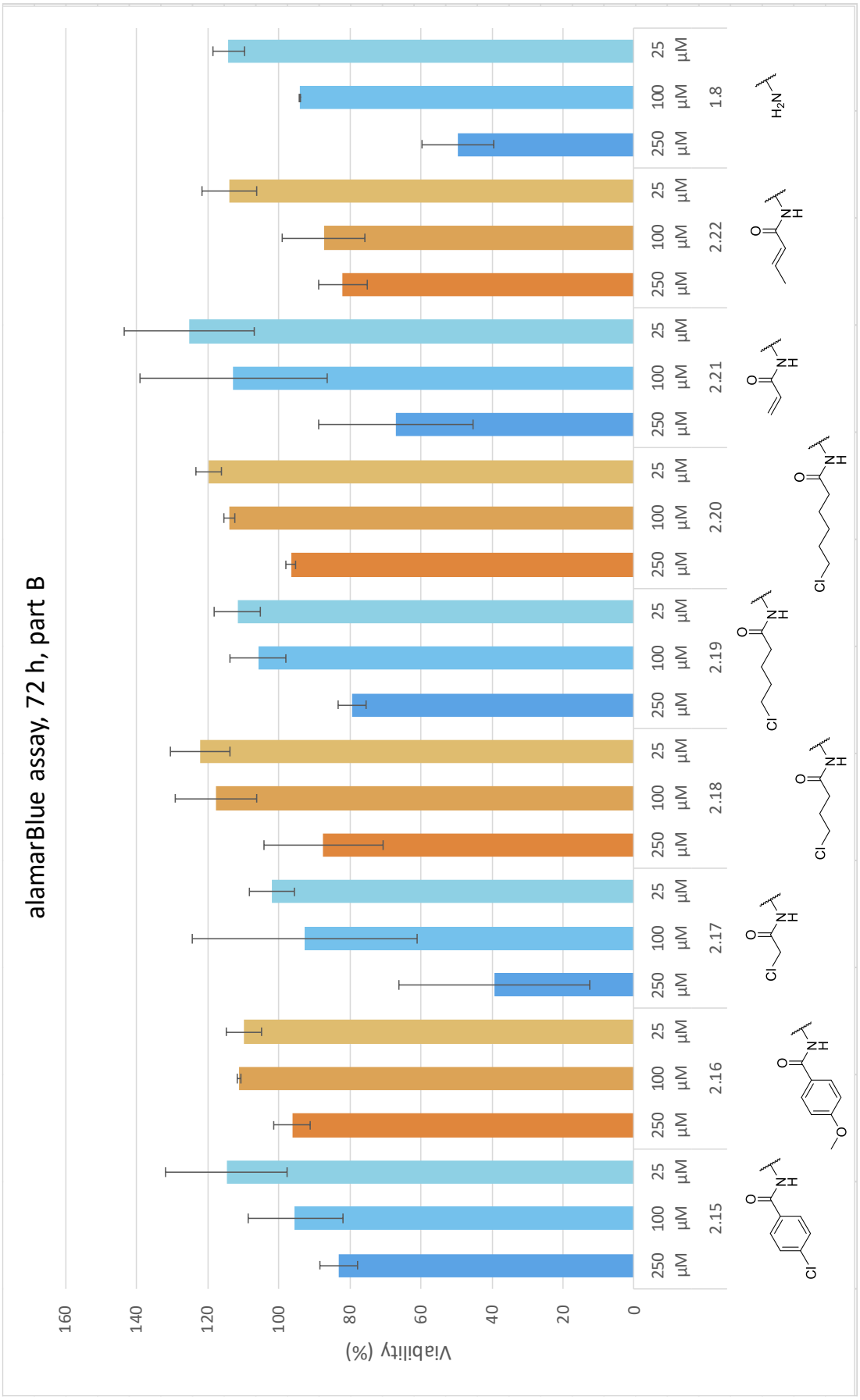

***Figure 2.5**. Inhibition of growth of MDA-MB-231 cells by queuine analogues in alamarBlue assay*

Table 2.2. *Inhibition of growth of MDA-MB-231 cells by queuine analogues in alamarBlue assay*

Compound n°	Percent viability of MDA-MB-231 cells		
	25 µM	100 µM	250 µM
2.4	105	103	87
2.7	147	127	81
2.8	127	120	100
2.9	139	119	79
2.10	118	126	116
2.11	128	126	118
2.12	125	130	95
2.13	99	117	96
2.14	103	97	95
2.15	115	95	83
2.16	110	111	98
2.17	102	93	39
2.18	122	118	87
2.19	112	106	76
2.20	120	114	97
2.21	125	113	67
2.22	114	87	82
1.8	114	94	50

The assays were repeated numerous times, using different incubation times and fresh compound dilutions, medium, cells and resazurin. However, each time the results obtained yielded similar results to **Table 2.2**, with all compounds seemingly increasing the viability of cancer cells.

An alternative hypothesis was put forward to rationalise these results. It was suggested that the compounds were interfering with one or some of the species involved in the reductive metabolism, *e.g.* NADH dehydrogenase. The quantitative nature of the alamarBlue assay is based on the assumption that the cells' reductive metabolism and viability is proportional, which could be incorrect in this case. The analogues' effect on cell metabolism could be the focus of future studies but was deemed out of scope for this project.

A different methodology that did not rely on cell metabolism was used. A Hoechst assay with fluorescent dye Hoechst 33258 was performed. The Hoechst 33258 dye (**2.25**, **Figure 2.6**) has an emission wavelength of 460 nm and exhibits fluorescence enhancement upon binding to A-T rich regions of double stranded DNA. Comparison of emission between the controls, blanks and treated wells provide quantitative cell viability values.[58,59]

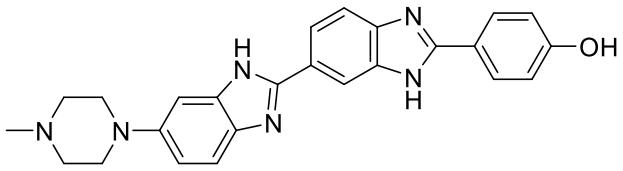

Hoechst 33258, **2.25**

Figure 2.6*. Chemical structure of Hoechst 33258 dye.*

The results of the assay with Hoechst 33258 are reported in **Figure 2.7** and **Table 2.3** below.

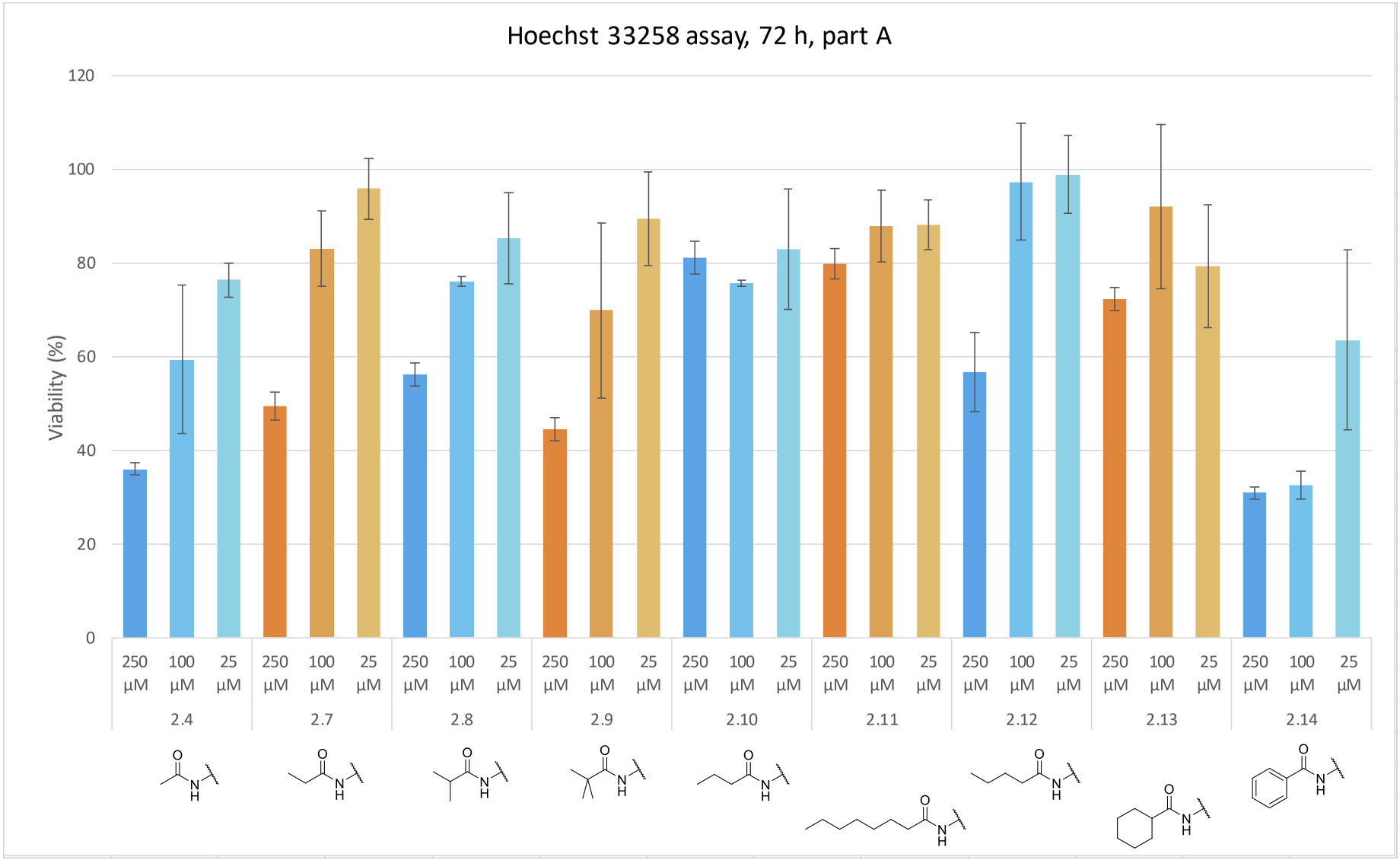
Hoechst 33258 assay, 72 h, part A
Viability (%)
120
100
80
60
40
20
0
250 µM
100 µM
25 µM
2.4
2.7
2.8
2.9
2.10
2.11
2.12
2.13
2.14

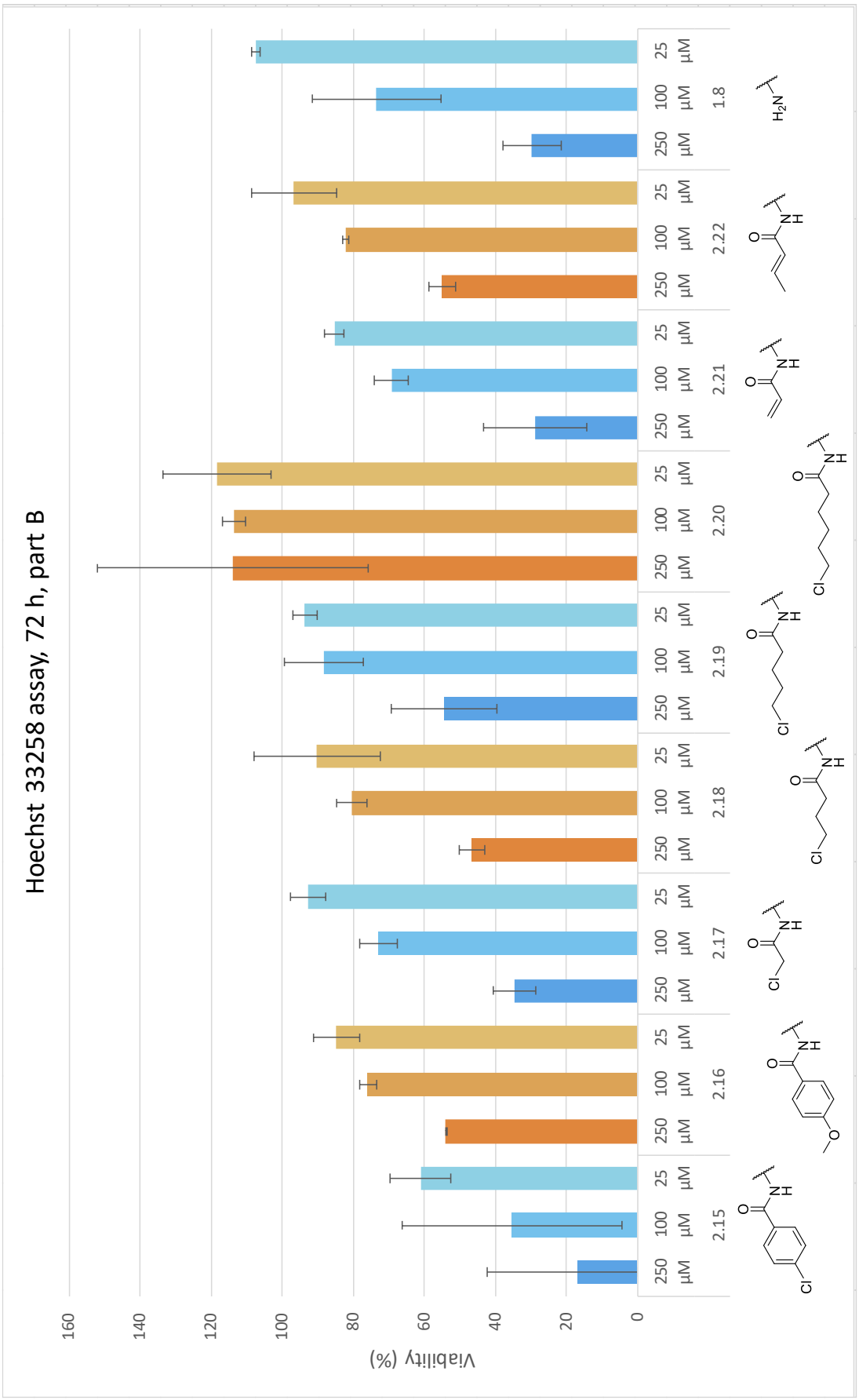

Figure 2.7. *Inhibition of growth of MDA-MB-231 cells by queuine analogues in Hoechst assay*

Table 2.3. *Inhibition of growth of MDA-MB-231 cells by queuine analogues in Hoechst assay*

Compound n°	Percent viability of MDA-MB-231 cells		
	25 µM	100 µM	250 µM
2.4	76	59	36
2.7	96	83	49
2.8	85	76	56
2.9	90	70	45
2.10	83	76	81
2.11	88	88	80
2.12	99	97	57
2.13	79	92	72
2.14	64	33	31
2.15	61	35	17
2.16	85	76	54
2.17	93	73	35
2.18	90	80	46
2.19	94	88	54
2.20	118	114	114
2.21	85	69	29
2.22	97	82	55
1.8	107	73	30

The compounds with the strongest inhibitory effect were **2.4**, **2.14** and **2.15**, with 61 – 76% viability at 250 µM and 17 – 36% viability at 25 µM. Aromatic analogues **2.14** – **2.16** showed good inhibition overall and **2.14** and **2.15** had the strongest inhibitory effect of all compounds at 25 µM (64% and 61%, respectively). Aliphatic analogues **2.4** and **2.7** – **2.13** showed varying degrees of inhibition. Compounds containing a short or branched alkyl side-chain (**2.4**, **2.7** – **2.9**) had a consistent dose-effect correlation with low inhibition at 25 µM and modest inhibition at 250 µM (36 – 56% viability). The remaining aliphatic analogues (**2.10** – **2.13**) had weak inhibition overall and did not show a correlation between concentration and viability.

All electrophilic analogues except **2.20** had good dose-dependent viability values similar to small alkyl analogues **2.4** and **2.7** – **2.9**. For chloroalkanes **2.17** – **2.19**, the inhibitory effect

increases as the chain length decreases. The same chain length trend is observed for Michael acceptors **2.21** and **2.22**. The shorter-chained electrophilic analogues **2.17** and **2.21** had good inhibition at higher concentrations (35% and 29% viability at 250 µM, respectively) with values comparable to the short chain alkyl analogues, **2.4** and **2.7** – **2.9**. Surprisingly, compound **2.20** gave rise to viability values over 100% across all concentrations and did not follow the trend of the other chloroalkanes. It is yet to be determined if these results are an anomaly or if **2.20** encourages cancer growth.

$PreQ_0$ (**1.8**) exhibited the highest variation across concentration of all compounds with 107% at 25 µM, 73% at 100 µM and 30% at 250 µM. $PreQ_0$ appeared to promote cancer growth at low concentrations while having an inverse effect at higher concentrations. The cytotoxic effect of $preQ_0$ has been observed before in a study by Kui Hong *et al*[60] where the molecule induced a growth inhibition of 62% in HeLa cells (38% viability) and 57% in HepG2 cells (43% viability) at the concentration of 1142 µM after a 24 h incubation. However, to the best of the author's knowledge, the increase in viability caused by $preQ_0$ at 25 µM has not been reported in the scientific literature and deserves further investigation.

3. Conclusion

A new and efficient synthetic method for the functionalisation of the 2-position on $preQ_0$ was successfully developed. This new synthesis allows for shorter reaction times over the previous method and employs a faster and more reliable purification method with trituration in methanol. Different hydrolysis conditions were explored and the work-up was optimised for the selective cleavage of amides at the 7-position.

Novel $preQ_0$ analogues **2.4** and **2.7** – **2.22** were synthesised by using the newly-developed method. The compounds were assessed against the MDA-MB-231 cancer cell line in alamarBlue and Hoechst assays. Compounds **2.4**, **2.14** and **2.15** were found to strongly inhibit cancer cell growth in the cell line, especially at higher concentrations. $PreQ_0$ was included in the assays alongside the library of analogues and was seen to increase viability at low concentrations and decrease viability at higher concentrations.

The assay results showed that $preQ_0$ analogues containing small alkyl side-chains or aromatic moieties at the 2-position inhibited MDA-MB-231 cell growth the most. Short-chain electrophilic substituents were found to have comparable inhibition to their alkane counterparts. Future work could be aimed at determining whether employing electrophilic or unfunctionalised side-chains is the best strategy in the development of anticancer compounds.

The aromatic analogues offered the strongest inhibition at lower concentrations and excellent inhibition at the highest concentrations. However, only three aromatic analogues were included in the assay so future efforts could focus on creating an expanded library of aromatic compounds, possibly including heterocycles. Furthermore, two-dimensional libraries with variation at the 2- and 5-position could be explored to determine if position 5 can contribute to the cytotoxicity of the compounds. Future studies could also aim to functionalise $preQ_0$ with amine bonds rather than the amide bonds explored in this project. Finally, running compounds **2.4**, **2.7** – **2.22** and **1.8** in identical Hoechst assays against healthy human cells could determine if their activity is selective towards cancer cells.

4. Experimental

4.1. General indications

All reactions were carried out under argon atmosphere. Unless specified otherwise, all solvents and reagents were used without prior purification and were of reagent or technical grade. The hexane used was of HPLC grade. Anhydrous THF was acquired from an encapsulated solvent purification system. Pyridine and triethylamine were distilled over calcium hydride before use. The concentrated hydrochloric acid used was 36% w/v. All glassware was oven-dried at 250 °C overnight prior to each procedure.

^{1}H NMR and ^{13}C NMR were performed on a 400 MHz Agilent spectrometer at the frequency indicated on the reported spectroscopic data and all samples were analysed in DMSO-d_6 relative to residual solvent peaks (δH = 2.50 ppm; δC = 39.51 ppm). All ^{13}C NMR experiments were ran with proton decoupling on. Additional 2D NMR experiments can be found in the Appendix. Infra-red spectra were obtained as neat solids from a Perkin-Elmer attenuated total reflectance (ATR) Fourier-transform IR (FTIR) spectrometer and only significant absorptions are presented. Melting points were recorded on a Griffin melting point apparatus and readings obtained are uncorrected. High-resolution mass spectrometry experiments were carried out by the Mass Spectrometry Unit of the School of Chemistry of the University of Dublin TCD using 1% DMSO in methanol as solvent.

4.2. Synthetic procedures

4.2.1. Synthesis of 2-chloro-3-oxopropanenitrile (2.2)

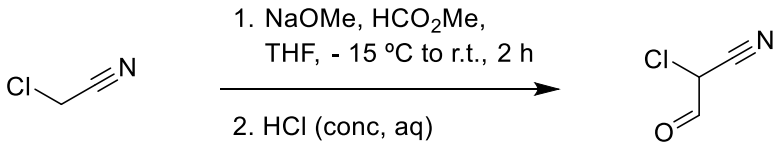

Sodium methoxide (7.14 g, 132.00 mmol) was added to a two-neck 1 L flask containing anhydrous tetrahydrofuran. The resulting suspension was flushed with argon and cooled to -15 °C in an ice-acetone bath. Methyl formate (9.00 mL, 147.00 mmol) was added dropwise to the solution over 10 min. The reaction mixture was left to stir for 20 min, after which chloroacetonitrile (8.30 mL, 132.00 mmol) was added dropwise over 2 h. The reaction was

cooled to 0 °C and concentrated hydrochloric acid (12.0 mL) was added dropwise to the reaction mixture, causing its colour to change from yellow to bright red and a white precipitate to appear. The crude suspension was filtered through celite and the filtrate was concentrated *in vacuo*, yielding a brown oil. The oil was used immediately and without further purification in the synthesis of **1.8**.

4.2.2. Synthesis of 7-cyano-7-deazaguanine (preQ$_0$) (1.8)

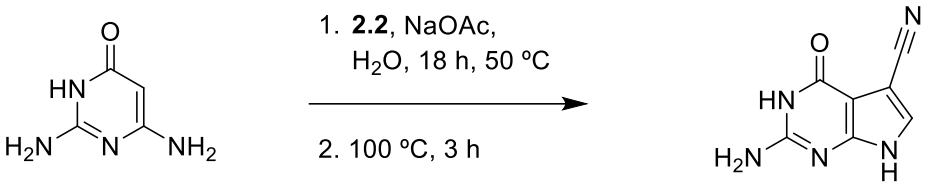

Sodium acetate (4.35 g, 53.0 mmol) and 2,4-diamino-6-hydroxypyrimidine (5.35 g, 44.4 mmol) in water (0.6 M) were stirred together at 50 °C in a 1 L round bottom flask. Then, a solution of 2-chloro-3-oxopropanenitrile in water (0.07 g/mL) was added dropwise to the reaction mixture over 30 min. The resulting suspension was stirred for 18 h at 50 °C, which caused it to become cream-coloured. The reaction mixture was then heated to 100 °C for 3 h and the mixture was allowed to cool to room temperature before being filtered *in vacuo*. The filtered solid was washed with water (100 mL) followed by acetone (100 mL). The isolated solids were then dissolved in aqueous potassium hydroxide (20 g/L, 200 mL), resulting in a brown solution. The solution was treated with activated charcoal (10 g) and left to stir for 30 min. The charcoal was removed by filtration and the filtrate was cooled to 0 °C and acidified to pH 2 with concentrated hydrochloric, causing a pale cream precipitate to form. The suspension was then filtered and the solid was dried using azeotropic distillation with toluene and methanol. The resulting waxy pellets were crushed with mortar and pestle and dried in a desiccator, affording a pale cream amorphous solid (4.22 g, 57%).

^{1}H NMR (400 MHz, dmso) δ 11.99 (s, 1H), 10.78 (s, 1H), 7.57 (d, *J* = 2.4 Hz, 1H), 6.50 (s, 2H).

The spectroscopic data is consistent with the scientific literature.[49-52]

4.2.3. Synthesis of *N*-(5-cyano-4-oxo-4,7-dihydro-3*H*-pyrrolo[2,3-*d*]pyrimidin-2-yl)acetamide (2.4)

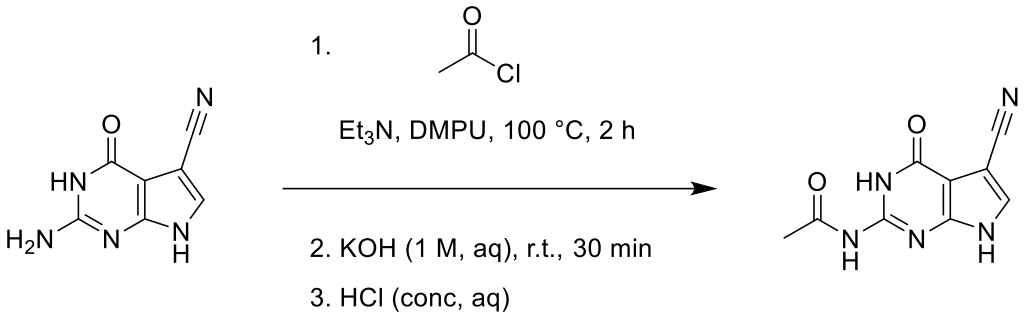

A suspension of 7-cyano-7-deazaguanine (150 mg, 0.856 mmol) in anhydrous DMPU (5 mL) in a 50 mL round bottom flask was treated with distilled triethylamine (0.48 mL, 3.426 mmol). The mixture was cooled to 0 °C in an ice bath, after which distilled acetyl chloride (0.24 mL, 3.426 mmol) was added dropwise to the mixture. The reaction was then heated to 100 °C for 2 h, after which ^{1}H NMR analysis indicated full consumption of the starting material. The reaction mixture was allowed to cool to room temperature and was treated with aqueous potassium hydroxide (1 M, 5 mL) and left to stir for 30 min. Then, the mixture was acidified to pH 2 with concentrated hydrochloric acid, causing a precipitate to form which was collected *via* vacuum filtration. The collected solids were triturated in methanol (5 mL) for 30 min and filtered under vacuum and the process was repeated once more, affording a light brown powder (119 mg, 64%).

^{1}H NMR (400 MHz, dmso) δ 12.65 (s, 1H), 11.95 (s, 1H), 11.58 (s, 1H), 7.92 (d, *J* = 2.7 Hz, 1H), 2.17 (s, 3H).

^{13}C NMR (101 MHz, dmso) δ 173.5, 155.5, 148.5, 148.1, 130.1, 115.2, 102.9, 86.2, 23.8.

HRMS (ESI) exact mass calculated for [$C_9H_7N_5O_2$] requires *m*/*z* 217.0600, found *m*/*z* 216.0528 [M - H]$^{-}$

FTIR (ν_{max}, cm^{-1}) 3142, 2975, 2230 (C≡N st.), 1632, 1248

M.p. >300 °C

4.2.4. Synthesis of *N*-(5-cyano-4-oxo-4,7-dihydro-3*H*-pyrrolo[2,3-*d*]pyrimidin-2-yl)propionamide (2.7)

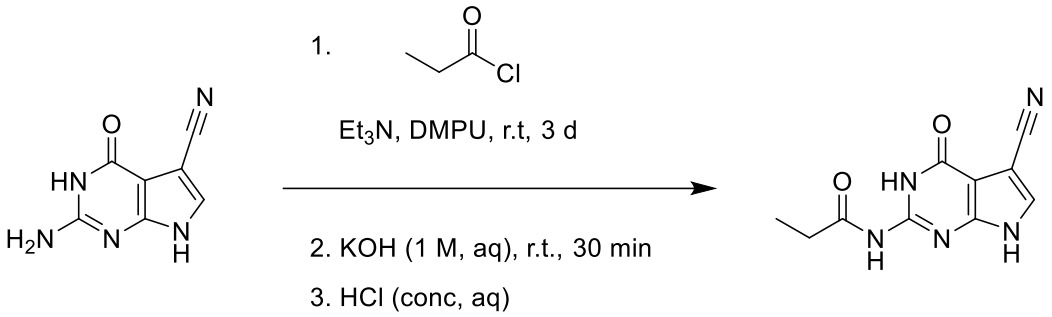

A suspension of 7-cyano-7-deazaguanine (150 mg, 0.856 mmol) in anhydrous DMPU (5 mL) in a 50 mL round bottom flask was treated with distilled triethylamine (0.48 mL, 3.426 mmol). Distilled propionyl chloride (0.30 mL, 3.426 mmol) was then added dropwise to the mixture. The reaction was then left to stir at room temperature for 3 d, after which ^{1}H NMR analysis indicated full consumption of the starting material. The reaction mixture was treated with aqueous potassium hydroxide (1 M, 5 mL) and left to stir for 30 min. Then, the mixture was acidified to pH 2 with concentrated hydrochloric acid, causing a precipitate to form which was collected *via* vacuum filtration. The collected solids were triturated in a 1:1 mixture of methanol and dichloromethane (5 mL) for 30 min and filtered under vacuum, affording an off-white powder (33 mg, 17%).

^{1}H NMR (400 MHz, dmso) δ 12.64 (s, 1H), 11.97 (s, 1H), 11.53 (s, 1H), 7.92 (s, 1H), 2.46 (q, *J* = 7.5 Hz, 2H), 1.07 (t, *J* = 7.5 Hz, 3H).

^{13}C NMR (101 MHz, dmso) δ 177.0, 155.5, 148.6, 148.1, 130.1, 115.2, 102.9, 86.2, 29.3, 8.7.

HRMS (ESI) exact mass calculated for [$C_{10}H_9N_5O_2$] requires *m*/*z* 231.0756, found *m*/*z* 230.0689 [M - H]$^{-}$

FTIR (ν_{max}, cm^{-1}) 3184, 2948, 2228 (C≡N st.), 1630, 1248

M.p. >300 °C

4.2.5. Synthesis of *N*-(5-cyano-4-oxo-4,7-dihydro-3*H*-pyrrolo[2,3-*d*]pyrimidin-2-yl)isobutyramide (2.8)

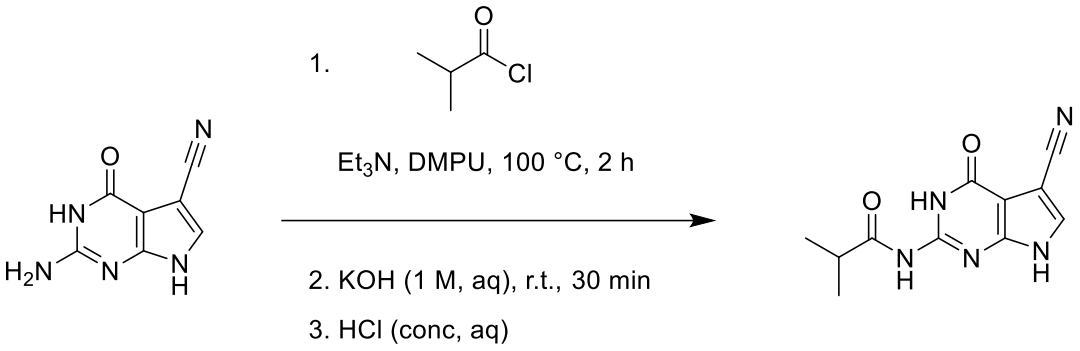

A suspension of 7-cyano-7-deazaguanine (75 mg, 0.428 mmol) in anhydrous DMPU (1 mL) in a 10 mL microwave vial was treated with distilled triethylamine (0.24 mL, 1.712 mmol). Distilled isobutyryl chloride (0.18 mL, 1.712 mmol) was then added dropwise to the mixture. The reaction was then heated to 100 °C for 2 h, after which ^{1}H NMR analysis indicated full consumption of the starting material. The reaction mixture was allowed to cool to room temperature and was treated with aqueous potassium hydroxide (1 M, 1 mL) and left to stir for 30 min. Then, the mixture was acidified to pH 2 with concentrated hydrochloric acid, causing a precipitate to form which was collected *via* vacuum filtration. The collected solids were triturated in methanol (5 mL) for 10 min and filtered under vacuum, affording a white powder (43 mg, 41%).

^{1}H NMR (400 MHz, dmso) δ 12.63 (s, 1H), 11.99 (s, 1H), 11.55 (s, 1H), 7.92 (s, 1H), 2.76 (hept, *J* = 6.8 Hz, 1H), 1.11 (d, *J* = 6.8 Hz, 6H).

^{13}C NMR (101 MHz, dmso) δ 180.3, 155.7, 148.6, 148.3, 130.3, 115.3, 103.0, 86.4, 34.9, 19.0.

HRMS (ESI) exact mass calculated for [$C_{11}H_{11}N_5O_2$] requires *m*/*z* 245.0913, found *m*/*z* 246.0988 $[M + H]^+$

FTIR (ν_{max}, cm^{-1}) 3203, 2946, 2225 (C≡N st.), 1643, 1246

M.p. >300 °C

4.2.6. Synthesis of *N*-(5-cyano-4-oxo-4,7-dihydro-3*H*-pyrrolo[2,3-*d*]pyrimidin-2-yl)pivalamide (2.9)

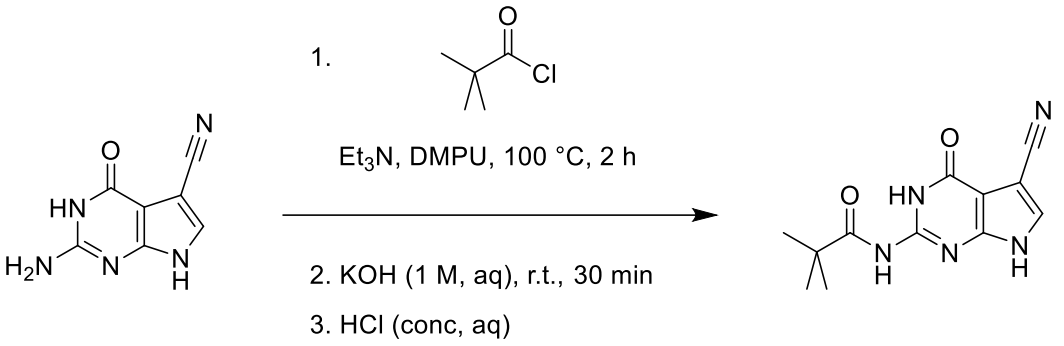

A suspension of 7-cyano-7-deazaguanine (75 mg, 0.428 mmol) in anhydrous DMPU (1 mL) in a 10 mL microwave vial was treated with distilled triethylamine (0.24 mL, 1.712 mmol). Distilled pivaloyl chloride (0.21 mL, 1.712 mmol) was added dropwise to the mixture. The reaction was then heated to 100 °C for 2 h, after which ^{1}H NMR analysis indicated full consumption of the starting material. The reaction mixture was allowed to cool to room temperature and was treated with aqueous potassium hydroxide (1 M, 1 mL) and left to stir for 30 min. Then, the mixture was acidified to pH 2 with concentrated hydrochloric acid, causing a precipitate to form which was collected *via* vacuum filtration. The collected solids were triturated in methanol (5 mL) for 10 min and filtered under vacuum, affording an off-white powder (31 mg, 28%).

^{1}H NMR (400 MHz, dmso) δ 12.56 (s, 1H), 12.10 (s, 1H), 10.98 (s, 1H), 7.94 (s, 1H), 1.24 (s, 9H).

^{13}C NMR (101 MHz, dmso) δ 181.2, 155.8, 148.5, 148.5, 130.3, 115.2, 103.1, 86.3, 40.1, 26.3.

HRMS (ESI) exact mass calculated for [$C_{12}H_{13}N_5O_2$] requires *m*/*z* 259.1069, found *m*/*z* 260.1138 $[M + H]^+$

FTIR (ν_{max}, cm^{-1}) 3180, 2972, 2228 (C≡N st.), 1648, 1240

M.p. >300 °C

4.2.7. Synthesis of *N*-(5-cyano-4-oxo-4,7-dihydro-3*H*-pyrrolo[2,3-*d*]pyrimidin-2-yl)butyramide (2.10)

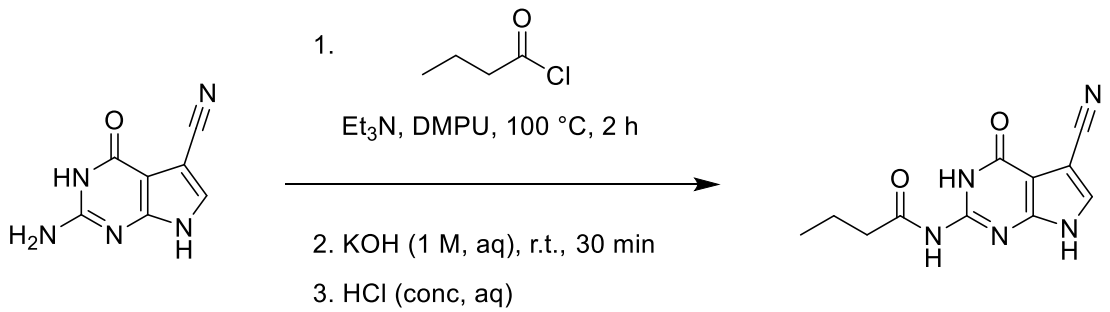

A suspension of 7-cyano-7-deazaguanine (75 mg, 0.428 mmol) in anhydrous DMPU (1 mL) in a 10 mL microwave vial was treated with distilled triethylamine (0.24 mL, 1.712 mmol). Distilled butyryl chloride (0.18 mL, 1.712 mmol) was then added dropwise to the mixture. The reaction was then heated to 100 °C for 2h, after which ^{1}H NMR analysis indicated full consumption of the starting material. The reaction mixture was allowed to cool to room temperature before being treated with aqueous potassium hydroxide (1 M, 1 mL) and was left to stir for 30 min. Then, the mixture was acidified to pH 2 with concentrated hydrochloric acid, causing a precipitate to form which was collected *via* vacuum filtration. The collected solids were triturated in methanol (5 mL) for 10 min and filtered under vacuum, affording an off-white powder (67 mg, 64%).

^{1}H NMR (400 MHz, dmso) δ 12.64 (s, 1H), 11.99 (s, 1H), 11.55 (s, 1H), 7.92 (s, 1H), 2.43 (t, *J* = 7.3 Hz, 2H), 1.61 (h, *J* = 7.3 Hz, 2H), 0.91 (t, *J* = 7.3 Hz, 3H).

^{13}C NMR (101 MHz, dmso) δ 176.2, 155.5, 148.5, 148.1, 130.1, 115.2, 102.9, 86.2, 37.8, 17.9, 13.4.

HRMS (ESI) exact mass calculated for [$C_{11}H_{11}N_5O_2$] requires *m*/*z* 245.0913, found *m*/*z* 246.0988 $[M + H]^+$

FTIR (ν_{max}, cm^{-1}) 3172, 2972, 2234 (C≡N st.), 1626, 1245

M.p. >300 °C

4.2.8. Synthesis of *N*-(5-cyano-4-oxo-4,7-dihydro-3*H*-pyrrolo[2,3-*d*]pyrimidin-2-yl)octanamide (2.11)

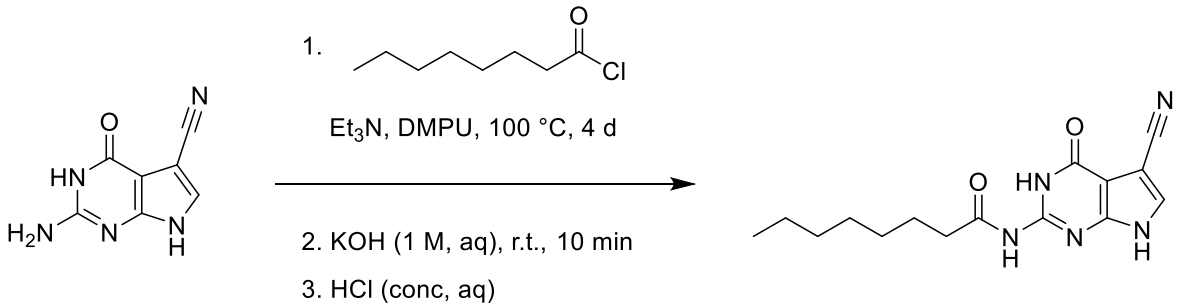

A suspension of 7-cyano-7-deazaguanine (75 mg, 0.428 mmol) in anhydrous DMPU (2.5 mL) in a 10 mL microwave vial was treated with distilled triethylamine (0.24 mL, 1.712 mmol). Distilled octanoyl chloride (0.29 mL, 3.426 mmol) was then added dropwise to the mixture. The reaction was then heated to 100 °C for 4 h, after which ^{1}H NMR analysis indicated full consumption of the starting material. The reaction mixture was allowed to cool to room temperature, treated with aqueous potassium hydroxide (1 M, 2.5 mL) and left to stir for 30 min. Then, the mixture was acidified to pH 2 with concentrated hydrochloric acid, causing a precipitate to form which was collected *via* vacuum filtration. The collected solids were triturated in methanol (5 mL) for 10 min and filtered under vacuum, affording an off-white powder (17 mg, 13%).

^{1}H NMR (400 MHz, dmso) δ 12.64 (s, 1H), 11.98 (s, 1H), 11.54 (s, 1H), 7.92 (d, *J* = 2.6 Hz, 1H), 2.44 (t, *J* = 7.4 Hz, 2H), 1.63 – 1.53 (m, 2H), 1.34 – 1.20 (m, 8H), 0.91 – 0.82 (m, *J* = 6.9 Hz, 3H).

^{13}C NMR (101 MHz, dmso) δ 176.4, 155.5, 148.5, 148.1, 130.1, 115.2, 102.9, 86.2, 35.9, 31.1, 28.3, 24.3, 22.0, 13.9.

HRMS (ESI) exact mass calculated for [$C_{15}H_{19}N_5O_2$] requires *m*/*z* 301.1539, found *m*/*z* 300.1471 $[M - H]^-$

FTIR (ν_{max}, cm^{-1}) 3140, 2931, 2867, 2232 (C≡N st.), 1651, 1246

M.p. >300 °C

4.2.9. Synthesis of *N*-(5-cyano-4-oxo-4,7-dihydro-3*H*-pyrrolo[2,3-*d*]pyrimidin-2-yl)pentanamide (2.12)

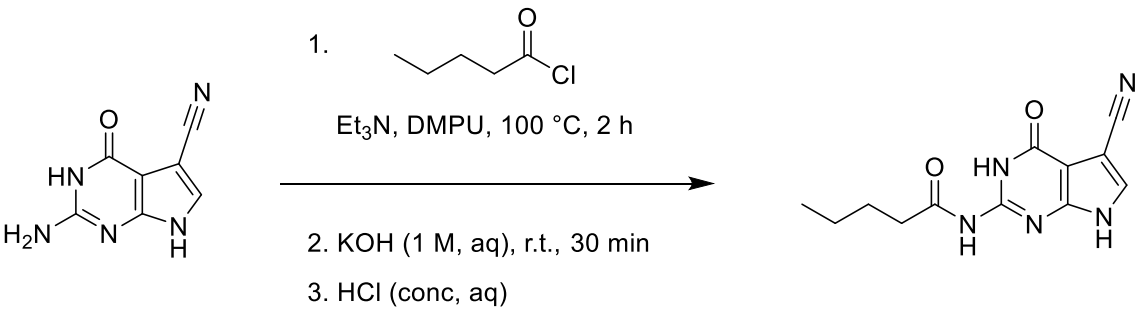

A suspension of 7-cyano-7-deazaguanine (75 mg, 0.428 mmol) in anhydrous DMPU (1 mL) in a 10 mL microwave vial was treated with distilled triethylamine (0.24 mL, 1.712 mmol). Valeroyl chloride (0.20 mL, 1.712 mmol) was then added dropwise to the mixture. The reaction was then heated to 100 °C for 2 h, after which ^{1}H NMR analysis indicated full consumption of the starting material. The reaction mixture was allowed to cool to room temperature and was treated with aqueous potassium hydroxide (1 M, 1 mL) and left to stir for 30 min. Then, the mixture was acidified to pH 2 with concentrated hydrochloric acid, causing a precipitate to form which was collected *via* vacuum filtration. The collected solids were triturated in methanol (5 mL) for 10 min and filtered under vacuum, affording a white powder (29 mg, 21%).

^{1}H NMR (400 MHz, dmso) δ 12.67 (s, 1H), 11.99 (s, 1H), 11.55 (s, 1H), 7.90 (d, *J* = 2.6 Hz, 1H), 2.45 (t, *J* = 7.4 Hz, 2H), 1.56 (p, *J* = 7.5 Hz, 2H), 1.31 (h, *J* = 7.5 Hz, 2H), 0.88 (t, *J* = 7.3 Hz, 3H).

^{13}C NMR (101 MHz, dmso) δ 176.5, 155.7, 148.6, 148.2, 130.2, 115.3, 103.0, 86.3, 35.7, 26.6, 21.7, 13.7.

HRMS (ESI) exact mass calculated for [$C_{12}H_{13}N_5O_2$] requires *m*/*z* 259.1069, found *m*/*z* 260.1144 $[M + H]^+$

FTIR (ν_{max}, cm^{-1}) 3146, 2957, 2231 (C≡N st.), 1650, 1245

M.p. >300 °C

4.2.10. Synthesis of *N*-(5-cyano-4-oxo-4,7-dihydro-3*H*-pyrrolo[2,3-*d*]pyrimidin-2-yl)cyclohexanecarboxamide (2.13)

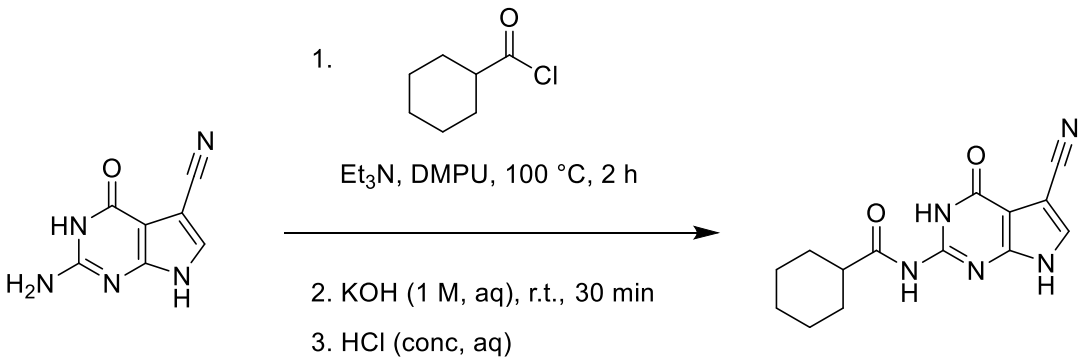

A suspension of 7-cyano-7-deazaguanine (75 mg, 0.428 mmol) in anhydrous DMPU (1 mL) in a 10 mL microwave vial was treated with distilled triethylamine (0.24 mL, 1.712 mmol). Distilled cyclohexanecarbonyl chloride (0.23 mL, 1.712 mmol) was added dropwise to the mixture. The reaction was then heated to 100 °C for 2 h, after which ^{1}H NMR analysis indicated full consumption of the starting material. The reaction mixture was allowed to cool to room temperature and was treated with aqueous potassium hydroxide (1 M, 1 mL) and left to stir for 30 min. Then, the mixture was acidified to pH 2 with concentrated hydrochloric acid, causing a precipitate to form which was collected *via* vacuum filtration. The collected solids were triturated in methanol (5 mL) for 10 min and filtered under vacuum, affording a white powder (65 mg, 53%).

^{1}H NMR (400 MHz, dmso) δ 12.63 (s, 1H), 12.00 (s, 1H), 11.50 (s, 1H), 7.91 (s, 1H), 1.82 (d, *J* = 12.0 Hz, 2H), 1.78 – 1.71 (m, *J* = 10.8 Hz, 2H), 1.66 – 1.60 (m, *J* = 7.9 Hz, 1H), 1.45 – 1.32 (m, 2H), 1.30 – 1.12 (m, 3H).

^{13}C NMR (101 MHz, dmso) δ 179.2, 155.6, 148.5, 148.3, 130.1, 115.2, 102.9, 86.2, 44.2, 28.6, 25.2, 24.9.

HRMS (ESI) exact mass calculated for [$C_{14}H_{15}N_5O_2$] requires *m*/*z* 285.1226, found *m*/*z* 284.1156 $[M - H]^-$

FTIR (ν_{max}, cm^{-1}) 3134, 2928, 2228 (C≡N st.), 1644, 1251

M.p. >300 °C

4.2.11. Synthesis of *N*-(5-cyano-4-oxo-4,7-dihydro-3*H*-pyrrolo[2,3-*d*]pyrimidin-2-yl)benzamide (2.14)

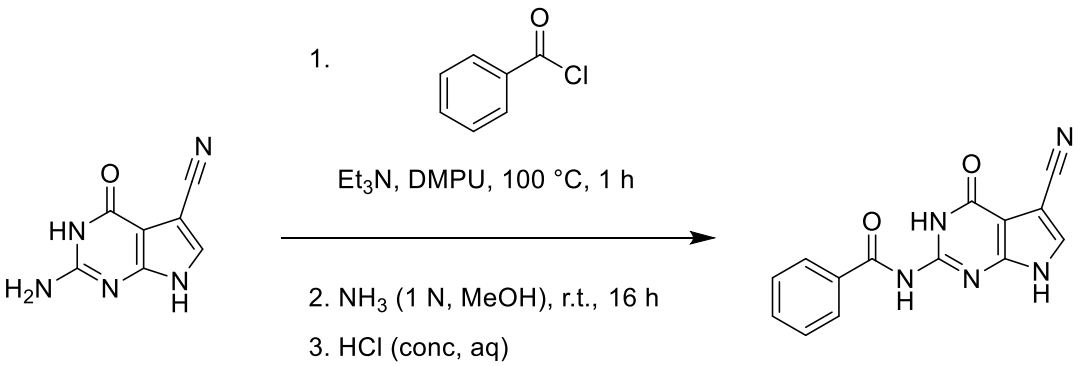

A suspension of 7-cyano-7-deazaguanine (150 mg, 0.856 mmol) in anhydrous DMPU (3 mL) in a 50 mL round bottom flask was treated with distilled triethylamine (0.48 mL, 3.426 mmol). Distilled benzoyl chloride (0.40 mL, 3.426 mmol) was added dropwise to the mixture. The reaction was then heated to 100 °C for 1 h, after which water (3 mL) was added and the suspension was transferred to a separating funnel. The solution was extracted with dichloromethane (3 x 20 mL) and the collected organics were concentrated *in vacuo*. The residue was then treated with methanolic ammonia (1 N, 3 mL) and the mixture was left to stir for 16 h. The solution was acidified to pH 2 with concentrated hydrochloric acid, causing a precipitate to form which was collected *via* vacuum filtration, affording a white powder (124 mg, 52%).

^{1}H NMR (400 MHz, dmso) δ 12.69 (s, 1H), 12.22 (s, 1H), 11.81 (s, 1H), 8.02 (d, *J* = 8.1 Hz, 3H), 7.97 (s, 1H), 7.67 (t, *J* = 7.3 Hz, 1H), 7.56 (t, *J* = 7.6 Hz, 3H).

^{13}C NMR (101 MHz, dmso) δ 169.0, 155.8, 148.4, 148.2, 133.1, 132.3, 130.4, 128.5, 128.4, 115.2, 103.4, 86.3.

HRMS (ESI) exact mass calculated for [$C_{14}H_9N_5O_2$] requires *m*/*z* 279.0756, found *m*/*z* 278.0687 $[M - H]^-$

FTIR (ν_{max}, cm^{-1}) 3173, 2229 (C≡N st.), 1669, 1252

M.p. >300 °C

4.2.12. Synthesis of 4-chloro-*N*-(5-cyano-4-oxo-4,7-dihydro-3*H*-pyrrolo[2,3-*d*]pyrimidin-2-yl)benzamide (2.15)

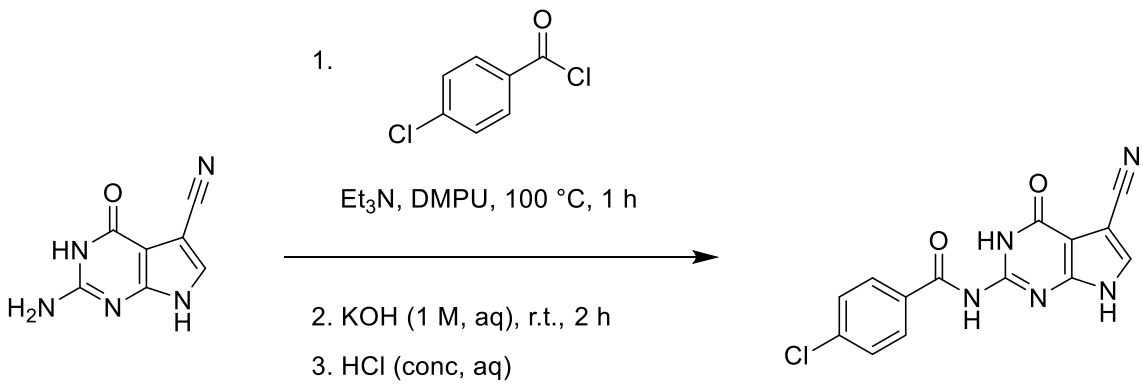

A suspension of 7-cyano-7-deazaguanine (150 mg, 0.856 mmol) in anhydrous DMPU (3 mL) in a 50 mL round bottom flask was treated with distilled triethylamine (0.48 mL, 3.426 mmol). Distilled 4-chlorobenzoyl chloride (0.44 mL, 3.426 mmol) was added dropwise to the mixture. The reaction was then heated to 100 °C for 1 h, after which aqueous potassium hydroxide (1 M, 3 mL) was added, turning the suspension into a solution. The solution was extracted with dichloromethane (3 x 20 mL) and the collected organics were concentrated *in vacuo*. The residue was then treated with aqueous potassium hydroxide (1 M, 10 mL) and left to stir for 2 h. Then, the suspension was centrifuged at 3750 rpm for 10 min and the liquid phase was collected and acidified to pH 2 with concentrated hydrochloric acid, causing a precipitate to form which was collected *via* vacuum filtration. The collected solids were triturated in methanol (5 mL) for 10 min and filtered under vacuum. This process was repeated three more times, affording a mustard powder (37 mg, 14%).

^{1}H NMR (400 MHz, dmso) δ 12.71 (s, 1H), 12.15 (s, 1H), 11.88 (s, 1H), 8.03 (d, *J* = 8.2 Hz, 2H), 7.98 (s, 1H), 7.64 (d, *J* = 8.2 Hz, 2H).

^{13}C NMR (101 MHz, dmso) δ 168.0, 155.8, 148.4, 148.0, 138.0, 131.2, 130.4, 130.4, 115.1, 103.5, 86.3.

HRMS (APCI) exact mass calculated for [$C_{14}H_8ClN_5O_2$] requires *m/z* 313.0367, found *m/z* 314.0436 $[M + H]^+$

FTIR (ν_{max}, cm^{-1}) 3347, 3173, 2237 (C≡N st.), 1651, 1262

M.p. >300 °C

4.2.13. Synthesis of *N*-(5-cyano-4-oxo-4,7-dihydro-3*H*-pyrrolo[2,3-*d*]pyrimidin-2-yl)-4-methoxybenzamide (2.16)

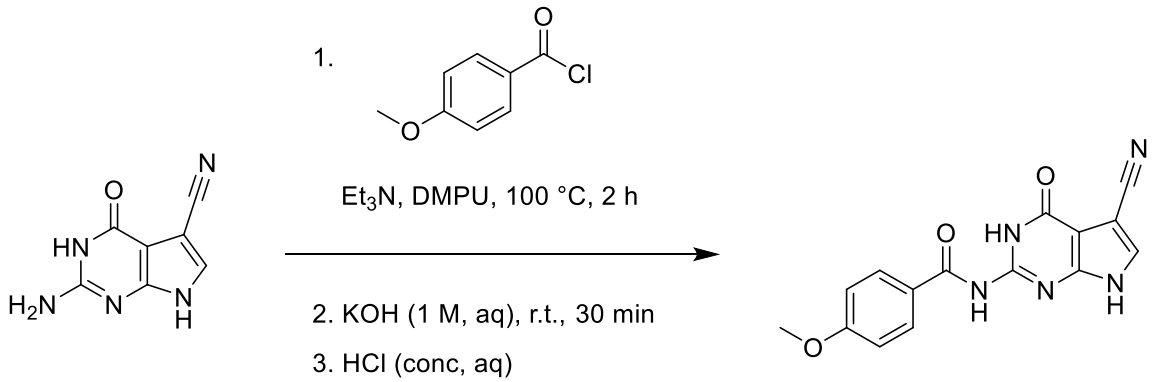

A suspension of 7-cyano-7-deazaguanine (75 mg, 0.428 mmol) in anhydrous DMPU (1 mL) in a 10 mL microwave vial was treated with distilled triethylamine (0.24 mL, 1.712 mmol). Distilled *p*-anisoyl chloride (0.23 mL, 1.712 mmol) was added dropwise to the mixture. The reaction was then heated to 100 °C for 2 h, after which ^{1}H NMR analysis indicated full consumption of the starting material. The reaction mixture was allowed to cool to room temperature and was treated with aqueous potassium hydroxide (1 M, 1 mL) and left to stir for 30 min. Then, the mixture was acidified to pH 2 with concentrated hydrochloric acid, causing a precipitate to form which was collected *via* vacuum filtration. The collected solids were triturated in methanol (5 mL) for 10 min and filtered under vacuum, affording a greenish yellow powder (43 mg, 33%).

^{1}H NMR (400 MHz, dmso) δ 12.66 (s, 1H), 12.30 (s, 1H), 11.65 (s, 1H), 8.05 (d, *J* = 8.8 Hz, 2H), 7.96 (d, *J* = 2.7 Hz, 1H), 7.08 (d, *J* = 8.8 Hz, 2H), 3.86 (s, 3H).

^{13}C NMR (101 MHz, dmso) δ 168.3, 163.2, 155.8, 148.5, 130.7, 130.3, 124.1, 115.2, 113.8, 103.3, 86.3, 55.6.

HRMS (ESI) exact mass calculated for [$C_{15}H_{11}N_5O_3$] requires *m*/*z* 309.0862, found *m*/*z* 308.0792 [M - H]$^{-}$

FTIR (ν_{max}, cm^{-1}) 3206, 2228 (C≡N st.), 1670, 1253

M.p. >300 °C

4.2.14. Synthesis of 2-chloro-*N*-(5-cyano-4-oxo-4,7-dihydro-3*H*-pyrrolo[2,3-*d*]pyrimidin-2-yl)acetamide (2.17)

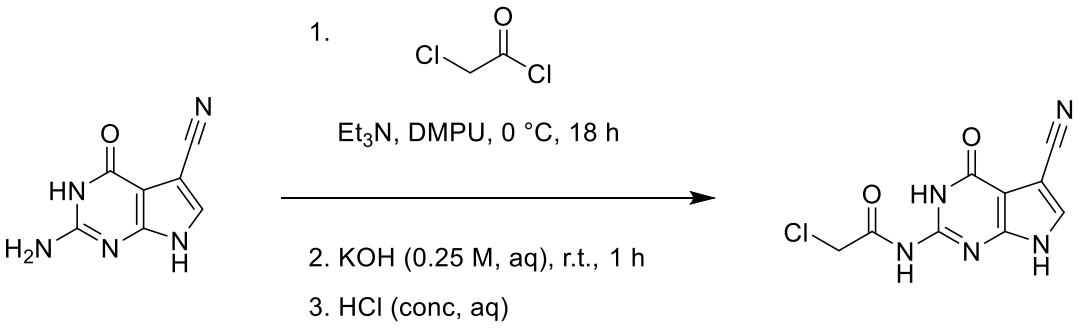

A suspension of 7-cyano-7-deazaguanine (150 mg, 0.856 mmol) in anhydrous DMPU (6 mL) in a 25 mL round bottom flask was treated with distilled triethylamine (0.48 mL, 3.426 mmol). The

mixture was cooled to 0 °C, after which chloroacetyl chloride (0.38 mL, 4.781 mmol) was added dropwise to the mixture. The reaction was then left to stir at 0 °C for 18 h. Then, the mixture was treated with aqueous potassium hydroxide (0.25 M, 6 mL) and left to stir at room temperature for 1 h, after which ^{1}H NMR analysis indicated total conversion to the desired product. Then, the solution was acidified to pH 2 with concentrated hydrochloric acid, diluted with water (50 mL), and refrigerated overnight, causing a precipitate to form. The precipitate was collected *via* vacuum filtration and the collected solids were washed with methanol (2 x 10 mL) to afford a yellow powder (97 mg, 41%).

^{1}H NMR (400 MHz, dmso) δ 12.74 (s, 1H), 11.87 (s, 1H), 11.63 (s, 1H), 7.94 (d, *J* = 2.8 Hz, 1H), 4.42 (s, 2H).

^{13}C NMR (101 MHz, dmso) δ 169.0, 155.6, 148.3, 147.3, 130.4, 115.1, 103.3, 86.4, 43.1.

HRMS (ESI) exact mass calculated for [$C_9H_6ClN_5O_2$] requires *m/z* 251.0210, found *m/z* 274.0106 $[M + Na]^+$

FTIR (ν_{max}, cm^{-1}) 3182, 2904, 2230 (C≡N st.), 1636, 1249

M.p. >300 °C

4.2.15. Synthesis of 4-chloro-*N*-(5-cyano-4-oxo-4,7-dihydro-3*H*-pyrrolo[2,3-*d*]pyrimidin-2-yl)butanamide (2.18)

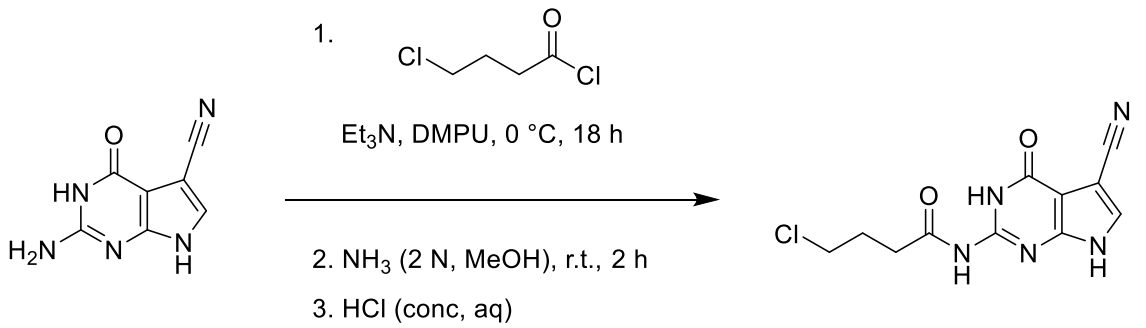

A suspension of 7-cyano-7-deazaguanine (150 mg, 0.856 mmol) in anhydrous DMPU (6 mL) in a 25 mL round bottom flask was treated with triethylamine (0.48 mL, 3.426 mmol). The mixture

was cooled to 0 °C, after which distilled 4-chlorobutyryl chloride (0.38 mL, 3.424 mmol) was added dropwise to the mixture. The reaction was then left to stir at 0 °C for 18 h. Then, the mixture was treated with methanolic ammonia (2 N, 6 mL) and left to stir at room temperature for 2 h. Then, the solution was acidified to pH 2 with concentrated hydrochloric acid, diluted with water (30 mL) and refrigerated overnight, causing a precipitate to form. The precipitate was collected *via* vacuum filtration and the collected solids were triturated in methanol (5 mL) for 10 min and filtered under vacuum to afford a white powder (93 mg, 39%).

^{1}H NMR (400 MHz, dmso) δ 12.66 (s, 1H), 11.91 (s, 1H), 11.61 (s, 1H), 7.90 (d, *J* = 2.7 Hz, 1H), 3.69 (t, *J* = 6.5 Hz, 2H), 2.62 (t, *J* = 7.2 Hz, 2H), 2.03 (p, *J* = 6.8 Hz, 2H).

^{13}C NMR (101 MHz, dmso) δ 175.3, 155.6, 148.6, 148.0, 130.2, 115.2, 103.0, 86.3, 44.6, 33.2, 27.1.

HRMS (ESI) exact mass calculated for [$C_{11}H_{10}ClN_5O_2$] requires *m*/*z* 279.0523, found *m*/*z* 302.0424 $[M + Na]^+$

FTIR (ν_{max}, cm^{-1}) 3182, 2961, 2233 (C≡N st.), 1630, 1247

M.p. >300 °C

4.2.16. Synthesis of 5-chloro-*N*-(5-cyano-4-oxo-4,7-dihydro-3*H*-pyrrolo[2,3-*d*]pyrimidin-2-yl)pentanamide (2.19)

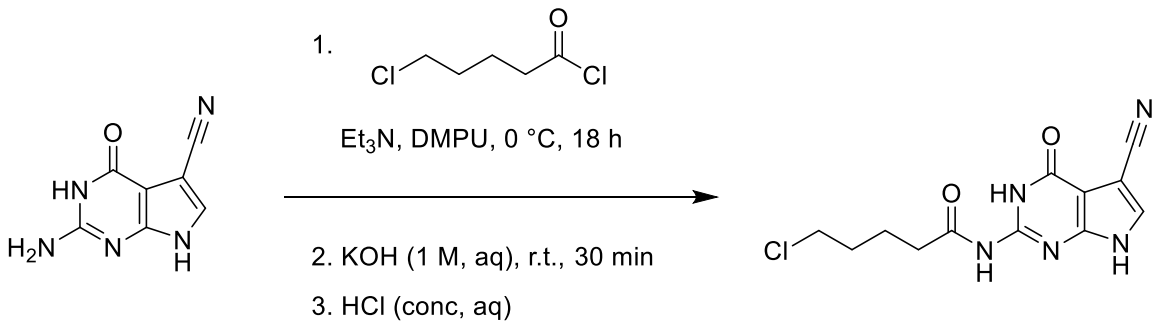

A suspension of 7-cyano-7-deazaguanine (150 mg, 0.856 mmol) in anhydrous DMPU (9 mL) in a 50 mL round bottom flask was treated with distilled triethylamine (0.48 mL, 3.426 mmol). The

mixture was cooled to 0 °C, after which distilled 5-chlorovaleroyl chloride (0.44 mL, 3.426 mmol) was added dropwise to the mixture. The reaction was then left to stir at 0 °C for 18 h, after which ^{1}H NMR indicated full consumption of the starting material. The mixture was then treated with aqueous potassium hydroxide (1 M, 9 mL) and left to stir at room temperature for 30 min. Then, the solution was acidified to pH 2 with concentrated hydrochloric acid, causing a precipitate to form which was collected *via* vacuum filtration, affording a white powder (52 mg, 21%).

^{1}H NMR (400 MHz, dmso) δ 12.65 (s, 1H), 11.95 (s, 1H), 11.57 (s, 1H), 7.92 (s, 1H), 3.66 (t, *J* = 6.0 Hz, 2H), 2.48 (s, 2H), 1.82 – 1.65 (m, 4H).

^{13}C NMR (101 MHz, dmso) δ 175.9, 155.6, 148.5, 148.0, 130.1, 115.2, 102.9, 86.2, 45.0, 35.1, 31.3, 21.7.

HRMS (ESI) exact mass calculated for [$C_{12}H_{12}ClN_5O_2$] requires *m*/*z* 293.0680, found *m*/*z* 292.0611 [M - H]$^{-}$

FTIR (ν_{max}, cm^{-1}) 3203, 2960, 2229 (C≡N st.), 1632, 1246

M.p. 292 – 296 °C (dec.)

4.2.17. Synthesis of 6-chloro-*N*-(5-cyano-4-oxo-4,7-dihydro-3*H*-pyrrolo[2,3-*d*]pyrimidin-2-yl)hexanamide (2.20)

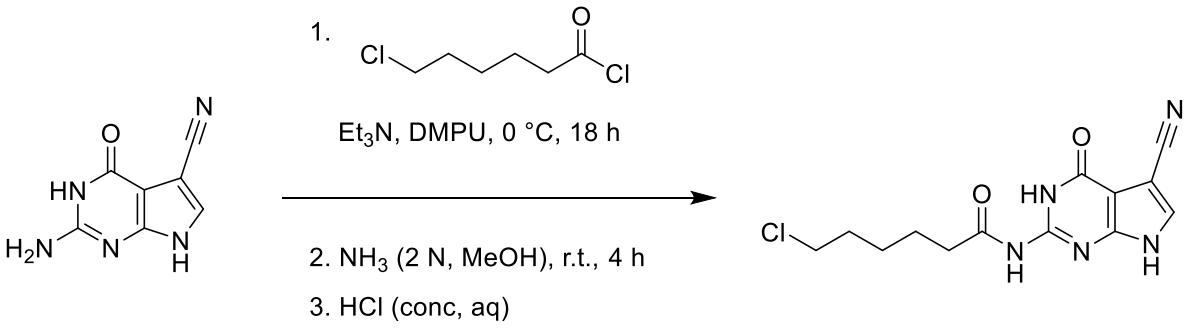

A suspension of 7-cyano-7-deazaguanine (103 mg, 0.59 mmol) in anhydrous DMPU (4 mL) in a 25 mL round bottom flask was treated with distilled triethylamine (0.33 mL, 2.34 mmol). The mixture was cooled to 0 °C, after which 4-chlorobutyryl chloride (0.44 mL, 2.34 mmol) was added

dropwise to the mixture. The reaction was then left to stir at 0 °C for 18 h. Then, the mixture was treated with methanolic ammonia (2 N, 4 mL) and left to stir at room temperature for 4 h. Then, the solution was acidified to pH 2 with concentrated hydrochloric acid, causing a precipitate to form. The precipitate was collected *via* vacuum filtration and the collected solids were dried in a desiccator before being triturated in methanol (5 mL) for 10 min and filtered under vacuum. The trituration and filtration steps were repeated thrice more to afford an off-white powder (76 mg, 42%).

^{1}H NMR (400 MHz, dmso) δ 12.65 (s, 1H), 11.98 (s, 1H), 11.56 (s, 1H), 7.91 (s, 1H), 3.64 (t, *J* = 6.6 Hz, 2H), 2.47 – 2.44 (m, *J* = 7.4 Hz, 2H), 1.73 (p, *J* = 7.0 Hz, 2H), 1.61 (p, *J* = 7.5 Hz, 2H), 1.41 (p, *J* = 7.6 Hz, 2H).

^{13}C NMR (101 MHz, dmso) δ 176.2, 155.5, 148.5, 148.0, 130.1, 115.2, 102.9, 86.2, 45.2, 35.8, 31.7, 25.7, 23.6.

HRMS (ESI) exact mass calculated for [$C_{13}H_{14}ClN_5O_2$] requires *m*/*z* 307.0836, found *m*/*z* 330.0727 $[M + Na]^+$

FTIR (ν_{max}, cm^{-1}) 3167, 2945, 2230 (C≡N st.), 1651, 1249

M.p. >300 °C

4.2.18. Synthesis of *N*-(5-cyano-4-oxo-4,7-dihydro-3*H*-pyrrolo[2,3-*d*]pyrimidin-2-yl)acrylamide (2.21)

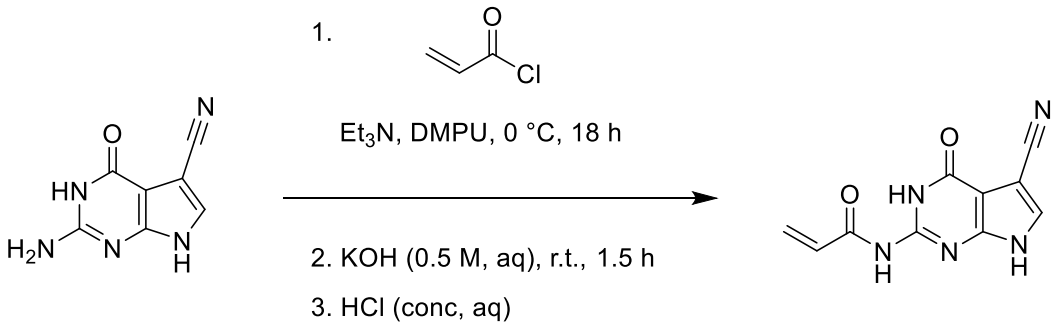

A suspension of 7-cyano-7-deazaguanine (150 mg, 0.856 mmol) in anhydrous DMPU (6 mL) in a 25 mL round bottom flask was treated with distilled triethylamine (0.48 mL, 3.426 mmol). The mixture was cooled to 0 °C, after which acryloyl chloride (0.28 mL, 3.424 mmol) was added

dropwise over 2 h. The reaction was then left to stir at 0 °C for 18 h. Then, the mixture was treated with aqueous potassium hydroxide (0.5 M, 6 mL) and left to stir at room temperature for 1.5 h. Then, the solution was acidified to pH 2 with concentrated hydrochloric acid, diluted with water (30 mL) and refrigerated overnight, causing a precipitate to form. The precipitate was collected *via* vacuum filtration and the collected solids were triturated in methanol (5 mL) for 10 min and filtered under vacuum. This process was repeated once more to afford a mustard powder (48 mg, 24%).

^{1}H NMR (400 MHz, dmso) δ 12.70 (s, 1H), 12.03 (s, 1H), 11.80 (s, 1H), 7.94 (d, *J* = 2.8 Hz, 1H), 6.55 (dd, *J* = 17.0, 9.9 Hz, 1H), 6.45 (dd, *J* = 17.0, 1.8 Hz, 1H), 5.99 (dd, *J* = 9.9, 1.8 Hz, 1H).

^{13}C NMR (101 MHz, dmso) δ 166.9, 155.6, 148.5, 148.1, 131.2, 130.3, 129.6, 115.2, 103.2, 86.3.

HRMS (ESI) exact mass calculated for [$C_{10}H_7N_5O_2$] requires *m*/*z* 229.0600, found *m*/*z* 228.0527 $[M - H]^-$

FTIR (ν_{max}, cm^{-1}) 3183, 2229 (C≡N st.), 1647, 1251

M.p. >300 °C

4.2.19. Synthesis of (*E*)-*N*-(5-cyano-4-oxo-4,7-dihydro-3*H*-pyrrolo[2,3-*d*]pyrimidin-2-yl)but-2-enamide (2.22)

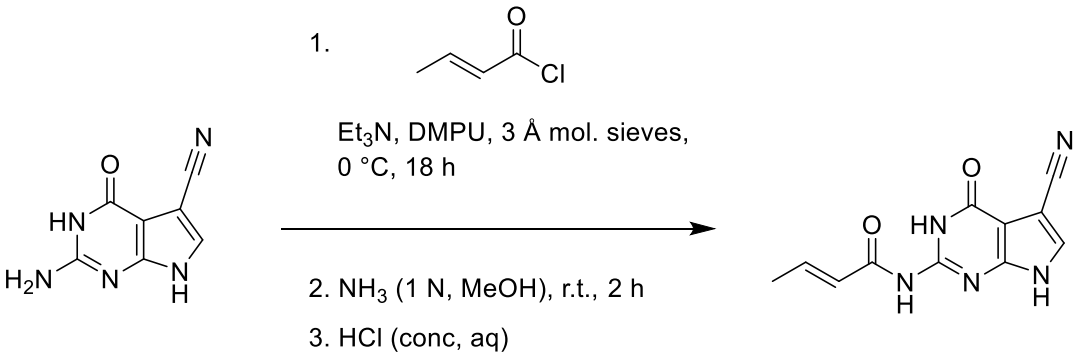

A suspension of 7-cyano-7-deazaguanine (150 mg, 0.856 mmol) in anhydrous DMPU (6 mL) and activated 3 Å molecular sieves in a 25 mL round bottom flask was treated with distilled triethylamine (0.48 mL, 3.426 mmol). The mixture was cooled to 0 °C, after which distilled

crotonyl chloride (0.33 mL, 3.424 mmol) was added dropwise to the mixture. The reaction was then left to stir at 0 °C for 18 h. Then, the mixture was treated with methanolic ammonia (1 N, 6 mL) and left to stir at room temperature for 2 h. Then, the solution was acidified to pH 2 with concentrated hydrochloric acid, causing a precipitate to form. The suspension was transferred to a 100 mL conical flask along with water (20 mL) and the flask was refrigerated overnight, causing additional precipitate to form. The precipitate was collected *via* vacuum filtration. The collected solids were then triturated in methanol (5 mL) for 30 min and filtered under vacuum and the process was repeated twice more, affording a mustard powder (16 mg, 7.7%).

^{1}H NMR (400 MHz, dmso) δ 12.66 (s, 1H), 12.11 (s, 1H), 11.61 (s, 1H), 7.93 (s, 1H), 7.04 (dq, *J* = 13.8, 6.8 Hz, 1H), 6.26 (d, *J* = 15.1 Hz, 1H), 1.91 (d, *J* = 6.8 Hz, 3H).

^{13}C NMR (101 MHz, dmso) δ 167.1, 155.6, 148.5, 148.4, 145.4, 130.2, 123.7, 115.2, 103.0, 86.3, 18.0.

HRMS (ESI) exact mass calculated for [$C_{11}H_9N_5O_2$] requires *m*/*z* 243.0756, found *m*/*z* 266.0650 $[M + Na]^+$

FTIR (ν_{max}, cm^{-1}) 3125, 2970, 2231 (C≡N st.), 1625, 1246

M.p. >300 °C

4.3. Biochemistry

4.3.1. Cell culture

MDA-MB-231 cells were provided by Dr. Vincent Kelly (School of Biochemistry, University of Dublin TCD) and were cultured in UltraCULTURE (Lonza) medium supplemented with 2 mM L-glutamine in antibiotic- and queuine-free conditions. All cell cultures were maintained in a humidified atmosphere at 37 °C and 5% CO_2. Media were warmed to 37 °C before use. Cells were cultured in 75 mL flasks.

4.3.2. Cell passaging

Subconfluent cells were first washed in 1X Dulbecco's phosphate-buffered saline (DPBS, Gibco). Cells were then detached using 2 mL of accutase solution (10% of 1X accutase in 1X DPBS) and incubated at 37 °C for up to 4 min. Cell detachment was checked under the microscope before addition of 8 mL of 1X DPBS to inactivate the accutase. The suspended cells were pelleted at 1000 rpm for 5 min in a centrifuge and resuspended in 1 mL of UltraCULTURE. Between a quarter to a sixth of the suspension was then used to seed the cells onto a fresh cell culture dish, depending on cell count before adding 10 mL of UltraCULTURE medium.

4.3.3. AlamarBlue viability assays

MDA-MB-231 cells were grown in UltraCULTURE medium with 2 mM L-glutamine supplement until confluency. Cells were counted and seeded on a 96-well plate at 5000 cells per well (well volume 100 µL, UltraCULTURE supplemented with 2 mM L-glutamine) before being treated with three different concentrations of **1.8**, **2.4** and **2.7** – **2.22** in DMSO (final concentrations 250 µM, 100 µM and 25 µM, 10% DMSO in UltraCULTURE with 2 mM L-glutamine) each in triplicate and grown for 72 h. After the desired time of incubation, 20 µL of alamarBlue (Invitrogen) was added to each well. Plates were then incubated for 4 h. Absorbance levels were measured using a microplate fluorometer (emission 540 nm, excitation 590 nm). Cell viability was expressed as a percentage of fluorescence in the treated cells in relation to untreated cells (taken as 100%).

4.3.4. Hoechst 33258 viability assays

MDA-MB-231 cells were grown in UltraCULTURE medium with 2 mM L-glutamine supplement until confluency. Cells were counted and seeded on a 96-well plate at 5000 cells per well (well volume 100 µL, UltraCULTURE supplemented with 2 mM L-glutamine) before being treated with three different concentrations of **1.8**, **2.4** and **2.7** – **2.22** in DMSO (final concentrations 250 µM, 100 µM and 25 µM, 10% DMSO in UltraCULTURE with 2 mM L-glutamine) each in triplicate and grown for 72 h. After the desired time of incubation, the medium was removed and 100 µL of Hoechst 33258 solution were added to each well. The plates were incubated for 5 min, the staining solution was removed and the wells were washed with PBS. Absorbance levels were measured using a microplate fluorometer (emission 360 nm, excitation 460 nm). Cell viability was expressed as a percentage of fluorescence in the treated cells in relation to untreated cells (taken as 100%).

5. References

1. S. Varghese, M. Cotter, F. Chevot, C. Fergus, C. Cunningham, K. H. Mills, S. J. Connon, J. M. Southern and V. P. Kelly, *Nucleic Acids Res.*, 2016, **45**, 2029–2039.
2. W. Baranowski, G. Dirheimer, J. A. Jakowicki and G. Keith, *Cancer Research*, 1994, **54**, 4468–4471.
3. S. Fowler, R. Roush and J. Wise, *Concepts of Biology***,** OpenStax, Rice University, 2017.
4. D. Voet and J. G. Voet, *Biochemistry*, N. J. Hoboken, Wiley, Fourth ed., 2017.

5. A. L. Lehninger and M. M. Cox, *Principles of Biochemistry*, W. H. Freeman, Science, Seventh ed., 2017.
6. Image modified from "Translation: Figure 3," by OpenStax College, Biology (CC BY 4.0).
7. F. Sun and G. Caetano-Anollés, *Complexity*, 2008, https://doi.org/10.1002/cplx.20255.
8. J. D. Watson, T. A. Baker, S. P. Bell, A. Gann, M. Levine and R. Losick, *Molecular Biology of the Gene*, Pearson/Benjamin Cummings, San Francisco, Sixth ed., 2008, 461-519.
9. M. Helm and J. D. Alfonzo, *Chemistry & Biology*, 2014, **21**, 174–185.
10. The RNA Modification Database, http://mods.rna.albany.edu/home, (accessed May 2019).
11. Modomics: a database of RNA modification pathways, http://modomics.genesilico.pl/modifications, (accessed April 2019).
12. S. Nishimura, *Prog. Nucleic Acid Res. Mol. Biol.*, 1983, **28**, 49–73.
13. N. Okada, N. Shindo-Okada and S. Nishimura, *Nucleic Acids Res.*, 1977, **4**, 415–423.
14. C. Fergus, D. Barnes, M. Alqasem and V. P. Kelly, *Nutrients*, 2015, **7**, 2897–2929.
15. W. R. Farkas, K. B. Jacobson and J. R. Katze, *Biochim. Biophys. Acta*, 1984, **781**, 64–75.
16. H. Kersten, *BioFactors*, 1988, **1**, 27–29.
17. C. Romier, J. E. Meyer and D. Suck, *FEBS Lett.*, 1997, **416**, 93–98.
18. Y. C. Chen, A. F. Brooks, D. M. Goodenough-Lashua, J. D. Kittendorf, H. D. Showalter and G. A. Garcia, *Nucleic Acids Res.*, 2011, **39**, 2834–2844.
19. G. A. Garcia, D. L. Tierney, S. Chong, K. Clark and J. E. Penner-Hahn, *Biochemistry*, 1996, **35**, 3133–3139.
20. M. Müller, C. Legrand, F. Tuorto, V. P. Kelly, Y. Atlasi, F. Lyko and A. E. Ehrenhofer-Murray, *Nucleic Acids Res.*, 2019, **47**, 3711–3727.
21. H. J. Grosjean, S. de Henau and D. M. Crothers, *Proc. Natl. Acad. Sci. U. S. A.*, 1978, **75**, 610–614.
22. F. Tuorto, C. Legrand, C. Cirzi, G. Federico, R. Liebers, M. Müller, A. E. Ehrenhofer-Murray, G. Dittmar, H. J. Grone and F. Lyko, *EMBO J.*, 2018, **37**, https://doi.org/10.15252/embj.201899777.
23. F. Meier, B. Suter, H. Grosjean, G. Keith and E. Kubli, *EMBO J.*, 1985, **4**, 823–827.
24. N. Okada, N. Shindo-Okada, S. Sato, Y. H. Itoh, K. Oka and S. Nishimura, *Proc. Natl. Acad. Sci. U. S. A.*, 1978, **75**, 4347–4251.
25. U. Gündüz, M. S. Elliott, P. H. Seubert, J. A. Houghton, P. J. Houghton, R. W. Trewyn and J. R. Katze, *Biochim. Biophys. Acta*, 1992, **1139**, 229–238.
26. W. Baranowski, G. Dirheimer, J. A. Jakowicki and G. Keith, *Cancer Res.*, 1994, **54**, 4468–4471.

27. U. Aytac and U. Gündüz, *Cancer Biochem. Biophys.*, 1994, **14**, 93–98.
28. B. S. Huang, R. T. Wu and K. Y. Chien, *Cancer Res.*, 1992, **52**, 4696–4700.
29. B. Emmerich, E. Zubrod, H. Weber, P. A. Maubach, H. Kersten and W. Kersten, *Cancer Res.*, 1985, **45**, 4308–4314.
30. G. Muraldhar, J. Ochieng and R. W. Trewyn, *Cancer Res.*, 1989, **49**, 7110–7114.
31. E. Randerath, H. P. Agrawal and K. Randerath, *Cancer Res.*, 1984, **44**, 1167–1171.
32. R. C. Morris, K. G. Brown and M. S. Elliott, *J. Biomol. Struct. Dyn.*, 1999, **16**, 757–774.
33. N. K. Howes and W. R. Farkas, *J. Biol. Chem.*, 1978, **253**, 9082–9087.
34. H. Akimoto, H. Nomura, M. Yoshida, N. Shindo-Okada, A. Hoshi and S. Nishimura, *J. Med. Chem.*, 1986, **29**, 1749–1753.
35. J. Kazius, R. McGuire and R. Bursi, *J. Med. Chem.*, 2005, **48**, 312–320.
36. L. Guterman, *Chem. Eng. News*, 2011, **89**, 19–26.
37. R. J. Flower, *Nat. Rev. Drug Discovery*, 2003, **2**, 179–191.
38. J. M. Shin, Y. M. Cho and G. Sachs, *J. Am. Chem. Soc.*, 2004 **126**, 7800–7811.
39. R. R. Yocum, D. J. Waxman, J. R. Rasmuttent and J. L. Stromincser, *Proc. Natl. Acad. Sci. U. S. A.*, 1979, **76**, 2730–2734.
40. P. Savi, J. Zachayus, N. Delesque-Touchard, C. Labouret, C. Hervé, M. Uzabiaga, J. Pereillo, J. Culouscou, F. Bono, P. Ferrara and J. Herbert, *Proc. Natl. Acad. Sci. U. S. A.*, 2006, **103**, 11069–11074.
41. M. S. Davids and J. R. Brown, *Future Oncol.*, 2014, **10**, 957–967.
42. R. A. Bauer, *Drug Discovery Today*, 2015, **20**, 1061–1073.
43. V. T. DeVita and E. Chu, *Cancer Res.*, 2008, **68**, 8643–8653.
44. R. K. Singh, S. Kumar, D. N. Prasad and T. R Bhardwaj, *Eur. J. Med. Chem.*, 2018, **10**, 401–433.
45. N. W. Gaikwad and W. J. Bodell, *Free Radic. Biol. Med.*, 2012, **52**, 340–347.
46. N. Zheng, S. Pang, T. Oe, C. Felix, S. Wehrli and I. Blair, *Curr. Drug Metab.*, 2006, **7**, 897–911.
47. M. Bean and H. Kohn, *J. Org. Chem.*, 2985, **50**, 293–298.
48. M. Santos and R. Moreira, *Mini-Rev. Med. Chem.*, 2007, **7**, 1040–1050.
49. A. F. Brooks, G. A. Garcia and H. D. H. Showalter, *Tetrahedron Lett.*, 2010, **51**, 4163–4165.
50. A. F. Brooks, PhD Thesis, University of Michigan, 2012.
51. A. V. Gangjee, E. Elzein, J. J. McGuire, S. F. Queener and R. L. Kisliuk, *J. Med. Chem.*, 2001, **44**, 1993–2003.

52. M. T. Migawa, J. M. Hinkley, G. C. Hoops and L. B. Townsend, *Synth. Commun.*, 1996, **26**, 3317–3322.
53. M. Cotter, PhD Thesis, The University of Dublin TCD, 2015.
54. K. Anzai and S. Suzuki, *Agric. Biol. Chem.*, 2014, **30**, 597–604.
55. G. J. Korinek and W. G. Schneider, *Can. J. Chem.*, **35**, 1157–1163.
56. L. P. Candeias, D. P. S. MacFarlane, S. L. W. McWhinnie, N. L. Maidwell, C. A. Roeschlaub, P. G. Sammes and R. Whittlesey, *J. Chem. Soc.*, 1998, **2**, 2333–2334.
57. S. Anoopkumar-Dukie, J. B. Carey, T. Conere, E. O'Sullivan, F. N. van Pelt and A. Allshire, *Br. J. Radiol.*, 2005, **78**, 945–947.
58. S. A. Latt and G. Stetten, *J. Histochem. Cytochem.*, 1976, **24**, 24–33.
59. F. G. Loontiens, P. Regenfuss, A. Zechel, L. Dumortier and R. M. Clegg, *Biochemistry*, 1990, **29**, 9029–9039.
60. D. Xu, M. Ma, Y. Liu, T. Zhou, K. Wang, Z. Deng and K. Hong, *Anticancer Agents Med. Chem.*, 2015, **15**, 285–290.

Appendix

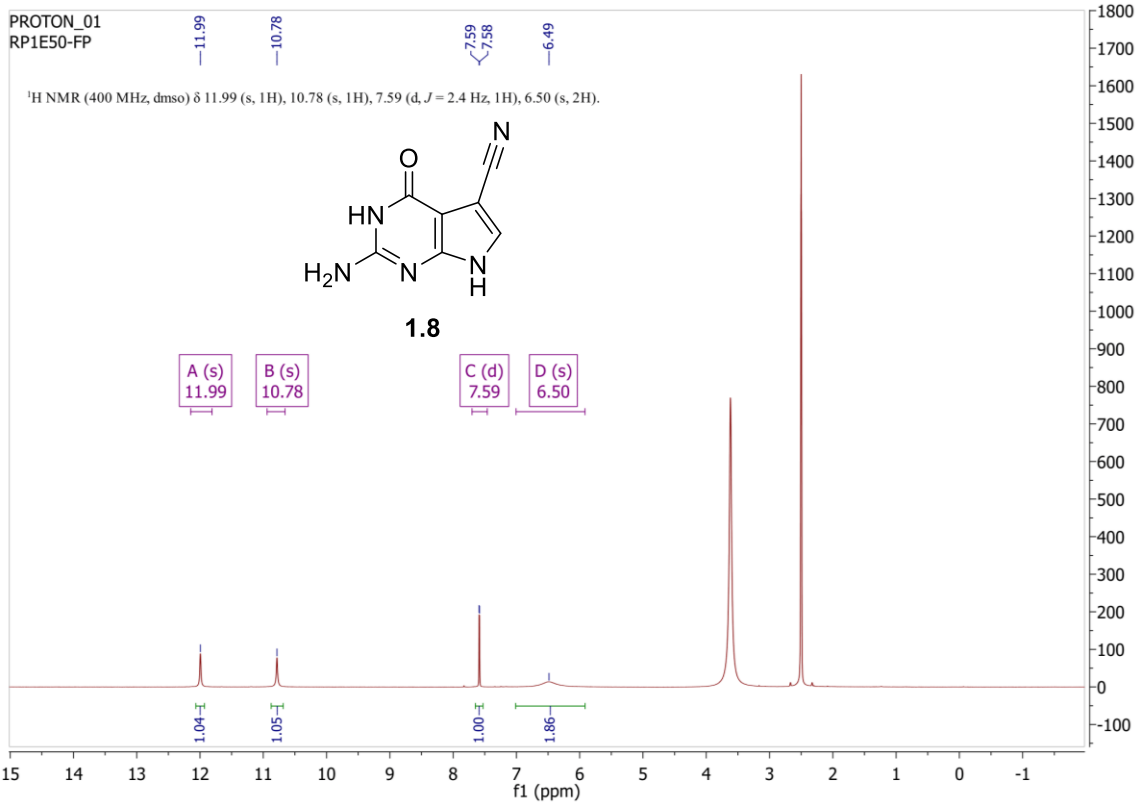
PROTON_01
RP1E50-FP
11.99
10.78
7.59
7.58
6.49
¹H NMR (400 MHz, dmso) δ 11.99 (s, 1H), 10.78 (s, 1H), 7.59 (d, J = 2.4 Hz, 1H), 6.50 (s, 2H).
1.8
A (s) 11.99
B (s) 10.78
C (d) 7.59
D (s) 6.50
1.04
1.05
1.00
1.86
f1 (ppm)

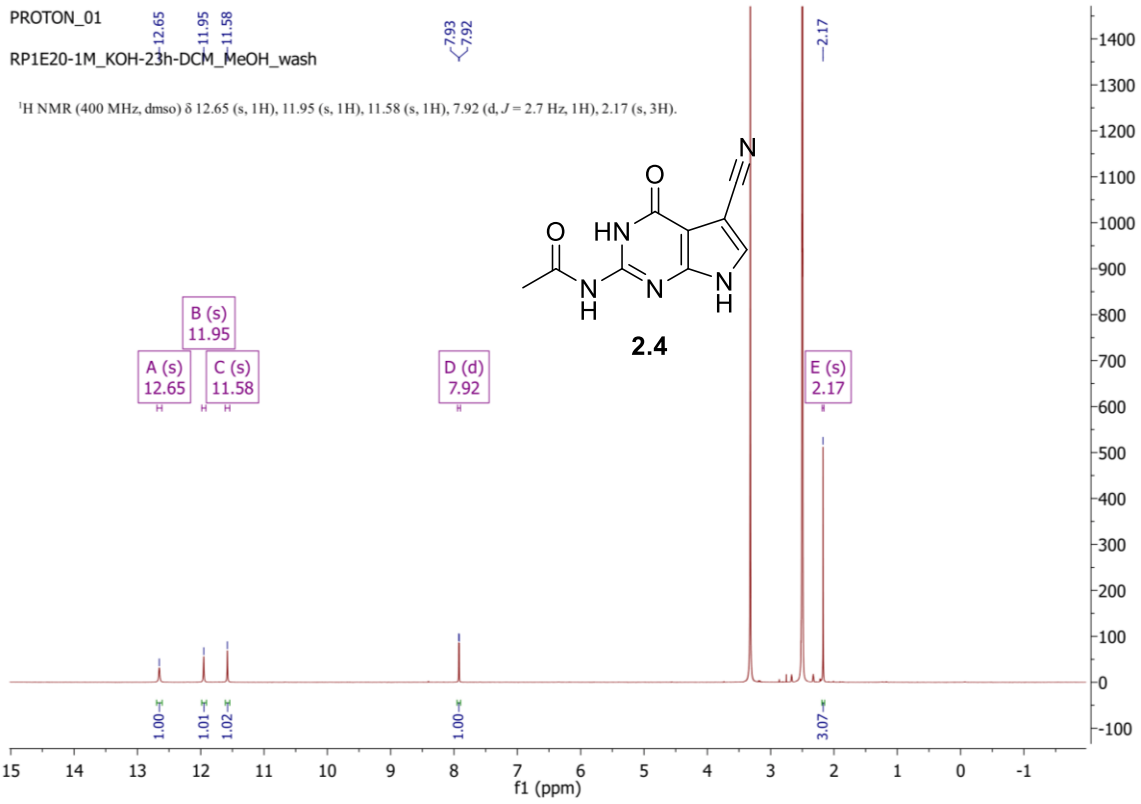
PROTON_01
RP1E20-1M_KOH-23h-DCM_MeOH_wash
12.65
11.95
11.58
7.93
7.92
2.17
¹H NMR (400 MHz, dmso) δ 12.65 (s, 1H), 11.95 (s, 1H), 11.58 (s, 1H), 7.92 (d, J = 2.7 Hz, 1H), 2.17 (s, 3H).
2.4
B (s) 11.95
A (s) 12.65
C (s) 11.58
D (d) 7.92
E (s) 2.17
1.00
1.01
1.02
1.00
3.07
f1 (ppm)

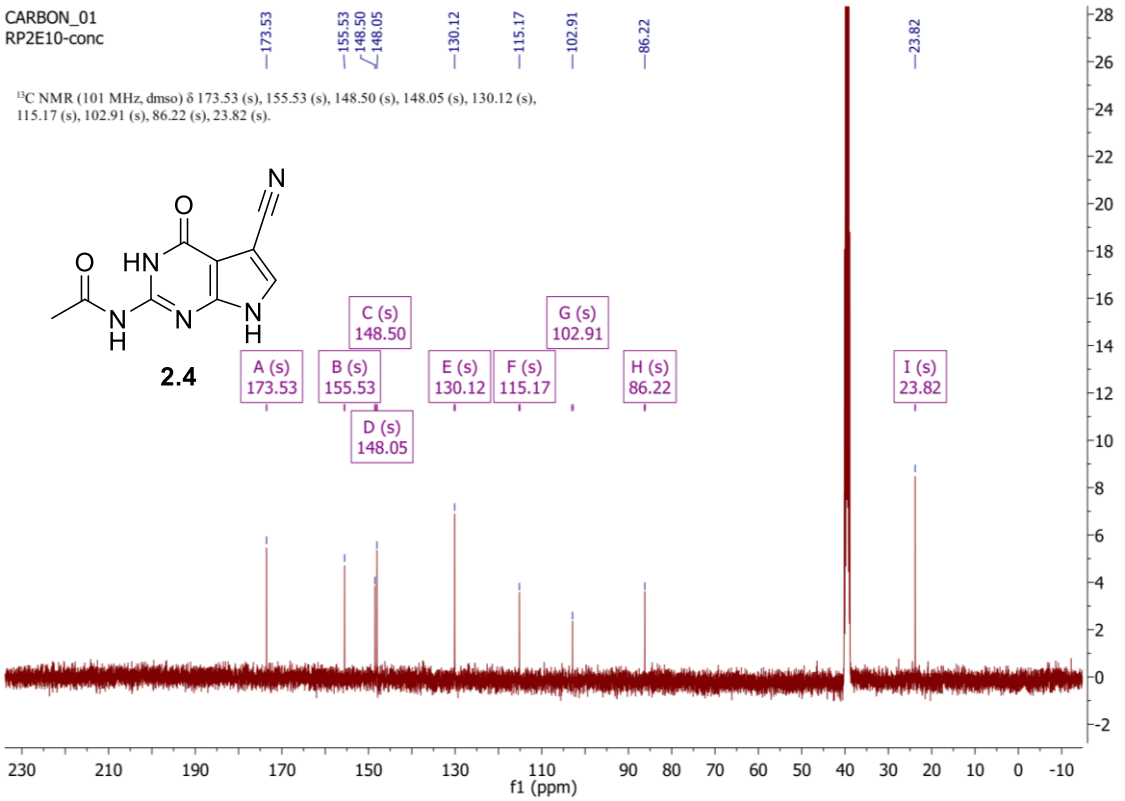
CARBON_01
RP2E10-conc
173.53
155.53
148.50
148.05
130.12
115.17
102.91
86.22
23.82
13C NMR (101 MHz, dmso) δ 173.53 (s), 155.53 (s), 148.50 (s), 148.05 (s), 130.12 (s), 115.17 (s), 102.91 (s), 86.22 (s), 23.82 (s).
2.4
A (s) 173.53
B (s) 155.53
C (s) 148.50
D (s) 148.05
E (s) 130.12
F (s) 115.17
G (s) 102.91
H (s) 86.22
I (s) 23.82
f1 (ppm)

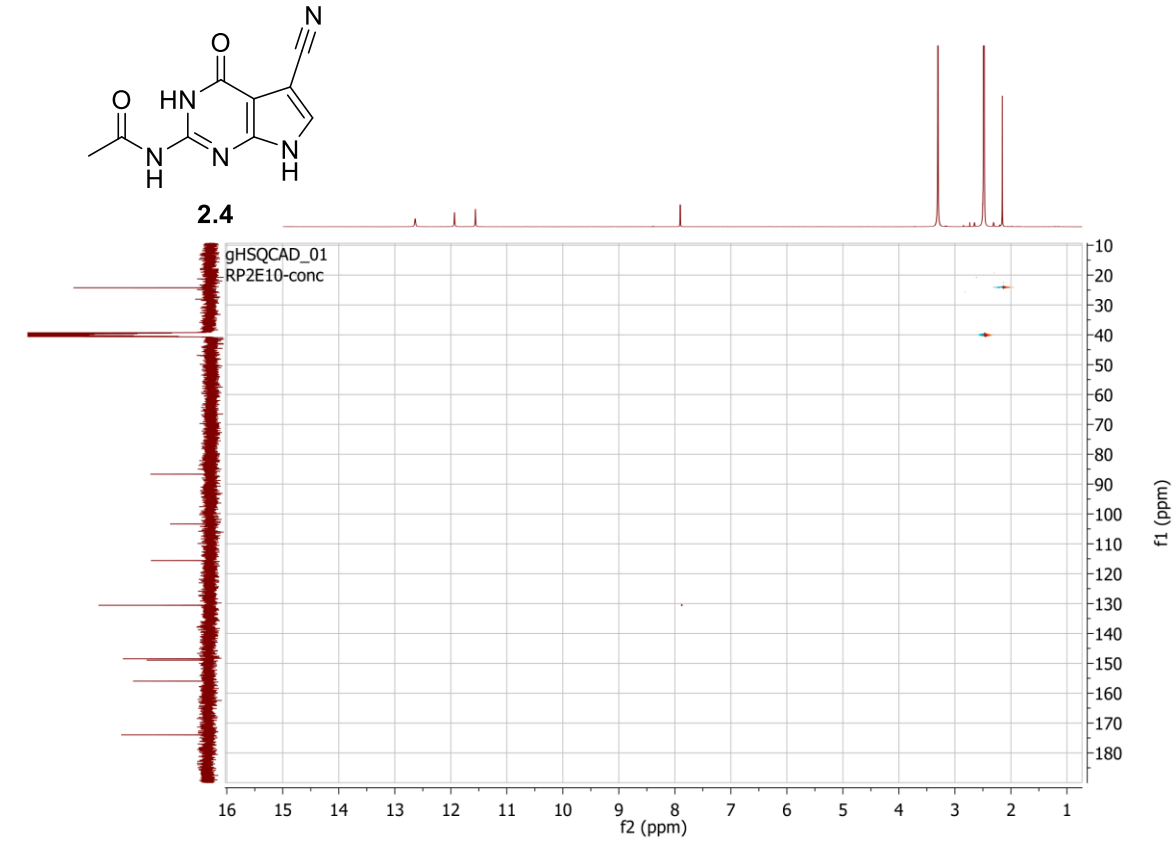
2.4
gHSQCAD_01
RP2E10-conc
f2 (ppm)
f1 (ppm)

Trinity College Dublin

Bruker Open Access LC-MS - Formula Identification Report

Sample-ID		Station	
Submitter		Supervisor	
Analysis Name	RP1E20-FP_RA3_01_15925.d	Acquisition Date	21/06/2018 13:24:08
Sample Description			

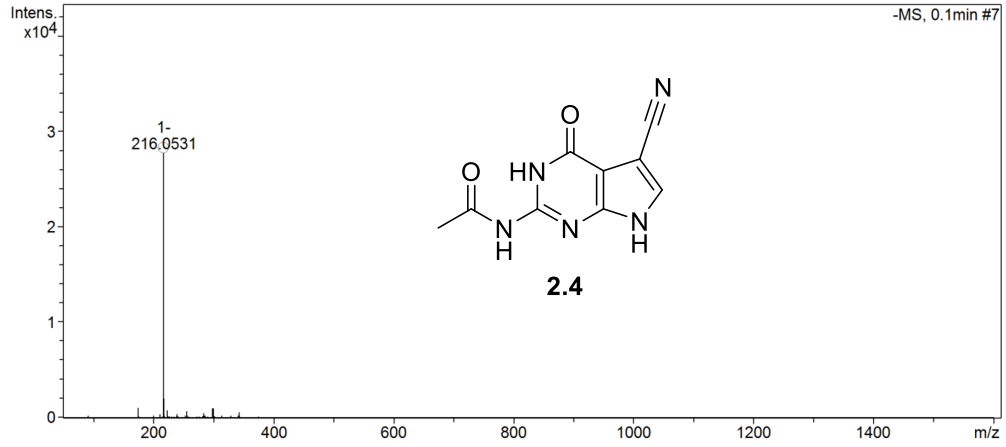

2.4

Meas. m/z	#	Ion Formula	m/z	err [mDa]	err [ppm]	rdb	N-Rule	e⁻ Conf	mSigma
216.053131	1	C9H6N5O2	216.052698	0.4	2.0	9.5	ok	even	25.9

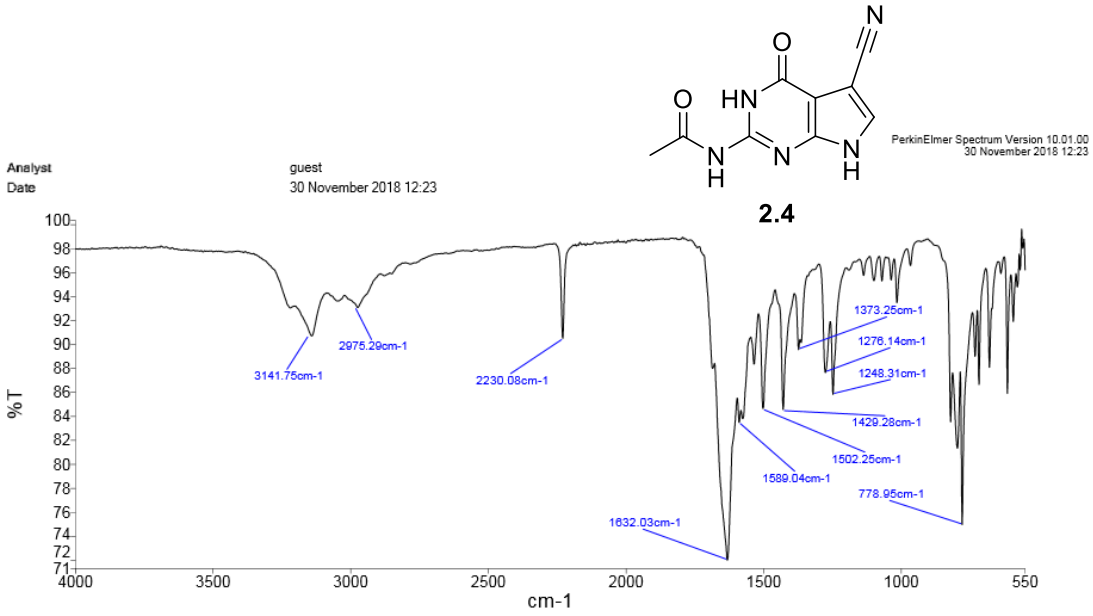

2.4

Sample Name	Description	Quality Checks
RPP01	Sample 001 By guest1 Date Friday, November 30 2018	The Quality Checks do not report any warnings for the sample.

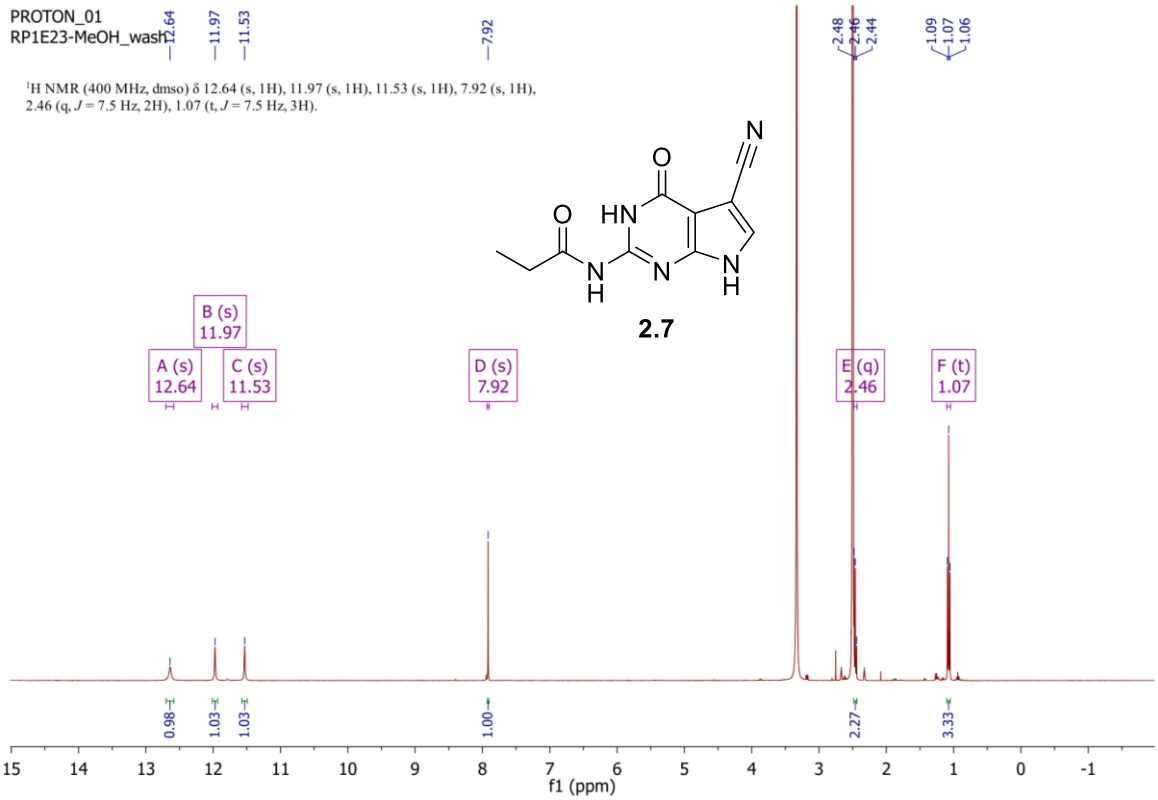
PROTON_01
RP1E23-MeOH_wash
12.64
11.97
11.53
7.92
2.48
2.46
2.44
1.09
1.07
1.06
^{1}H NMR (400 MHz, dmso) δ 12.64 (s, 1H), 11.97 (s, 1H), 11.53 (s, 1H), 7.92 (s, 1H), 2.46 (q, J = 7.5 Hz, 2H), 1.07 (t, J = 7.5 Hz, 3H).
2.7
B (s) 11.97
A (s) 12.64
C (s) 11.53
D (s) 7.92
E (q) 2.46
F (t) 1.07
0.98
1.03
1.03
1.00
2.27
3.33
f1 (ppm)

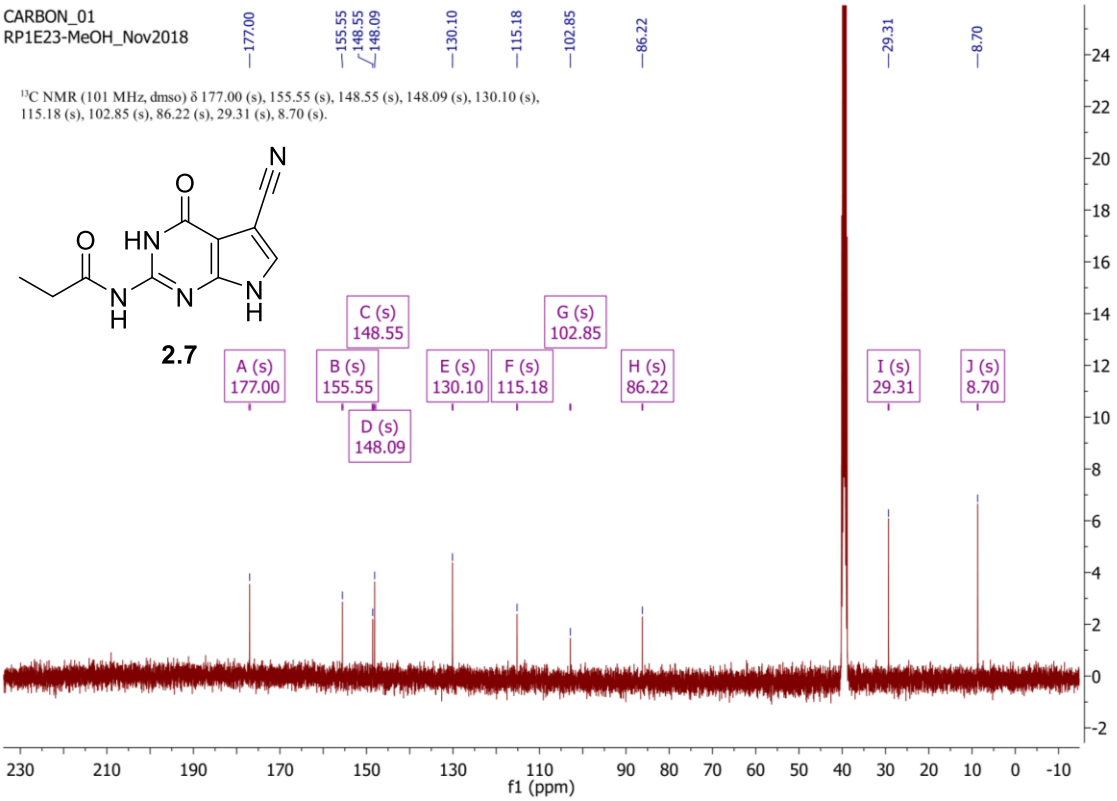
CARBON_01
RP1E23-MeOH_Nov2018
177.00
155.55
148.55
148.09
130.10
115.18
102.85
86.22
29.31
8.70
^{13}C NMR (101 MHz, dmso) δ 177.00 (s), 155.55 (s), 148.55 (s), 148.09 (s), 130.10 (s), 115.18 (s), 102.85 (s), 86.22 (s), 29.31 (s), 8.70 (s).
2.7
A (s) 177.00
B (s) 155.55
C (s) 148.55
D (s) 148.09
E (s) 130.10
F (s) 115.18
G (s) 102.85
H (s) 86.22
I (s) 29.31
J (s) 8.70
f1 (ppm)

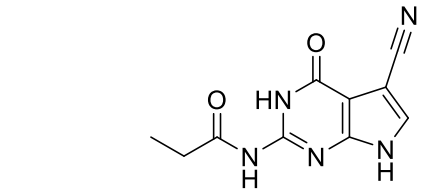

2.7

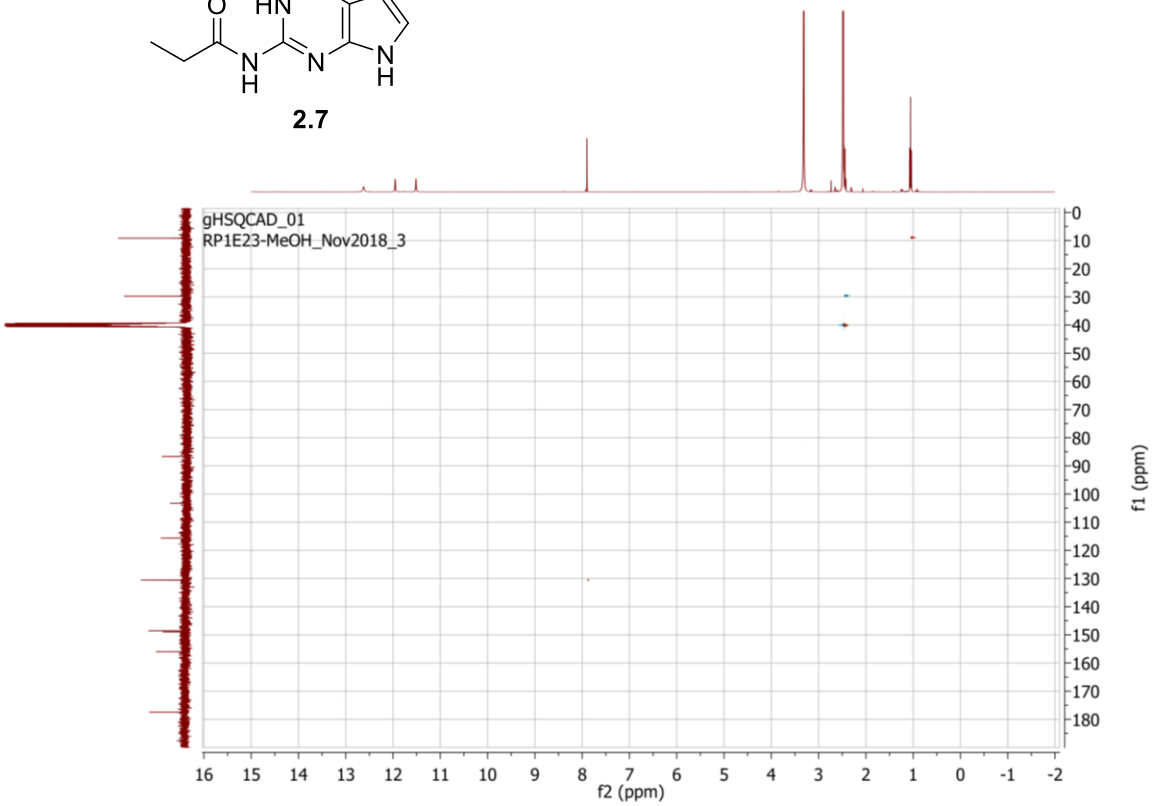

Trinity College Dublin

Bruker Open Access LC-MS - Formula Identification Report

Sample-ID		Station	
Submitter		Supervisor	
Analysis Name	RP1E23_RC8_01_18773.d	Acquisition Date	04/12/2018 16:44:19
Sample Description			

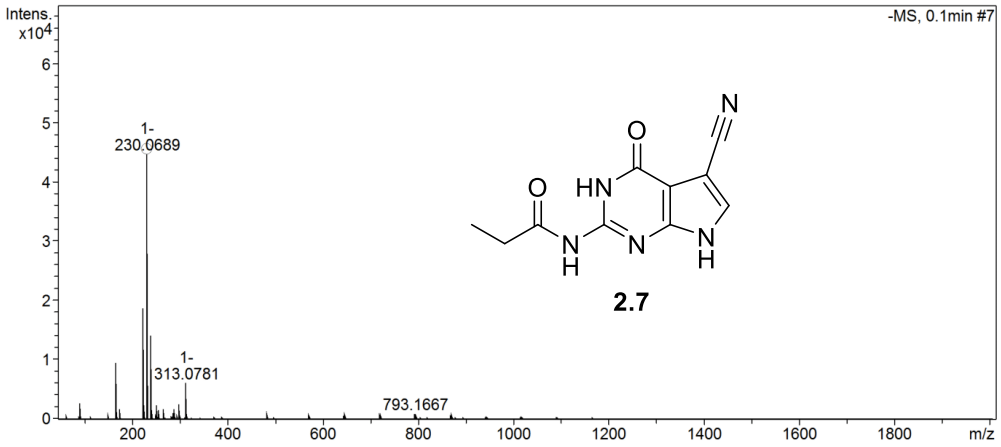

2.7

Meas. m/z	#	Ion Formula	m/z	err [mDa]	err [ppm]	rdb	N-Rule	e⁻ Conf	mSigma
230.068917	1	C10H8N5O2	230.068348	0.6	2.5	9.5	ok	even	43.1

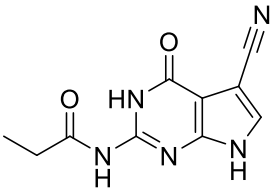

2.7

PerkinElmer Spectrum Version 10.01.00
30 November 2018 13:05

Analyst guest
Date 30 November 2018 13:05

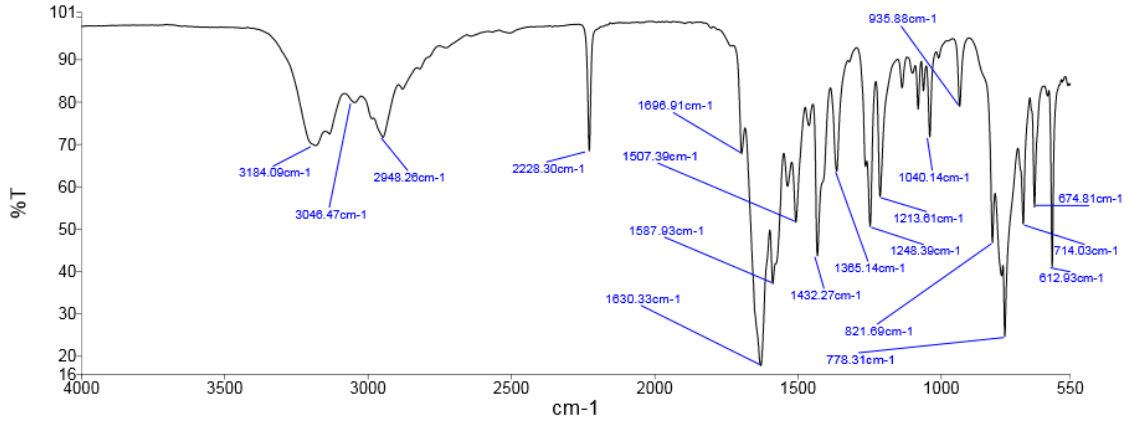

Sample Name	Description	Quality Checks
RPP02	Sample 002 By guest1 Date Friday, November 30 2018	The Quality Checks do not report any warnings for the sample.

PROTON_01
RP1E42-B

^{1}H NMR (400 MHz, dmso) δ 12.63 (s, 1H), 11.99 (s, 1H), 11.55 (s, 1H), 7.92 (s, 1H), 2.76 (hept, J = 6.8 Hz, 1H), 1.11 (d, J = 6.8 Hz, 6H).

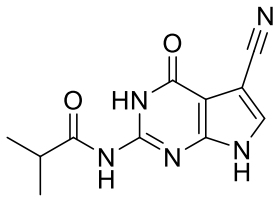

2.8

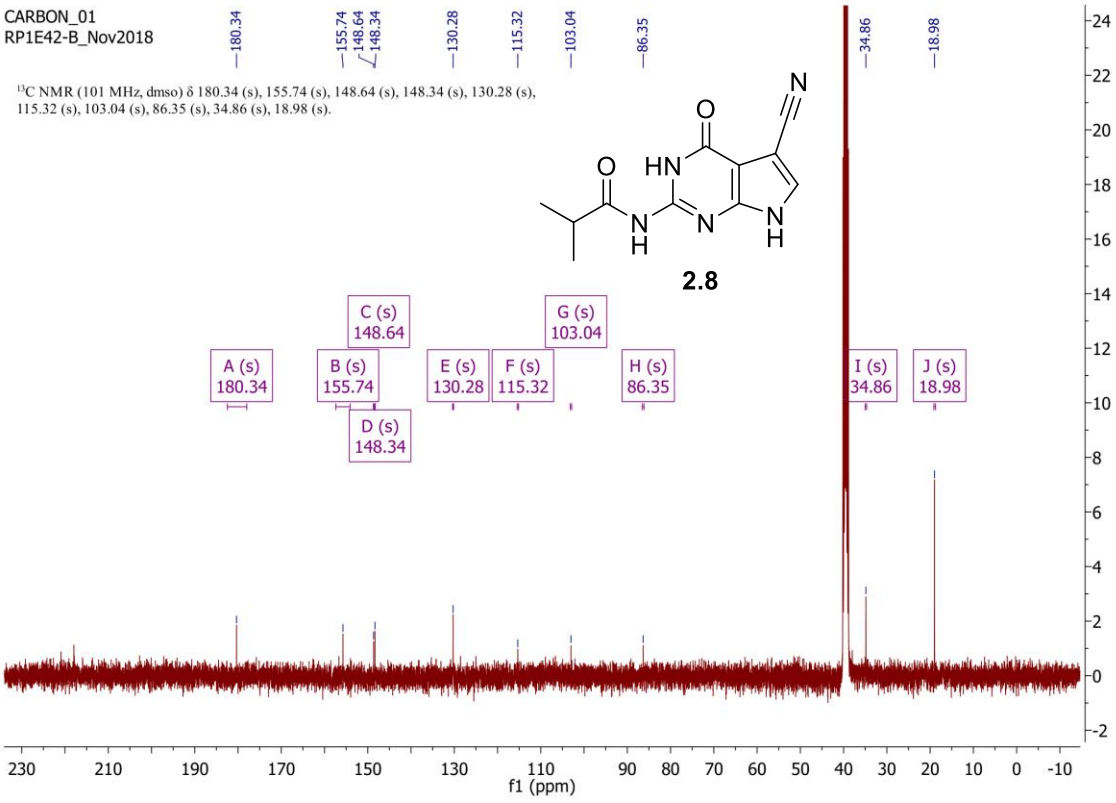
CARBON_01
RP1E42-B_Nov2018
180.34
155.74
148.64
148.34
130.28
115.32
103.04
86.35
34.86
18.98
13C NMR (101 MHz, dmso) δ 180.34 (s), 155.74 (s), 148.64 (s), 148.34 (s), 130.28 (s), 115.32 (s), 103.04 (s), 86.35 (s), 34.86 (s), 18.98 (s).
2.8
A (s) 180.34
B (s) 155.74
C (s) 148.64
D (s) 148.34
E (s) 130.28
F (s) 115.32
G (s) 103.04
H (s) 86.35
I (s) 34.86
J (s) 18.98
f1 (ppm)

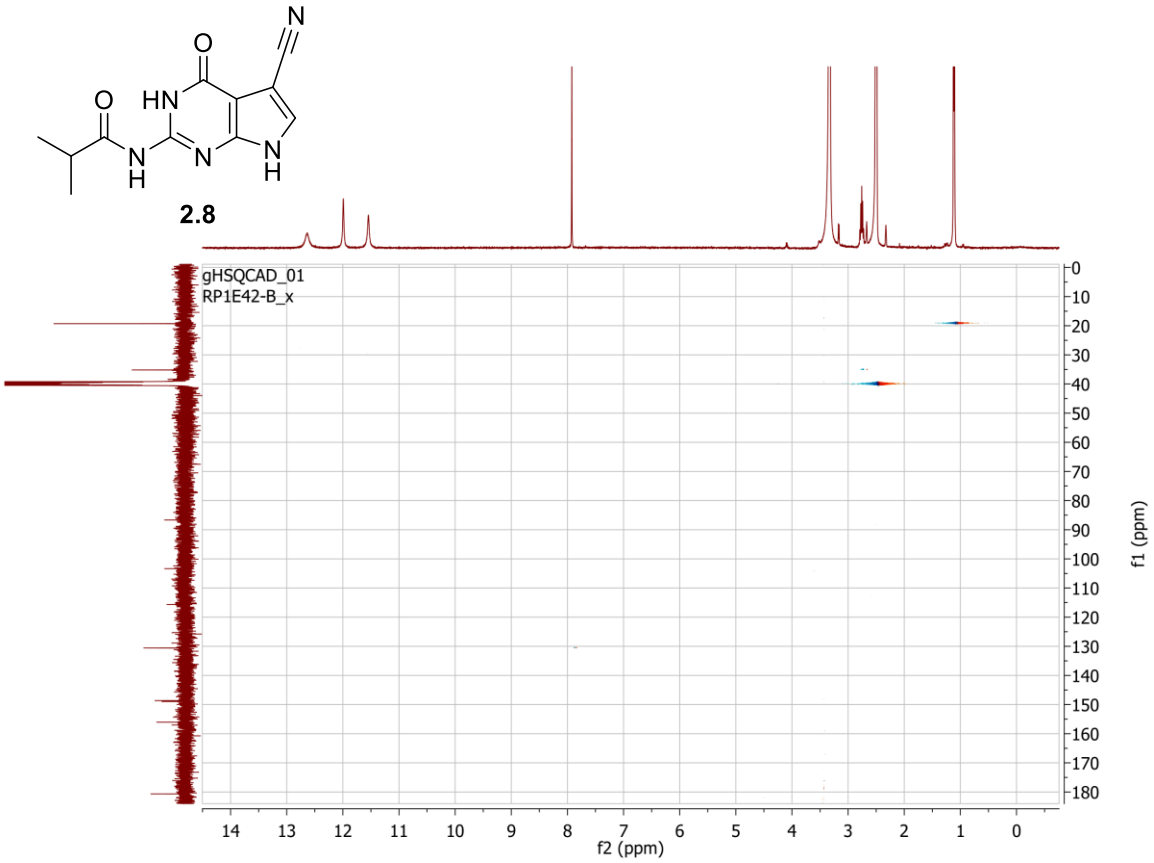
2.8
gHSQCAD_01
RP1E42-B_x
f2 (ppm)
f1 (ppm)

Trinity College Dublin

Bruker Open Access LC-MS - Formula Identification Report

Sample-ID		Station	
Submitter		Supervisor	
Analysis Name	RP1E42-B_RA7_01_15912.d	Acquisition Date	21/06/2018 12:30:46
Sample Description			

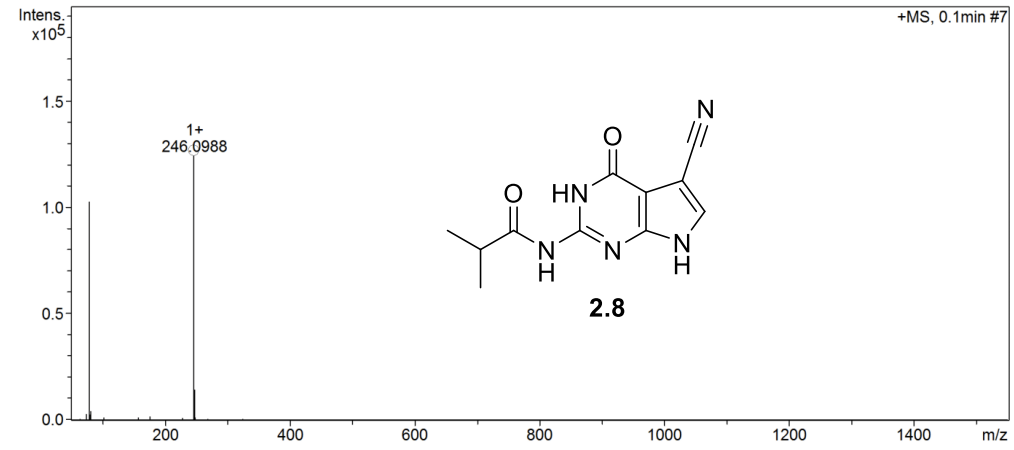

2.8

Meas. m/z	#	Ion Formula	m/z	err [mDa]	err [ppm]	rdb	N-Rule	e⁻ Conf	mSigma
246.098833	1	C11H12N5O2	246.098551	0.3	1.1	8.5	ok	even	14.7

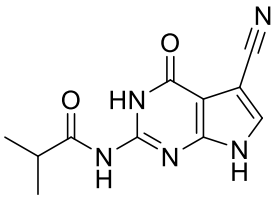

2.8

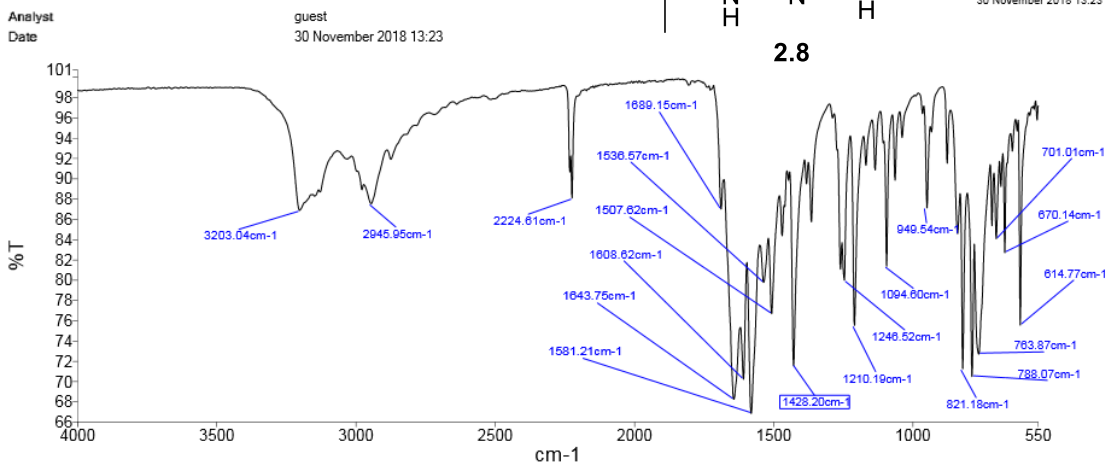

Sample Name	Description	Quality Checks
RPP03	Sample 003 By guest1 Date Friday, November 30 2018	The Quality Checks do not report any warnings for the sample.

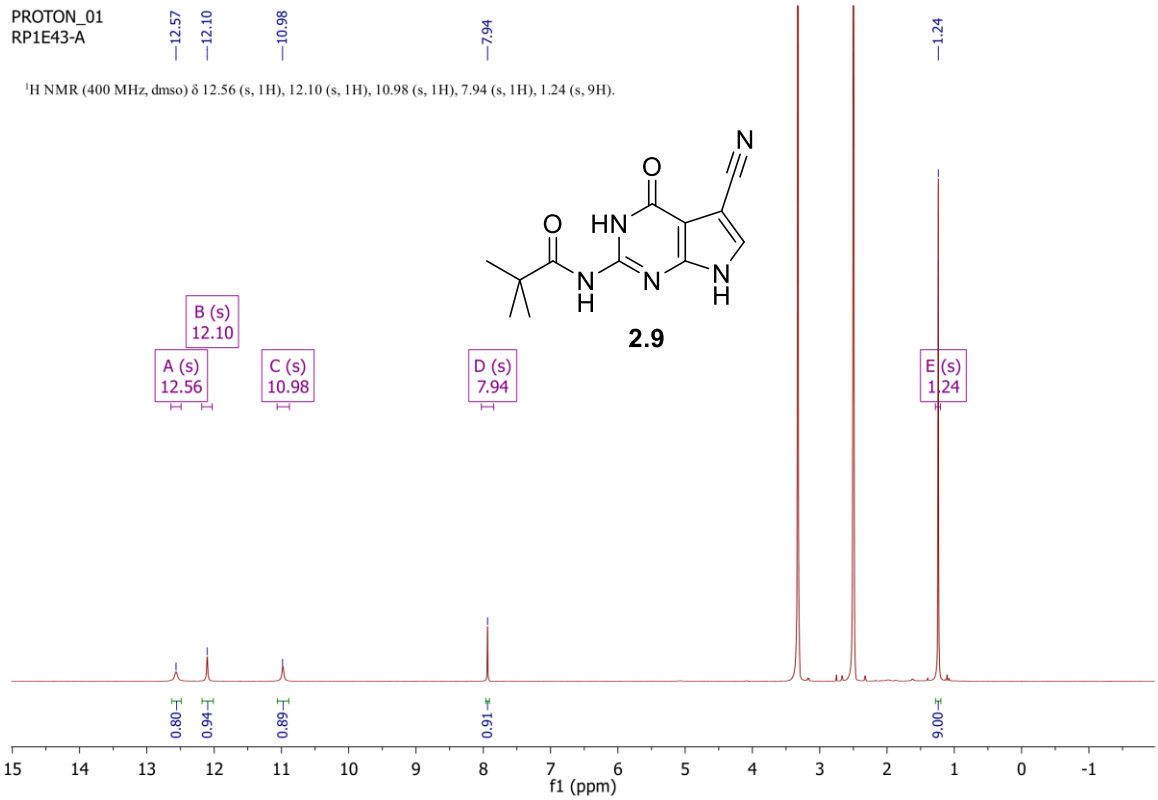
PROTON_01
RP1E43-A
12.57
12.10
10.98
7.94
1.24
¹H NMR (400 MHz, dmso) δ 12.56 (s, 1H), 12.10 (s, 1H), 10.98 (s, 1H), 7.94 (s, 1H), 1.24 (s, 9H).
2.9
B (s) 12.10
A (s) 12.56
C (s) 10.98
D (s) 7.94
E (s) 1.24
0.80
0.94
0.89
0.91
9.00
f1 (ppm)

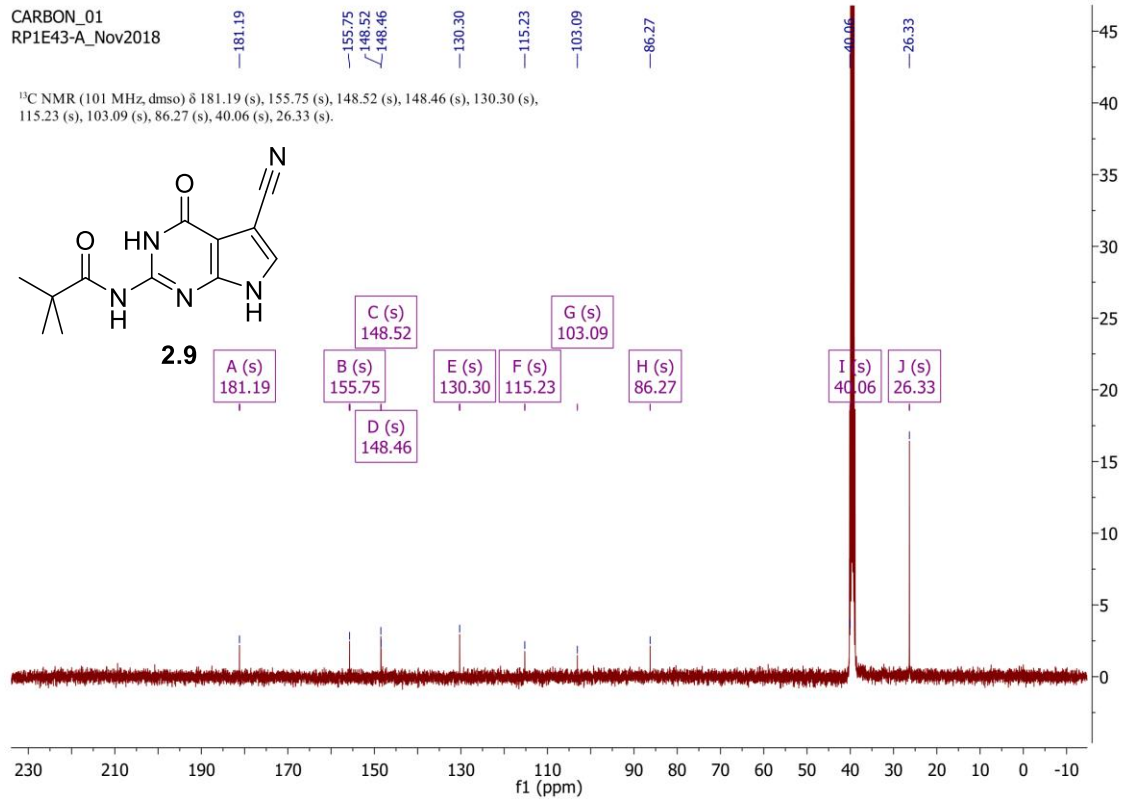
CARBON_01
RP1E43-A_Nov2018
181.19
155.75
148.52
148.46
130.30
115.23
103.09
86.27
40.06
26.33
¹³C NMR (101 MHz, dmso) δ 181.19 (s), 155.75 (s), 148.52 (s), 148.46 (s), 130.30 (s), 115.23 (s), 103.09 (s), 86.27 (s), 40.06 (s), 26.33 (s).
2.9
A (s) 181.19
B (s) 155.75
C (s) 148.52
D (s) 148.46
E (s) 130.30
F (s) 115.23
G (s) 103.09
H (s) 86.27
I (s) 40.06
J (s) 26.33
f1 (ppm)

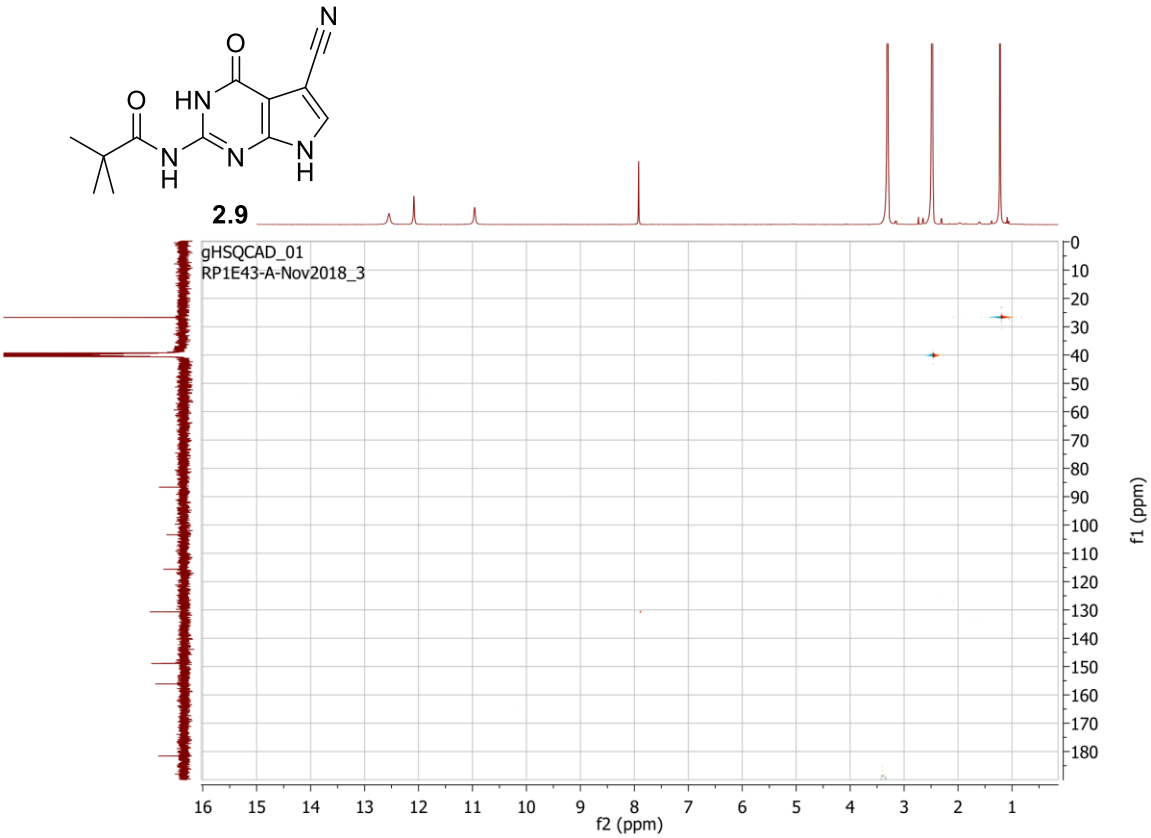

Trinity College Dublin

Bruker Open Access LC-MS - Formula Identification Report

Sample-ID		Station	
Submitter		Supervisor	
Analysis Name	RP1E43-A_RA8_01_15913.d	Acquisition Date	21/06/2018 12:34:02
Sample Description			

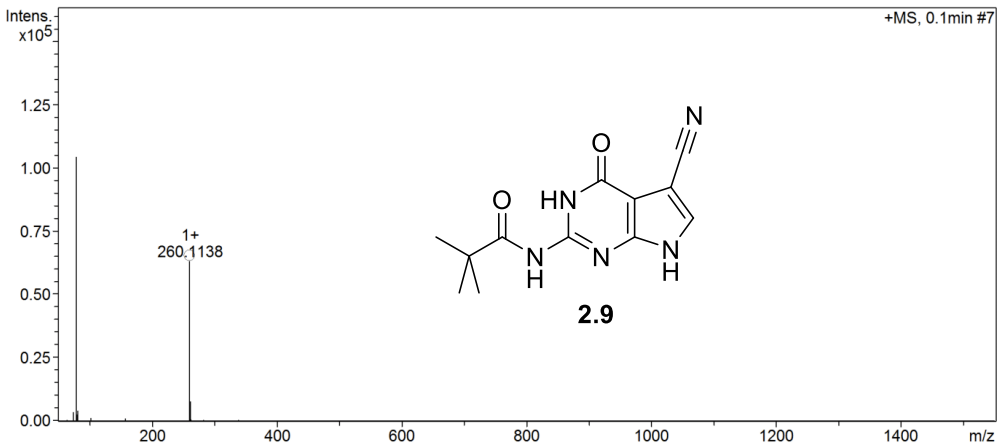

Meas. m/z	#	Ion Formula	m/z	err [mDa]	err [ppm]	rdb	N-Rule	e⁻ Conf	mSigma
260.113837	1	C12H14N5O2	260.114201	-0.4	-1.4	8.5	ok	even	16.4

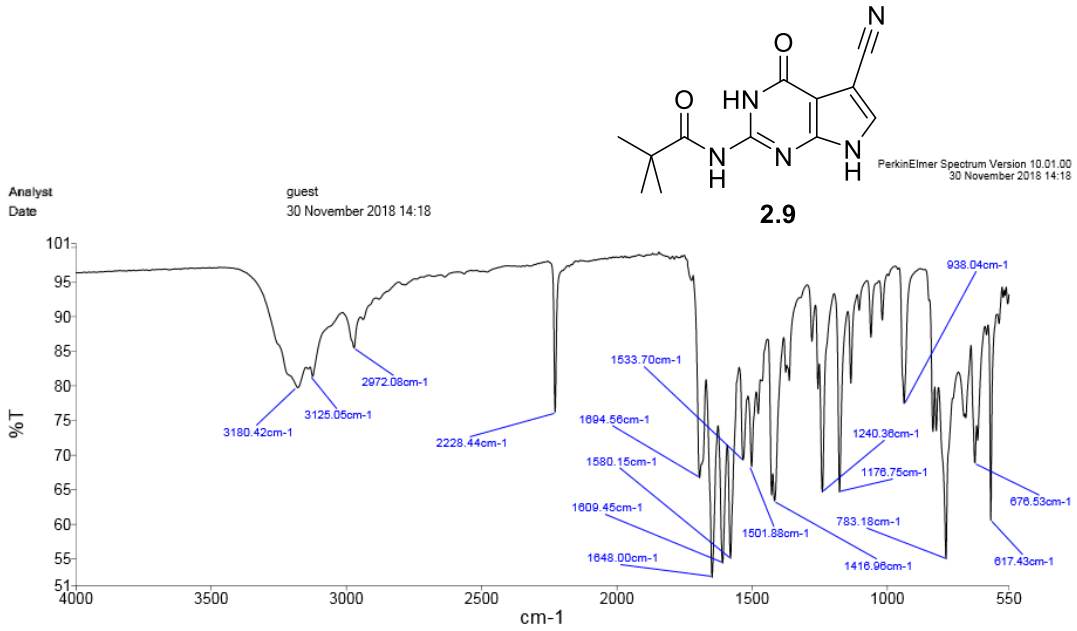

Sample Name	Description	Quality Checks
RPP04	Sample 004 By guest1 Date Friday, November 30 2018	The Quality Checks do not report any warnings for the sample.

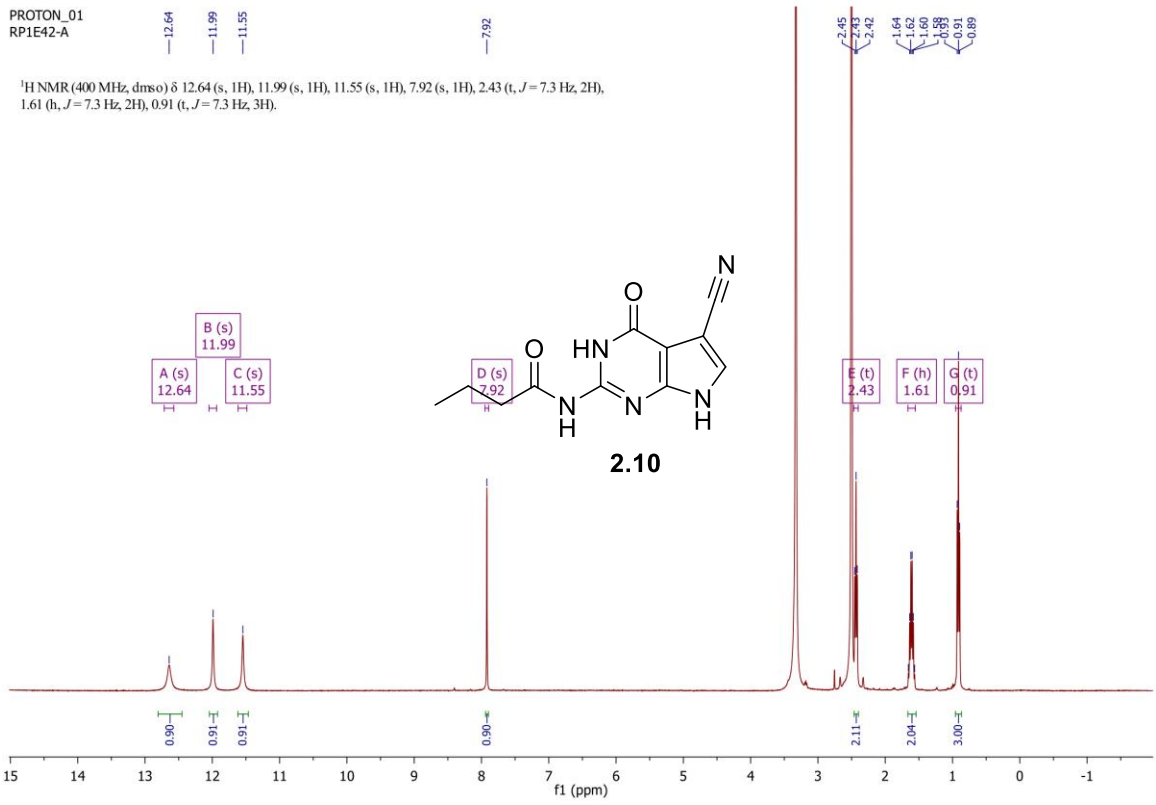

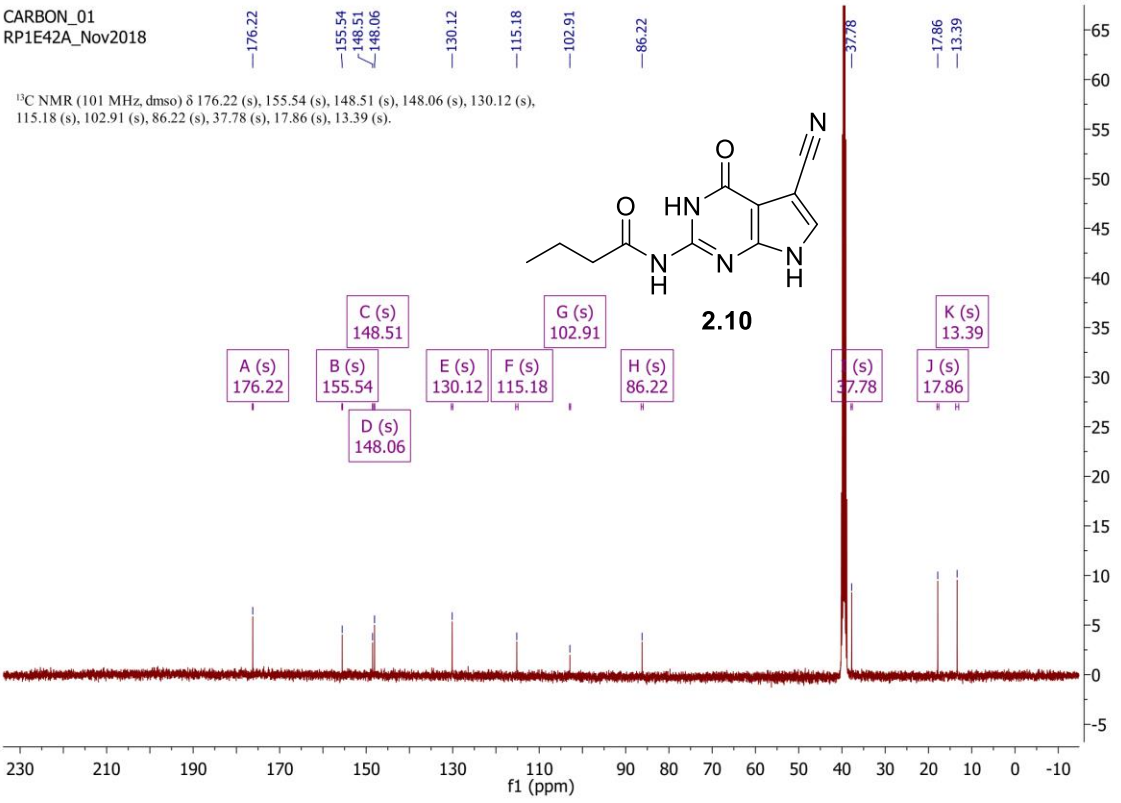
CARBON_01
RP1E42A_Nov2018
176.22
155.54
148.51
148.06
130.12
115.18
102.91
86.22
37.78
17.86
13.39
13C NMR (101 MHz, dmso) δ 176.22 (s), 155.54 (s), 148.51 (s), 148.06 (s), 130.12 (s), 115.18 (s), 102.91 (s), 86.22 (s), 37.78 (s), 17.86 (s), 13.39 (s).
2.10
A (s) 176.22
B (s) 155.54
C (s) 148.51
D (s) 148.06
E (s) 130.12
F (s) 115.18
G (s) 102.91
H (s) 86.22
J (s) 17.86
K (s) 13.39
f1 (ppm)

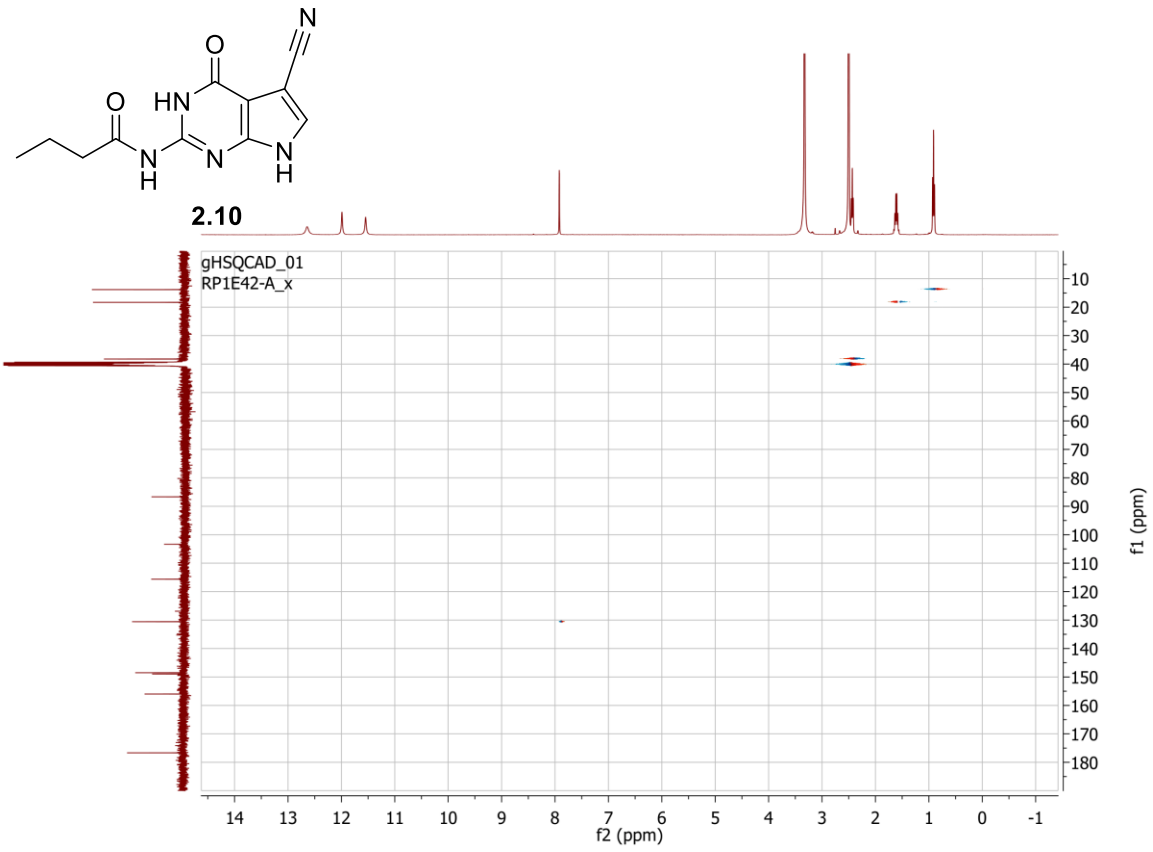
2.10
gHSQCAD_01
RP1E42-A_x
f2 (ppm)
f1 (ppm)

Trinity College Dublin

Bruker Open Access LC-MS - Formula Identification Report

Sample-ID		Station	
Submitter		Supervisor	
Analysis Name	RP1E42-A_RA6_01_15911.d	Acquisition Date	21/06/2018 12:27:26
Sample Description			

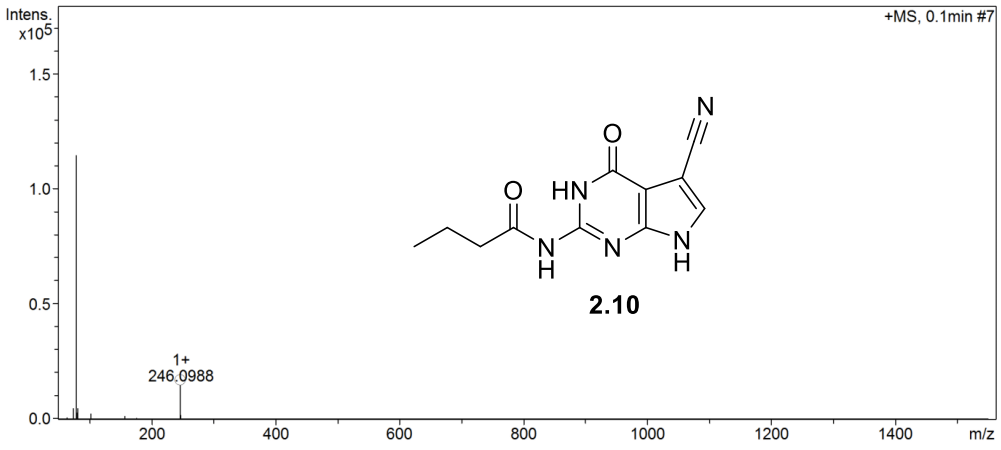

Meas. m/z	#	Ion Formula	m/z	err [mDa]	err [ppm]	rdb	N-Rule	e⁻ Conf	mSigma
246.098812	1	C11H12N5O2	246.098551	0.3	1.1	8.5	ok	even	10.1

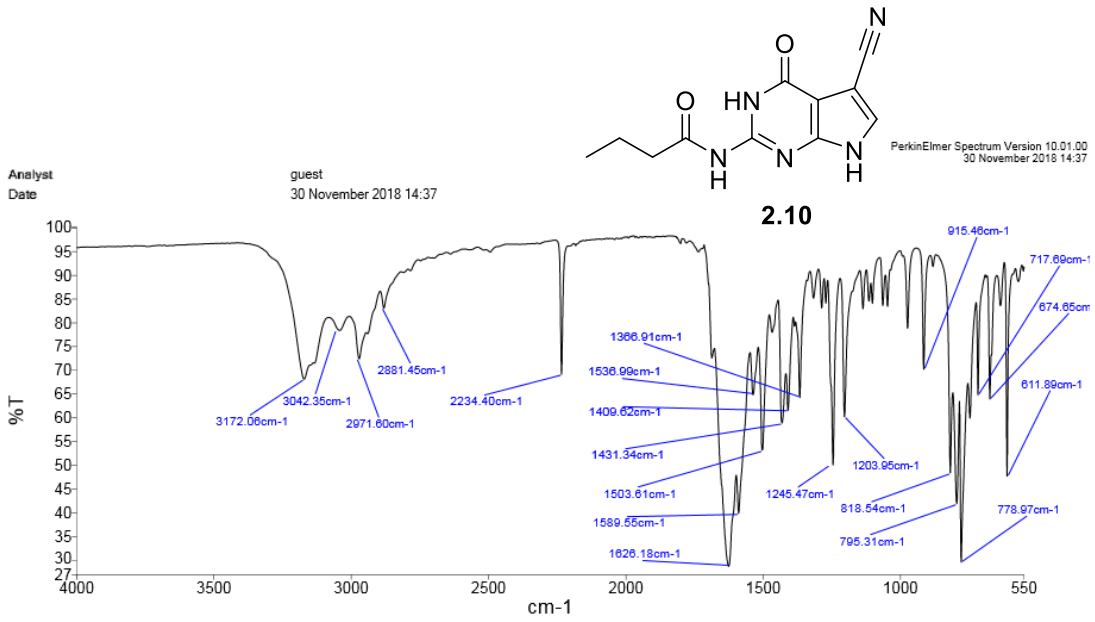

Sample Name	Description	Quality Checks
RPP06	Sample 006 By guest1 Date Friday, November 30 2018	The Quality Checks do not report any warnings for the sample.

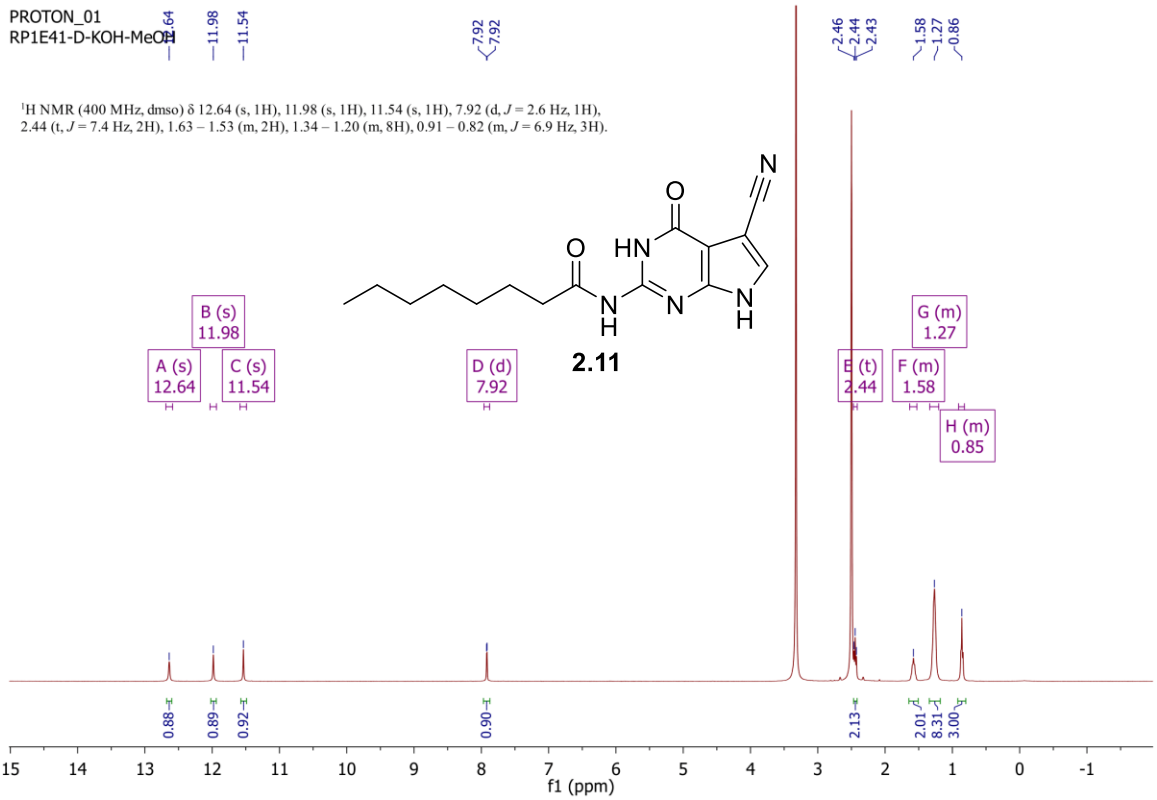
PROTON_01
RP1E41-D-KOH-MeOH
12.64
11.98
11.54
7.92
7.92
2.46
2.44
2.43
1.58
1.27
0.86
¹H NMR (400 MHz, dmso) δ 12.64 (s, 1H), 11.98 (s, 1H), 11.54 (s, 1H), 7.92 (d, J = 2.6 Hz, 1H), 2.44 (t, J = 7.4 Hz, 2H), 1.63 – 1.53 (m, 2H), 1.34 – 1.20 (m, 8H), 0.91 – 0.82 (m, J = 6.9 Hz, 3H).
B (s) 11.98
A (s) 12.64
C (s) 11.54
D (d) 7.92
E (t) 2.44
F (m) 1.58
G (m) 1.27
H (m) 0.85
2.11
0.88
0.89
0.92
0.90
2.13
2.01
8.31
3.00
f1 (ppm)

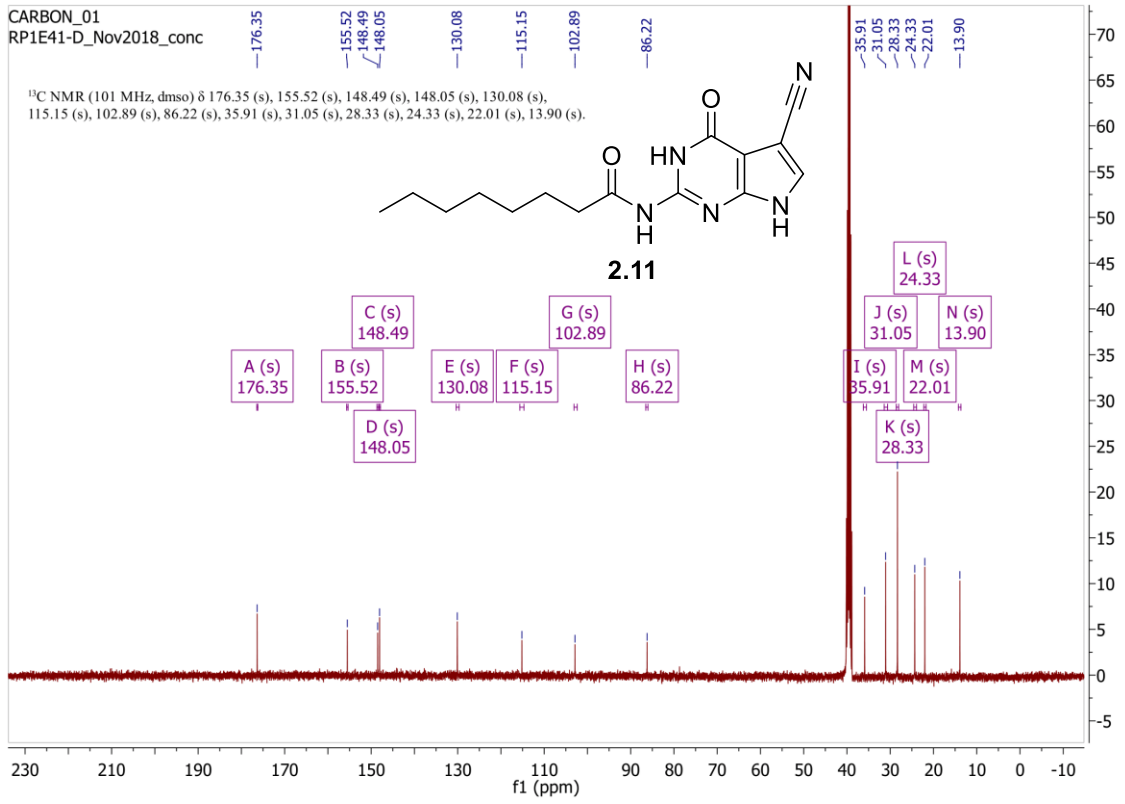
CARBON_01
RP1E41-D_Nov2018_conc
176.35
155.52
148.49
148.05
130.08
115.15
102.89
86.22
35.91
31.05
28.33
24.33
22.01
13.90
¹³C NMR (101 MHz, dmso) δ 176.35 (s), 155.52 (s), 148.49 (s), 148.05 (s), 130.08 (s), 115.15 (s), 102.89 (s), 86.22 (s), 35.91 (s), 31.05 (s), 28.33 (s), 24.33 (s), 22.01 (s), 13.90 (s).
A (s) 176.35
B (s) 155.52
C (s) 148.49
D (s) 148.05
E (s) 130.08
F (s) 115.15
G (s) 102.89
H (s) 86.22
I (s) 35.91
J (s) 31.05
K (s) 28.33
L (s) 24.33
M (s) 22.01
N (s) 13.90
2.11
f1 (ppm)

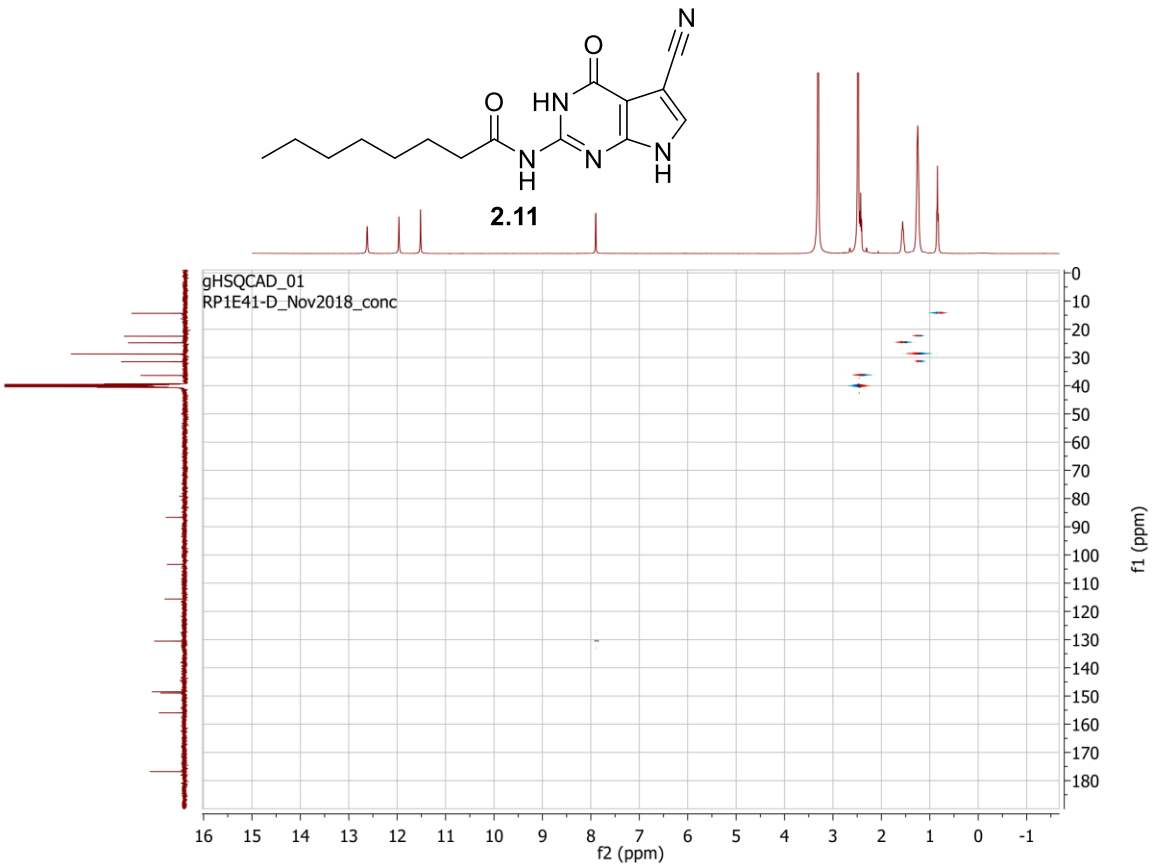

Trinity College Dublin

Bruker Open Access LC-MS - Formula Identification Report

Sample-ID		Station	
Submitter		Supervisor	
Analysis Name	RP1E41-D_RA5_01_15921.d	Acquisition Date	21/06/2018 13:08:20
Sample Description			

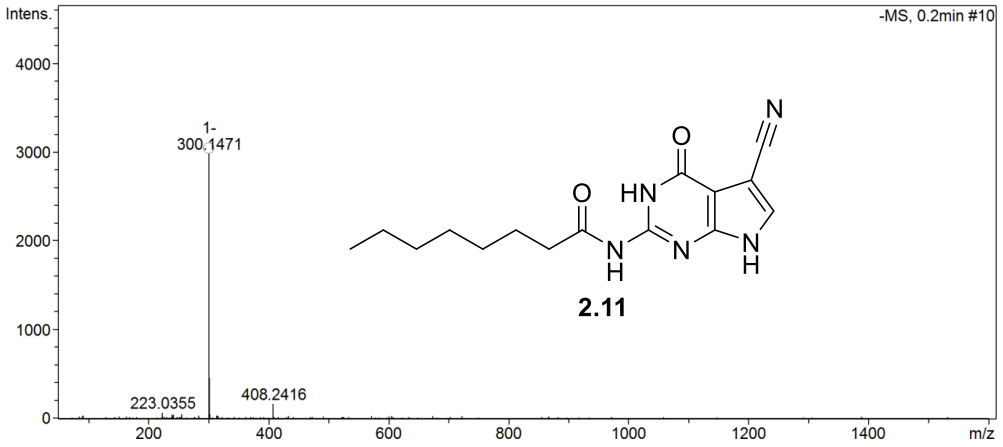

Meas. m/z	#	Ion Formula	m/z	err [mDa]	err [ppm]	rdb	N-Rule	e⁻ Conf	mSigma
300.147130	1	C15H18N5O2	300.146598	-0.5	-1.8	9.5	ok	even	17.8

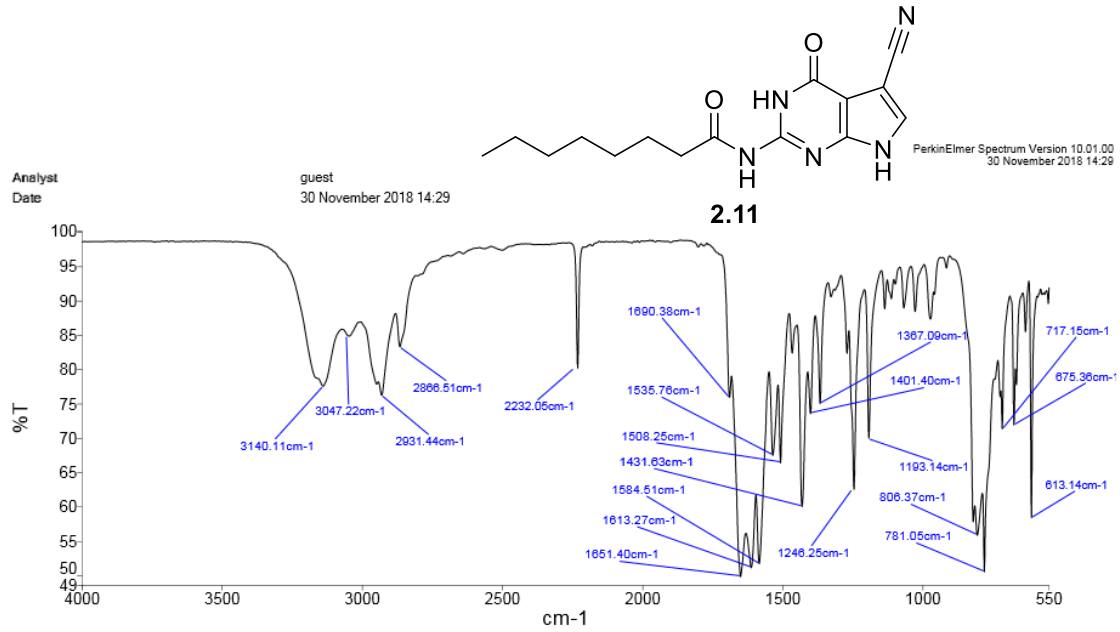

Sample Name	Description	Quality Checks
RPP05	Sample 005 By guest1 Date Friday, November 30 2018	The Quality Checks do not report any warnings for the sample.

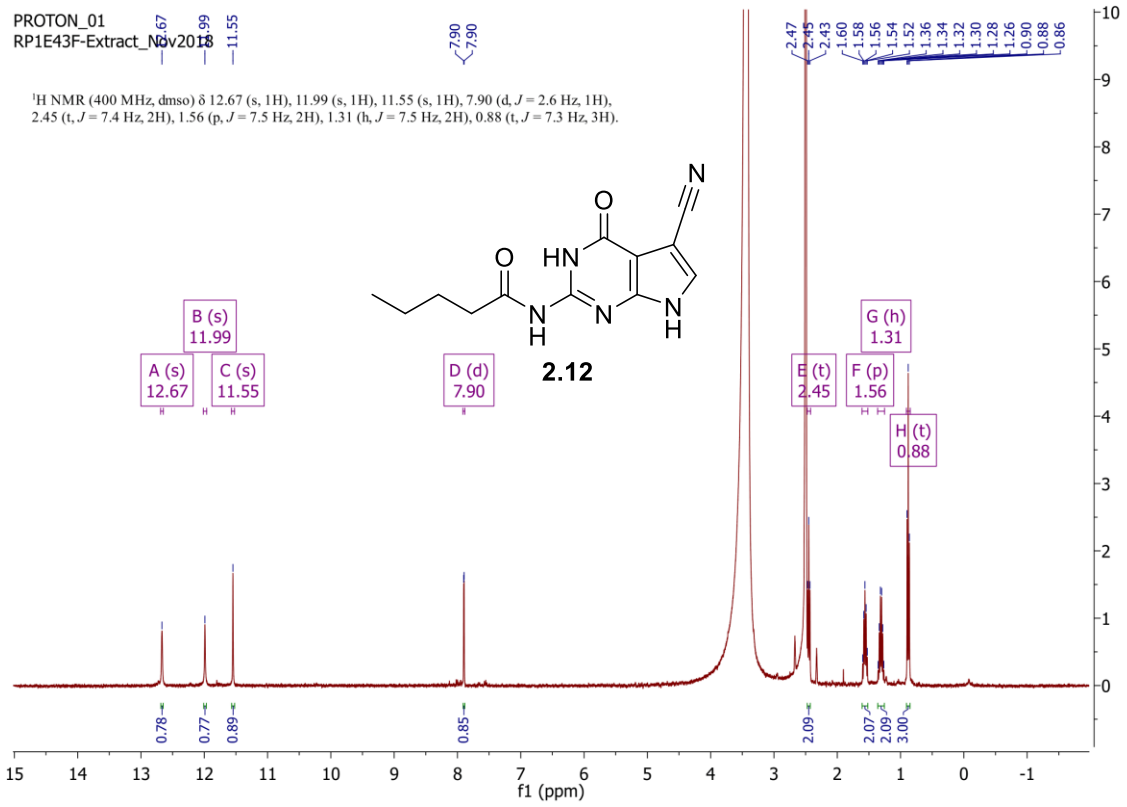

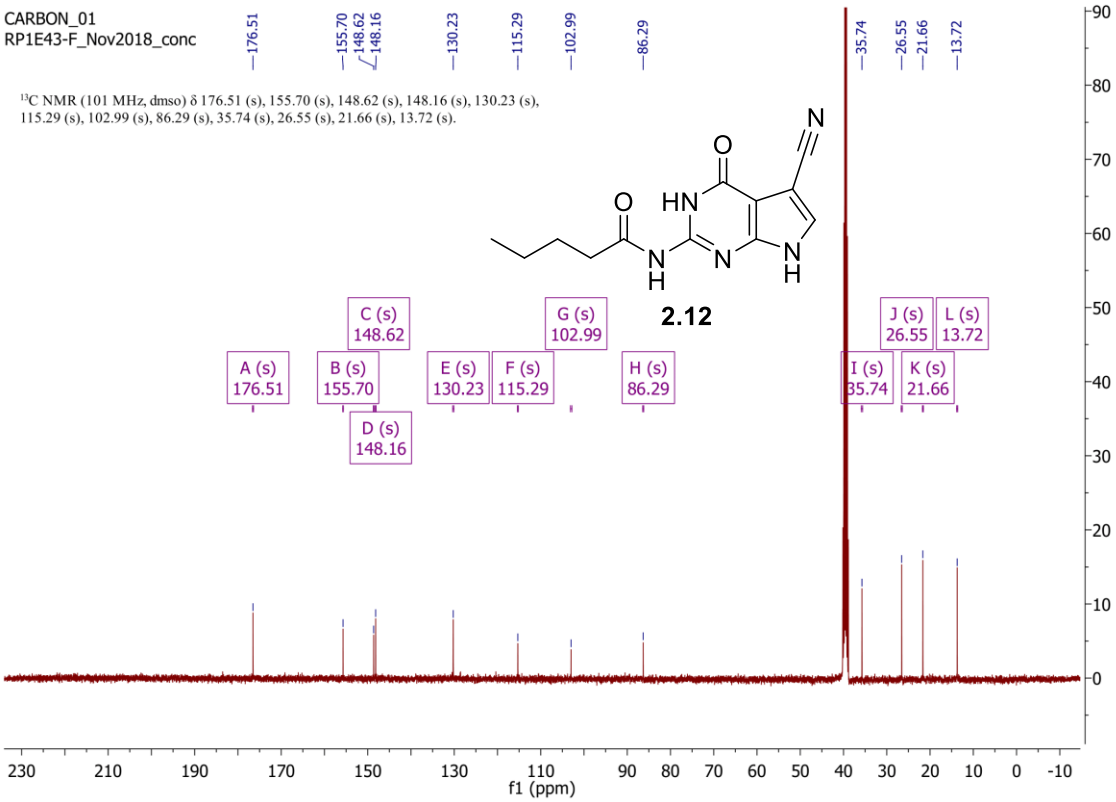
CARBON_01
RP1E43-F_Nov2018_conc
176.51
155.70
148.62
148.16
130.23
115.29
102.99
86.29
35.74
26.55
21.66
13.72
13C NMR (101 MHz, dmso) δ 176.51 (s), 155.70 (s), 148.62 (s), 148.16 (s), 130.23 (s), 115.29 (s), 102.99 (s), 86.29 (s), 35.74 (s), 26.55 (s), 21.66 (s), 13.72 (s).
2.12
A (s) 176.51
B (s) 155.70
C (s) 148.62
D (s) 148.16
E (s) 130.23
F (s) 115.29
G (s) 102.99
H (s) 86.29
I (s) 35.74
J (s) 26.55
K (s) 21.66
L (s) 13.72
f1 (ppm)

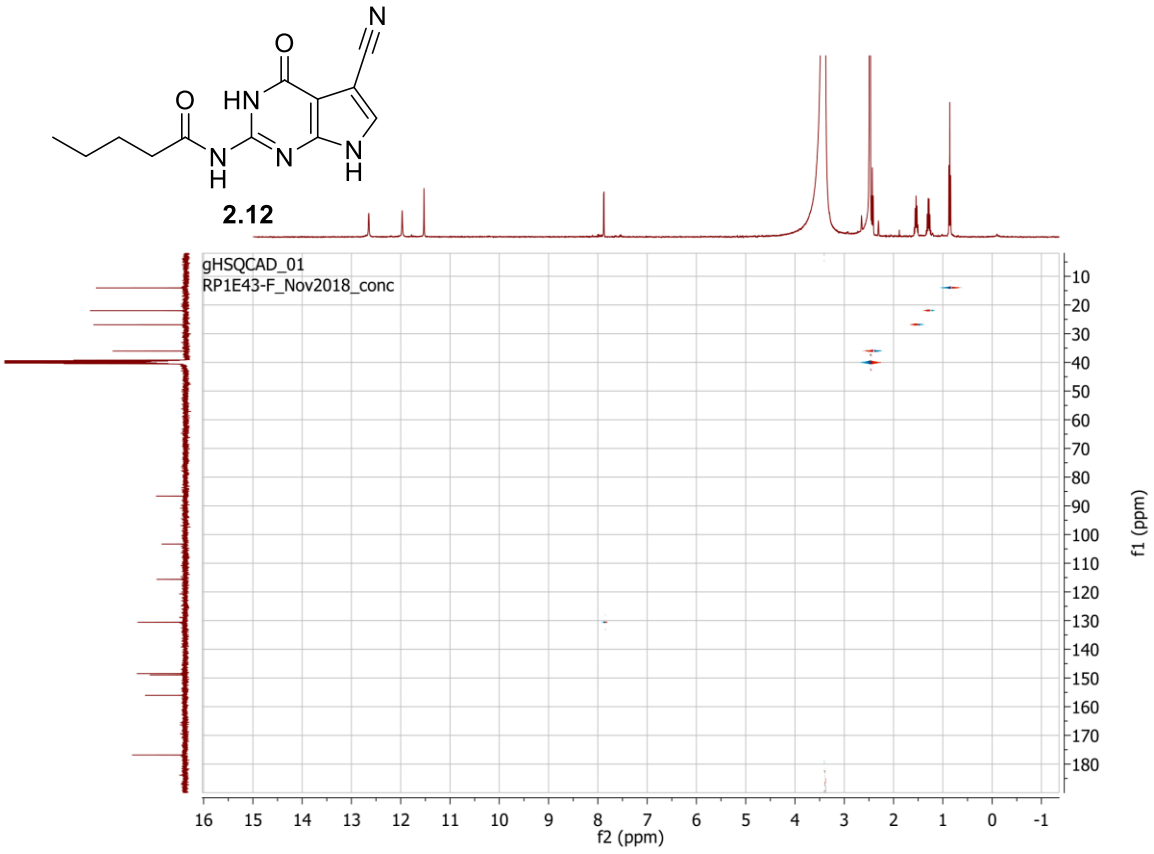
2.12
gHSQCAD_01
RP1E43-F_Nov2018_conc
f2 (ppm)
f1 (ppm)

Trinity College Dublin

Bruker Open Access LC-MS - Formula Identification Report

Sample-ID		Station	
Submitter		Supervisor	
Analysis Name	RP1E43-F_RB1_01_15914.d	Acquisition Date	21/06/2018 12:37:18
Sample Description			

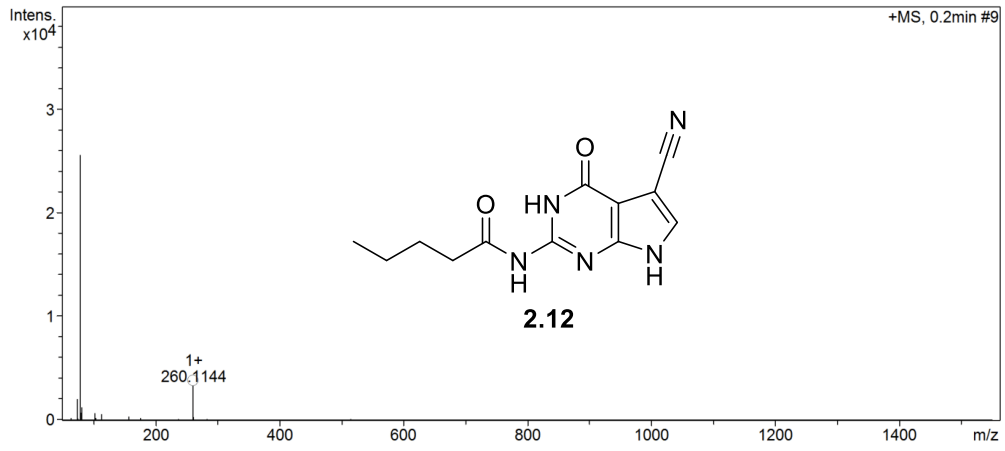

Meas. m/z	#	Ion Formula	m/z	err [mDa]	err [ppm]	rdb	N-Rule	e⁻ Conf	mSigma
260.114422	1	C12H14N5O2	260.114201	0.2	0.9	8.5	ok	even	35.1

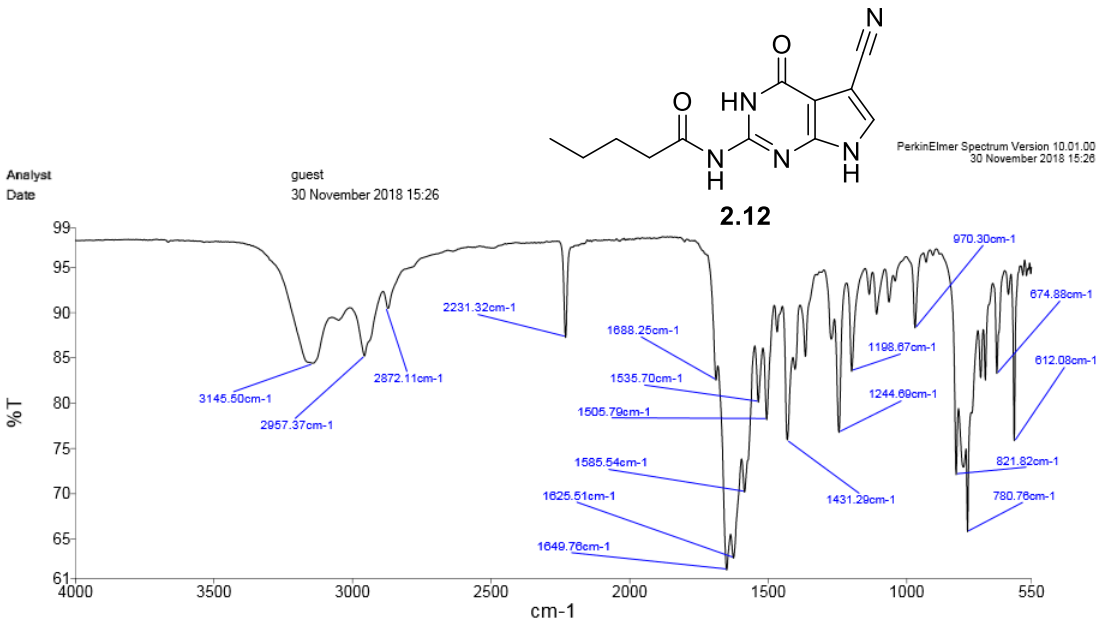

Sample Name	Description	Quality Checks
RPP11	Sample 011 By guest1 Date Friday, November 30 2018	The Quality Checks do not report any warnings for the sample.

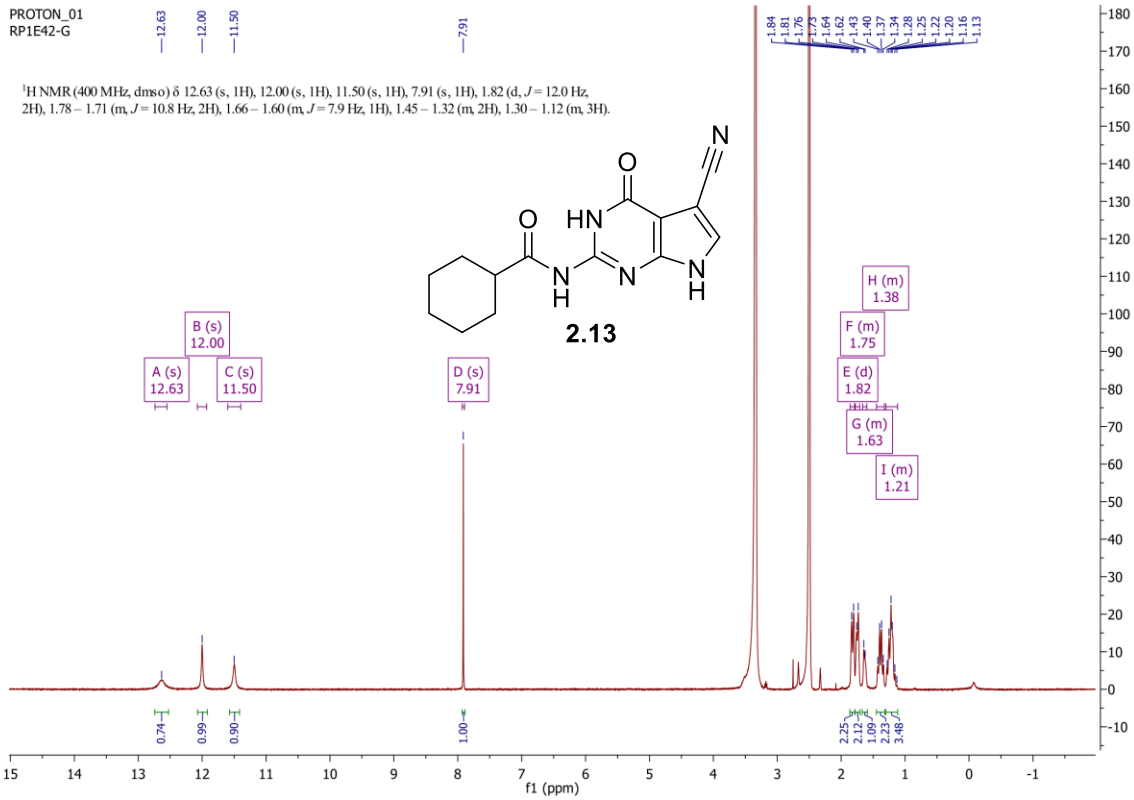
PROTON_01
RP1E42-G
12.63
12.00
11.50
7.91
1.84
1.81
1.78
1.76
1.73
1.64
1.62
1.43
1.40
1.37
1.34
1.28
1.25
1.22
1.20
1.16
1.13
[1]H NMR (400 MHz, dmso) δ 12.63 (s, 1H), 12.00 (s, 1H), 11.50 (s, 1H), 7.91 (s, 1H), 1.82 (d, J = 12.0 Hz, 2H), 1.78 – 1.71 (m, J = 10.8 Hz, 2H), 1.66 – 1.60 (m, J = 7.9 Hz, 1H), 1.45 – 1.32 (m, 2H), 1.30 – 1.12 (m, 3H).
2.13
A (s) 12.63
B (s) 12.00
C (s) 11.50
D (s) 7.91
E (d) 1.82
F (m) 1.75
G (m) 1.63
H (m) 1.38
I (m) 1.21
0.74
0.99
0.90
1.00
2.25
2.12
1.09
2.23
3.48
f1 (ppm)

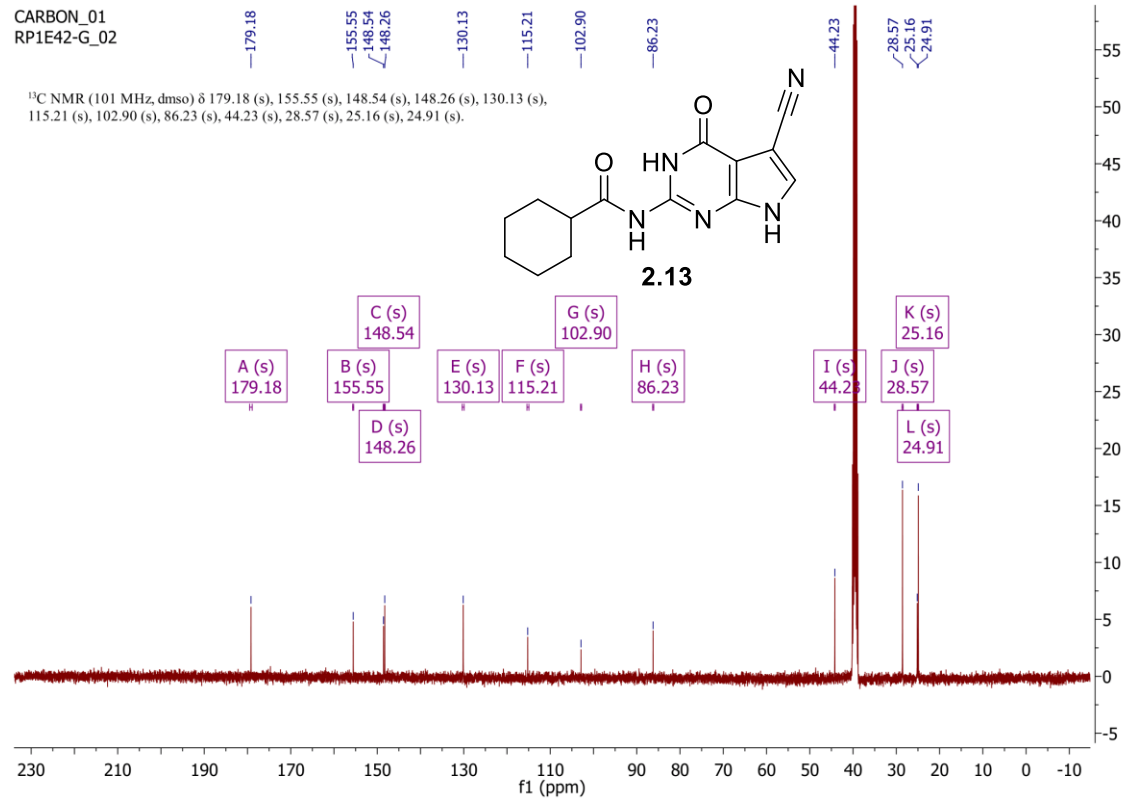
CARBON_01
RP1E42-G_02
179.18
155.55
148.54
148.26
130.13
115.21
102.90
86.23
44.23
28.57
25.16
24.91
[13]C NMR (101 MHz, dmso) δ 179.18 (s), 155.55 (s), 148.54 (s), 148.26 (s), 130.13 (s), 115.21 (s), 102.90 (s), 86.23 (s), 44.23 (s), 28.57 (s), 25.16 (s), 24.91 (s).
2.13
A (s) 179.18
B (s) 155.55
C (s) 148.54
D (s) 148.26
E (s) 130.13
F (s) 115.21
G (s) 102.90
H (s) 86.23
I (s) 44.23
J (s) 28.57
K (s) 25.16
L (s) 24.91
f1 (ppm)

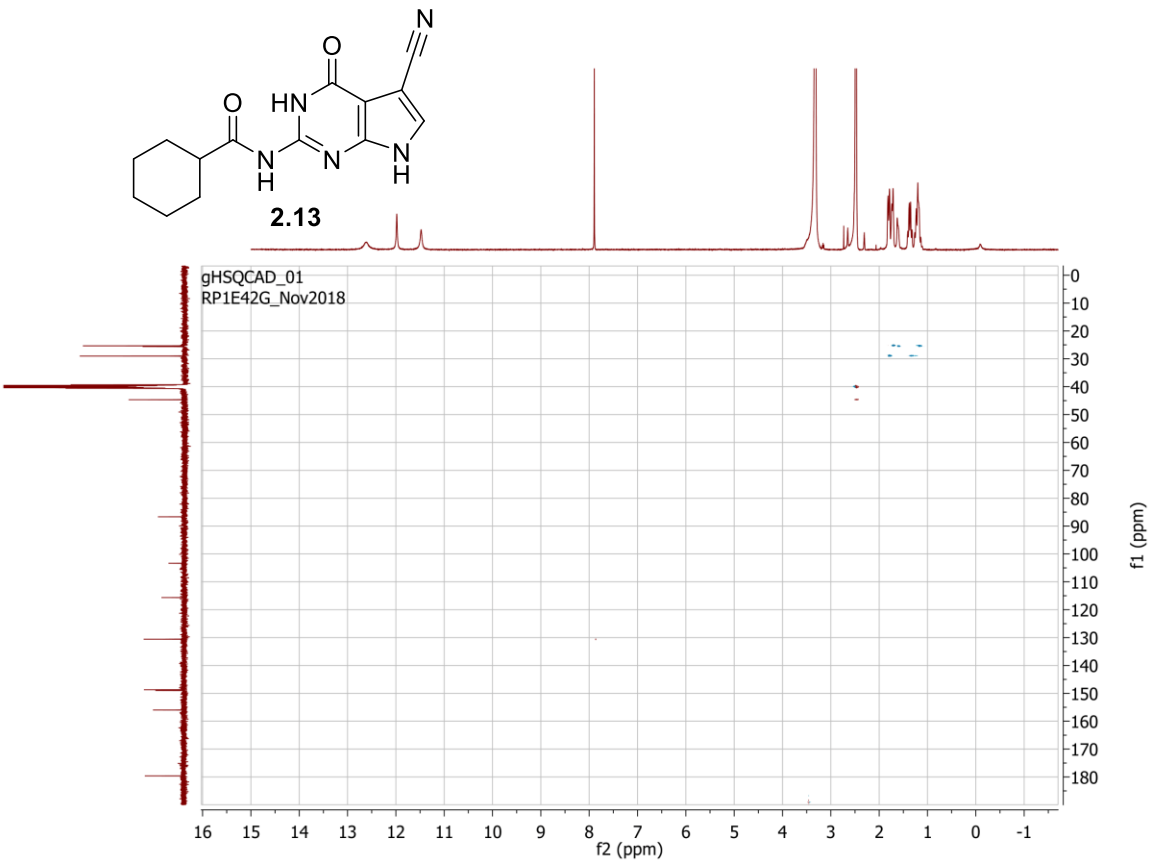
2.13
gHSQCAD_01
RP1E42G_Nov2018
f2 (ppm)
f1 (ppm)

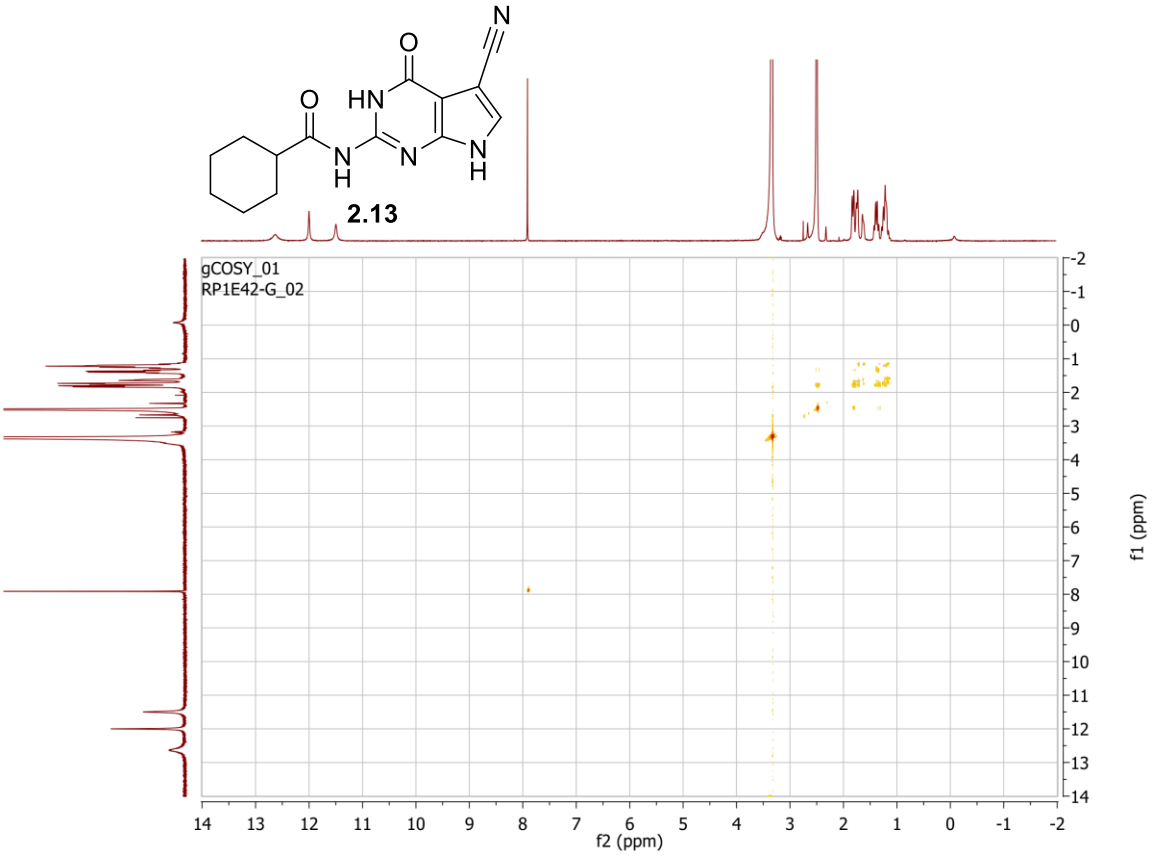
2.13
gCOSY_01
RP1E42-G_02
f2 (ppm)
f1 (ppm)

Trinity College Dublin

Bruker Open Access LC-MS - Formula Identification Report

Sample-ID		Station	
Submitter		Supervisor	
Analysis Name	RPE1E42-G_RA8_01_14199.d	Acquisition Date	29/03/2018 10:55:58
Sample Description			

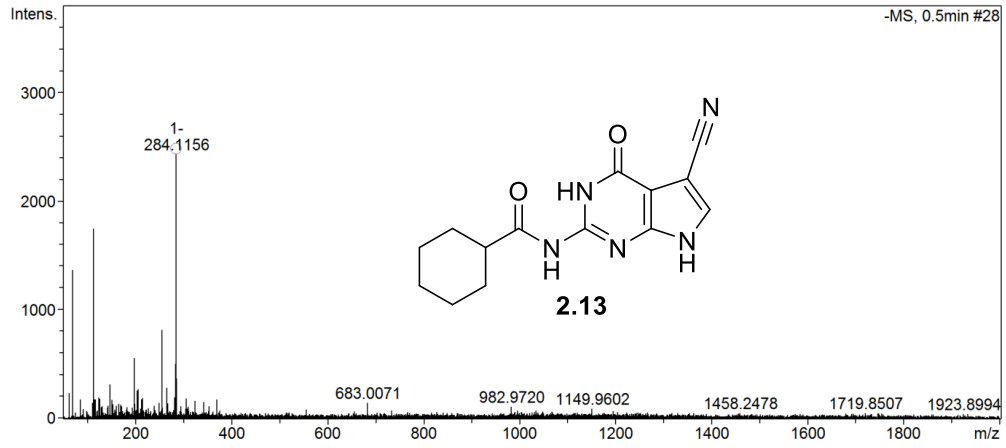

Meas. m/z	#	Ion Formula	m/z	err [mDa]	err [ppm]	rdb	N-Rule	e⁻ Conf	mSigma
284.115638	1	C14H14N5O2	284.115298	-0.3	-1.2	10.5	ok	even	13.2

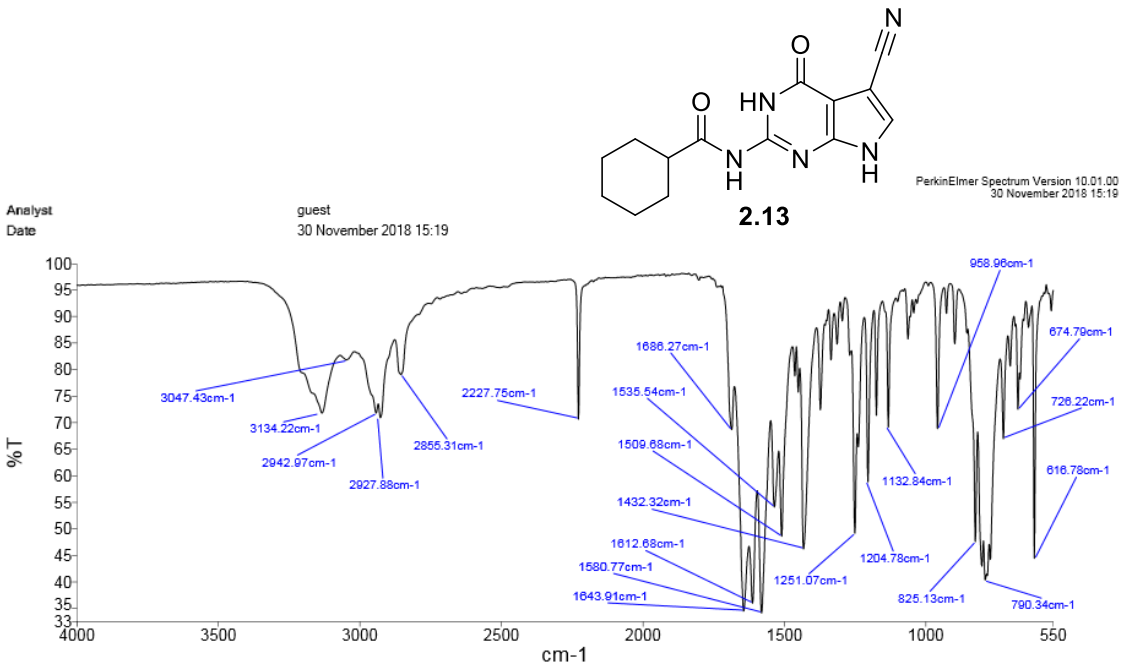

Sample Name	Description	Quality Checks
RPP10	Sample 010 By guest1 Date Friday, November 30 2018	The Quality Checks do not report any warnings for the sample.

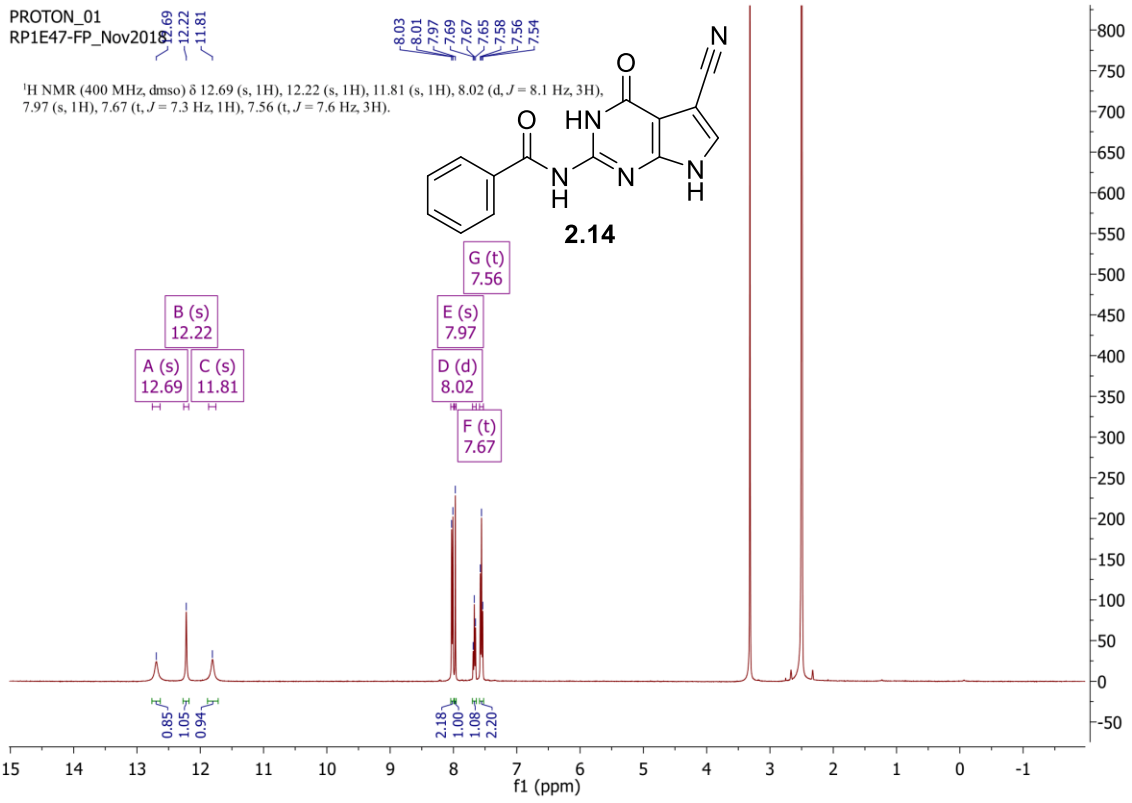
PROTON_01
RP1E47-FP_Nov2018
12.69
12.22
11.81
8.03
8.01
7.97
7.69
7.67
7.65
7.58
7.56
7.54
^{1}H NMR (400 MHz, dmso) δ 12.69 (s, 1H), 12.22 (s, 1H), 11.81 (s, 1H), 8.02 (d, J = 8.1 Hz, 3H), 7.97 (s, 1H), 7.67 (t, J = 7.3 Hz, 1H), 7.56 (t, J = 7.6 Hz, 3H).
2.14
G (t) 7.56
B (s) 12.22
E (s) 7.97
A (s) 12.69
C (s) 11.81
D (d) 8.02
F (t) 7.67
0.85
1.05
0.94
2.18
1.00
1.08
2.20
f1 (ppm)

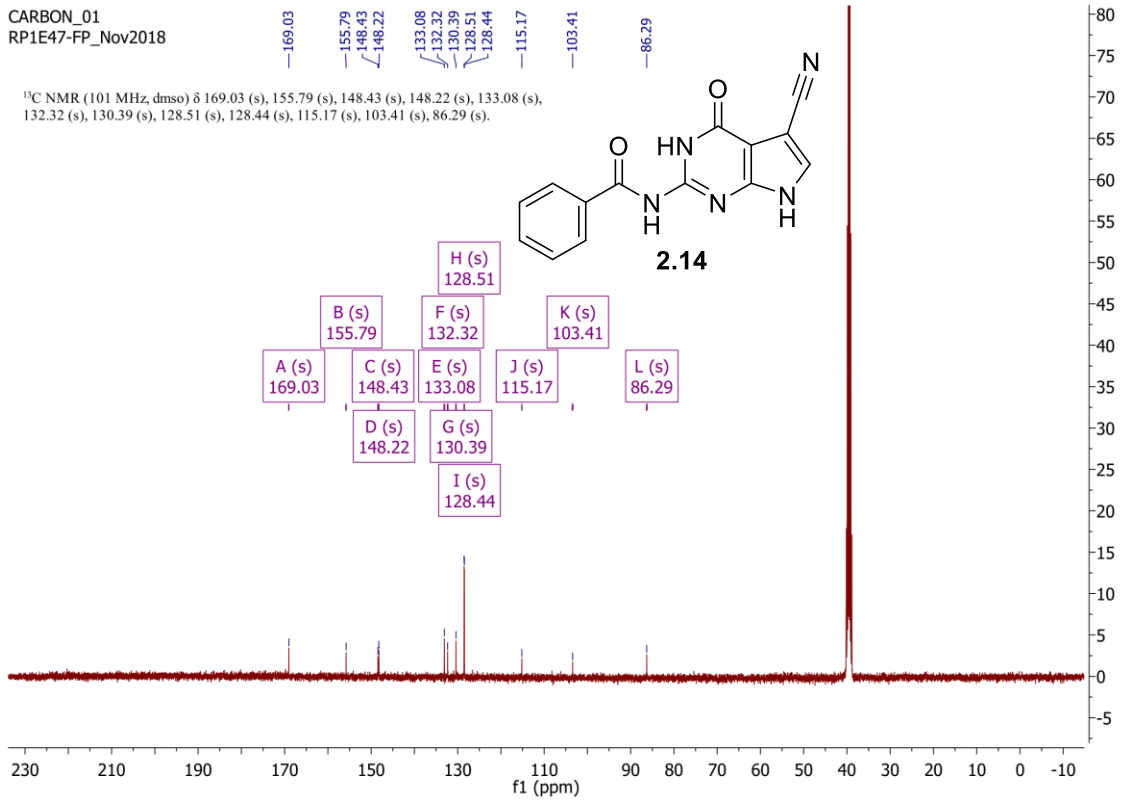
CARBON_01
RP1E47-FP_Nov2018
169.03
155.79
148.43
148.22
133.08
132.32
130.39
128.51
128.44
115.17
103.41
86.29
^{13}C NMR (101 MHz, dmso) δ 169.03 (s), 155.79 (s), 148.43 (s), 148.22 (s), 133.08 (s), 132.32 (s), 130.39 (s), 128.51 (s), 128.44 (s), 115.17 (s), 103.41 (s), 86.29 (s).
2.14
H (s) 128.51
B (s) 155.79
F (s) 132.32
K (s) 103.41
A (s) 169.03
C (s) 148.43
E (s) 133.08
J (s) 115.17
L (s) 86.29
D (s) 148.22
G (s) 130.39
I (s) 128.44
f1 (ppm)

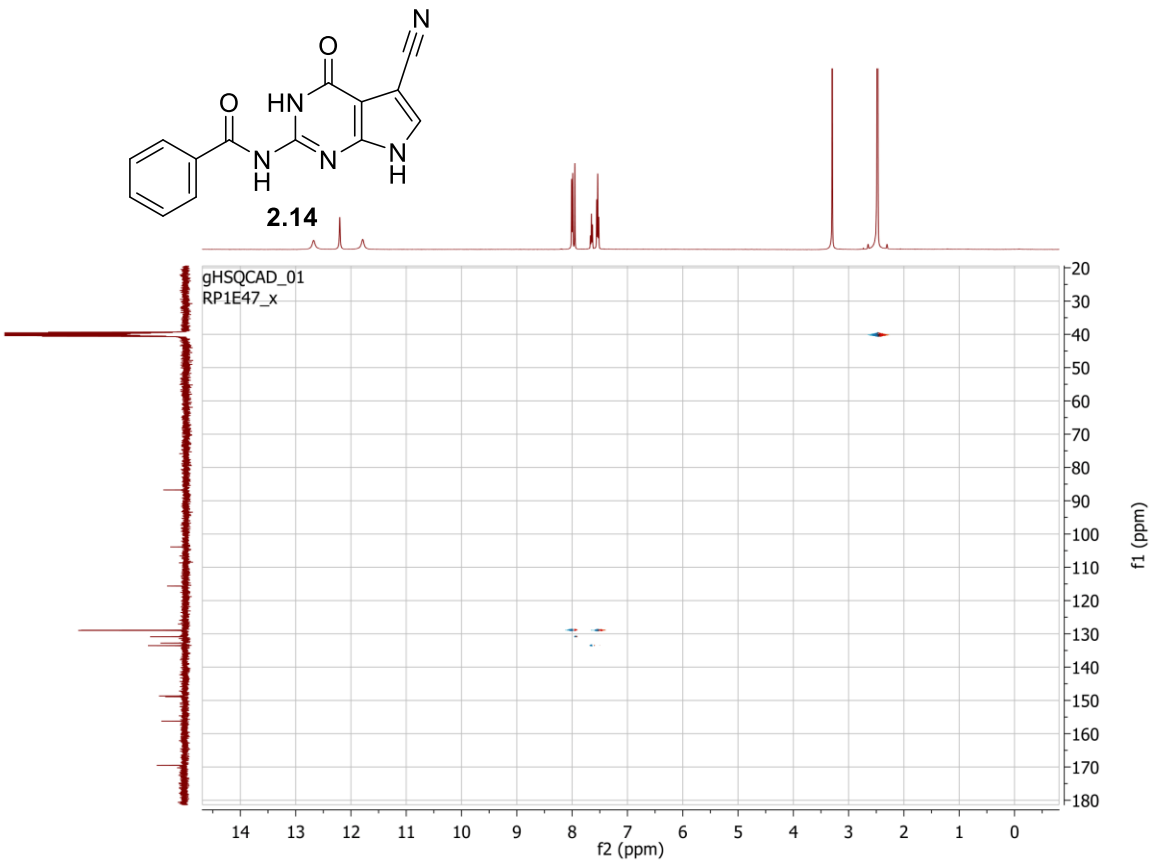

Trinity College Dublin

Bruker Open Access LC-MS - Formula Identification Report

Sample-ID		Station	
Submitter		Supervisor	
Analysis Name	RP1E47_RD5_01_18778.d	Acquisition Date	04/12/2018 17:00:45
Sample Description			

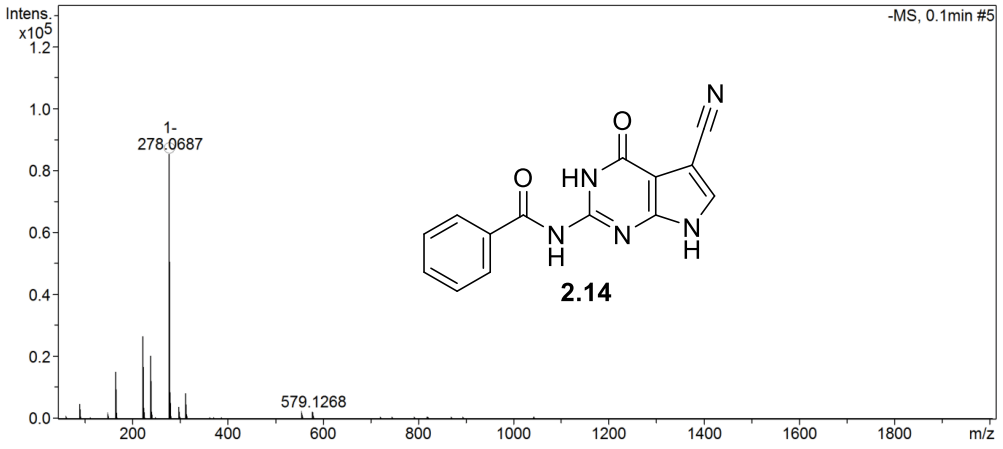

Meas. m/z	#	Ion Formula	m/z	err [mDa]	err [ppm]	rdb	N-Rule	e⁻ Conf	mSigma
278.068658	1	C14H8N5O2	278.068348	-0.3	-1.1	13.5	ok	even	42.6

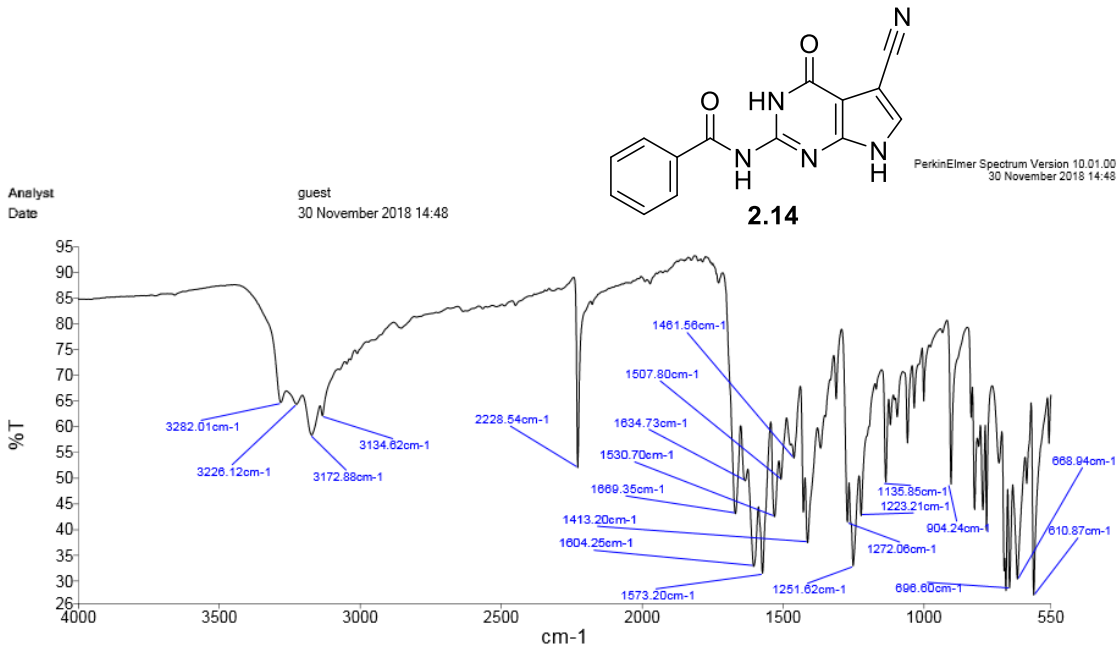

Sample Name	Description	Quality Checks
RPP07	Sample 007 By guest1 Date Friday, November 30 2018	The Quality Checks do not report any warnings for the sample.

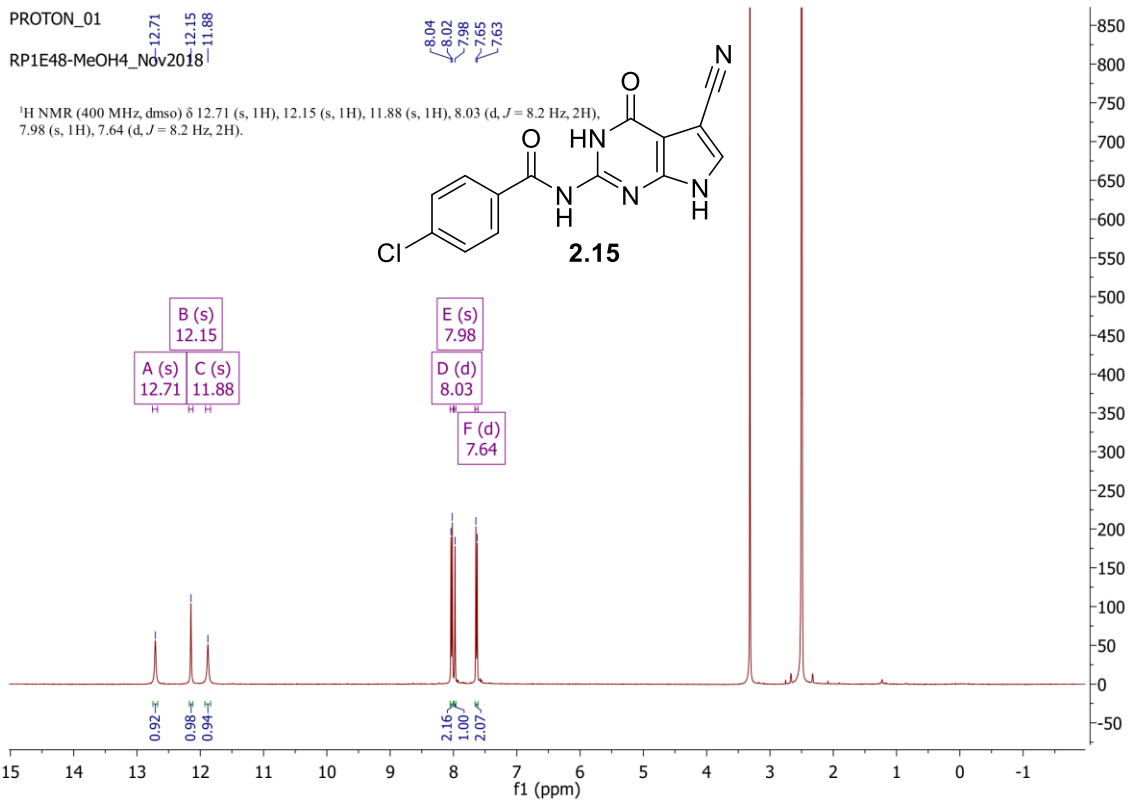

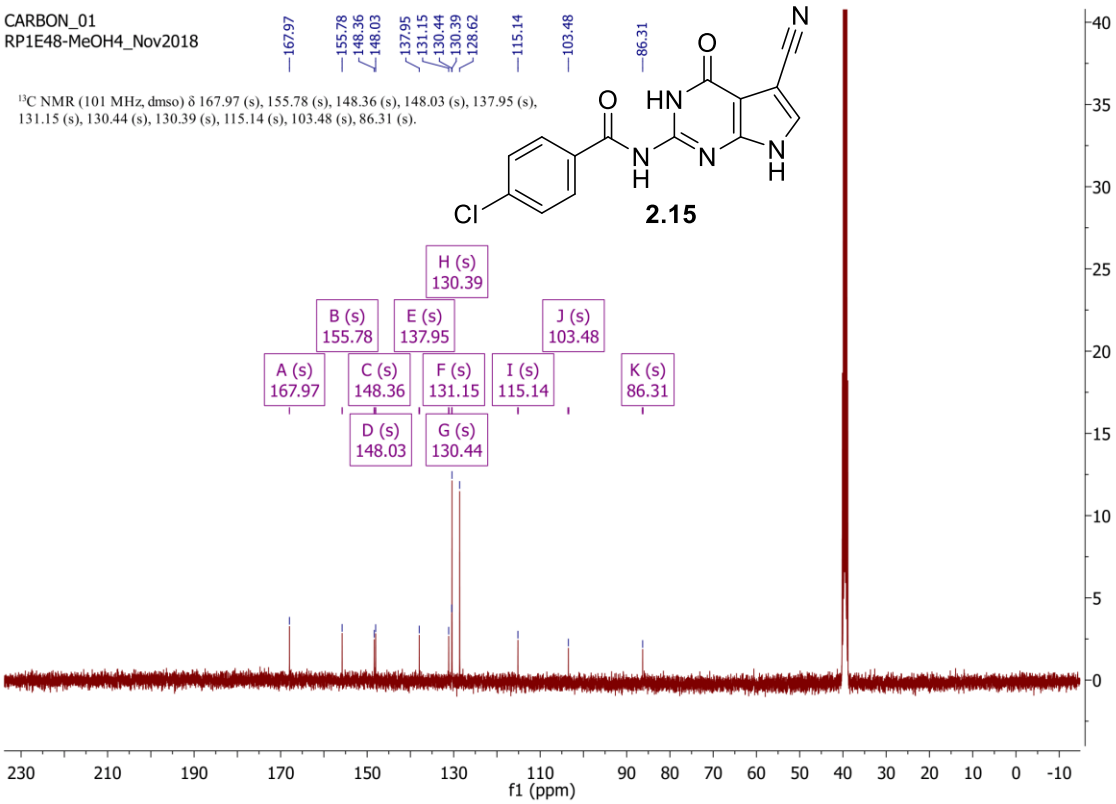
CARBON_01
RP1E48-MeOH4_Nov2018
167.97
155.78
148.36
148.03
137.95
131.15
130.44
130.39
128.62
115.14
103.48
86.31
13C NMR (101 MHz, dmso) δ 167.97 (s), 155.78 (s), 148.36 (s), 148.03 (s), 137.95 (s), 131.15 (s), 130.44 (s), 130.39 (s), 115.14 (s), 103.48 (s), 86.31 (s).
2.15
H (s) 130.39
B (s) 155.78
E (s) 137.95
J (s) 103.48
A (s) 167.97
C (s) 148.36
F (s) 131.15
I (s) 115.14
K (s) 86.31
D (s) 148.03
G (s) 130.44
f1 (ppm)

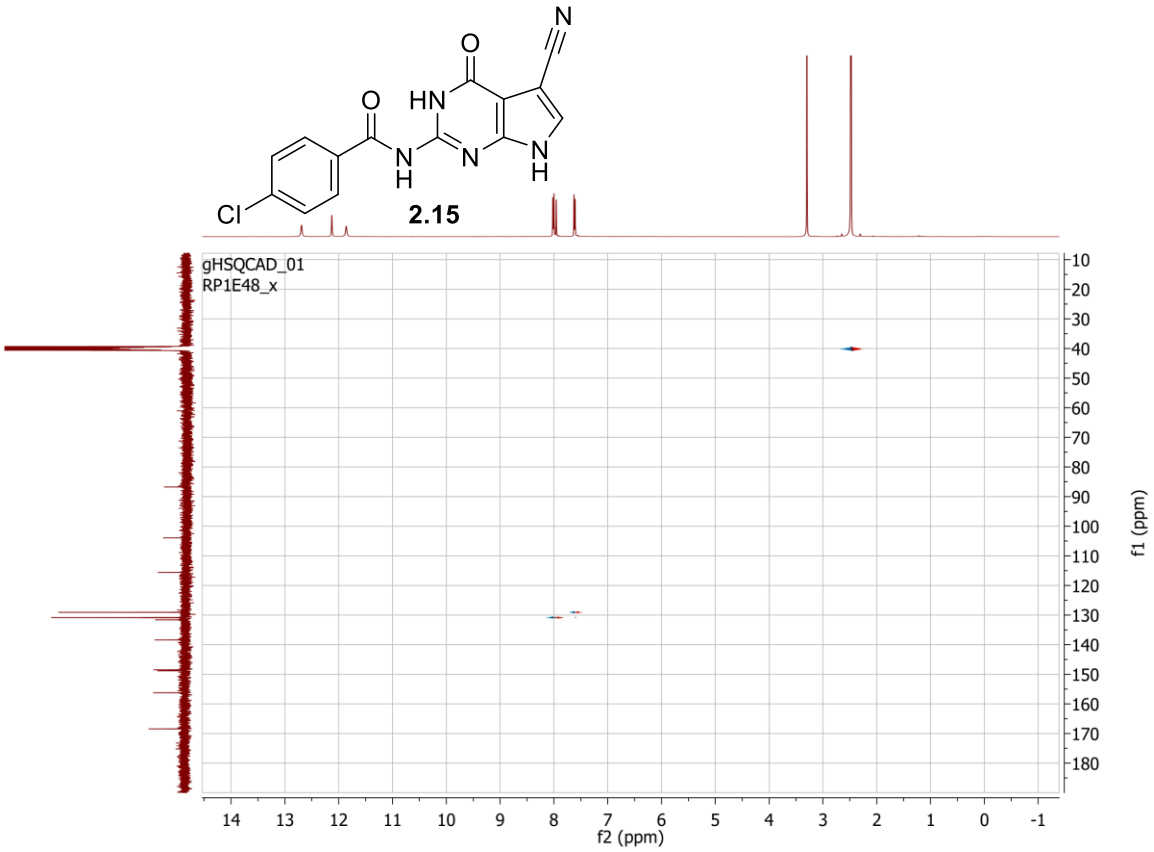
2.15
gHSQCAD_01
RP1E48_x
f2 (ppm)
f1 (ppm)

Trinity College Dublin

Bruker Open Access LC-MS - Formula Identification Report

Sample-ID		Station	
Submitter		Supervisor	
Analysis Name	RP1E48_RD2_01_18885.d	Acquisition Date	12/12/2018 11:03:34
Sample Description			

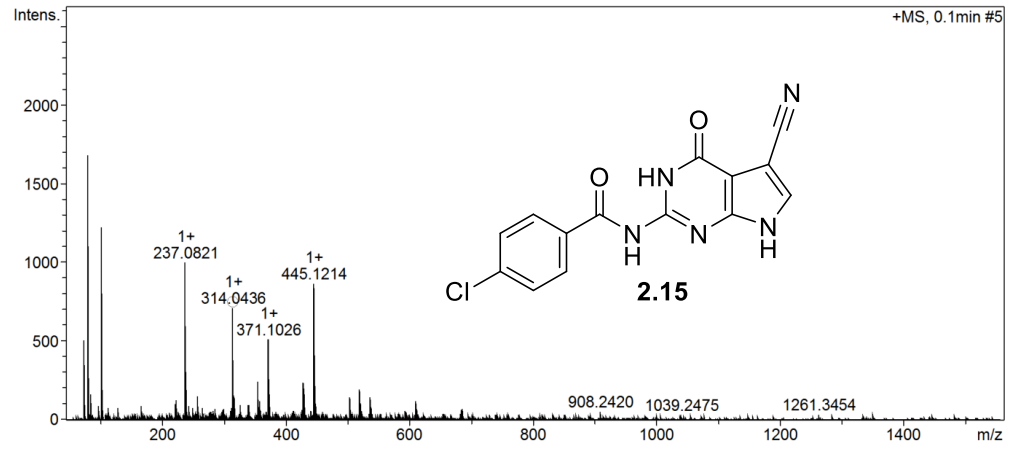

Meas. m/z	#	Ion Formula	m/z	err [mDa]	err [ppm]	rdb	N-Rule	e⁻ Conf	mSigma
314.043579	1	C14H9ClN5O2	314.043929	-0.4	-1.1	12.5	ok	even	62.4

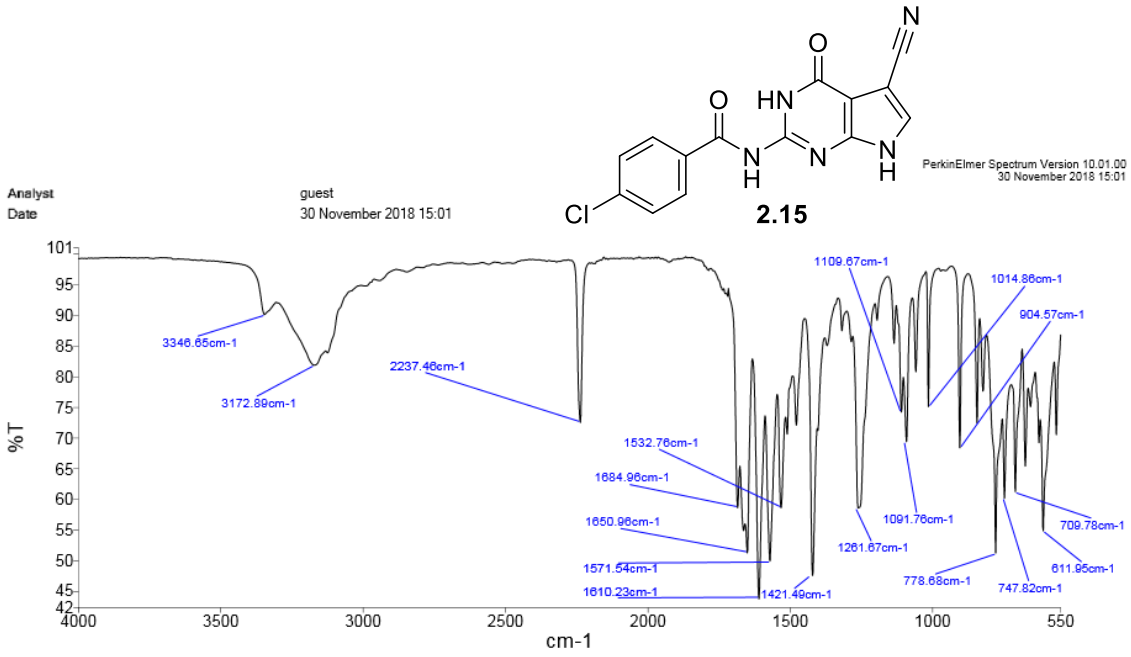

Sample Name	Description	Quality Checks
RPP08	Sample 008 By guest1 Date Friday, November 30 2018	The Quality Checks do not report any warnings for the sample.

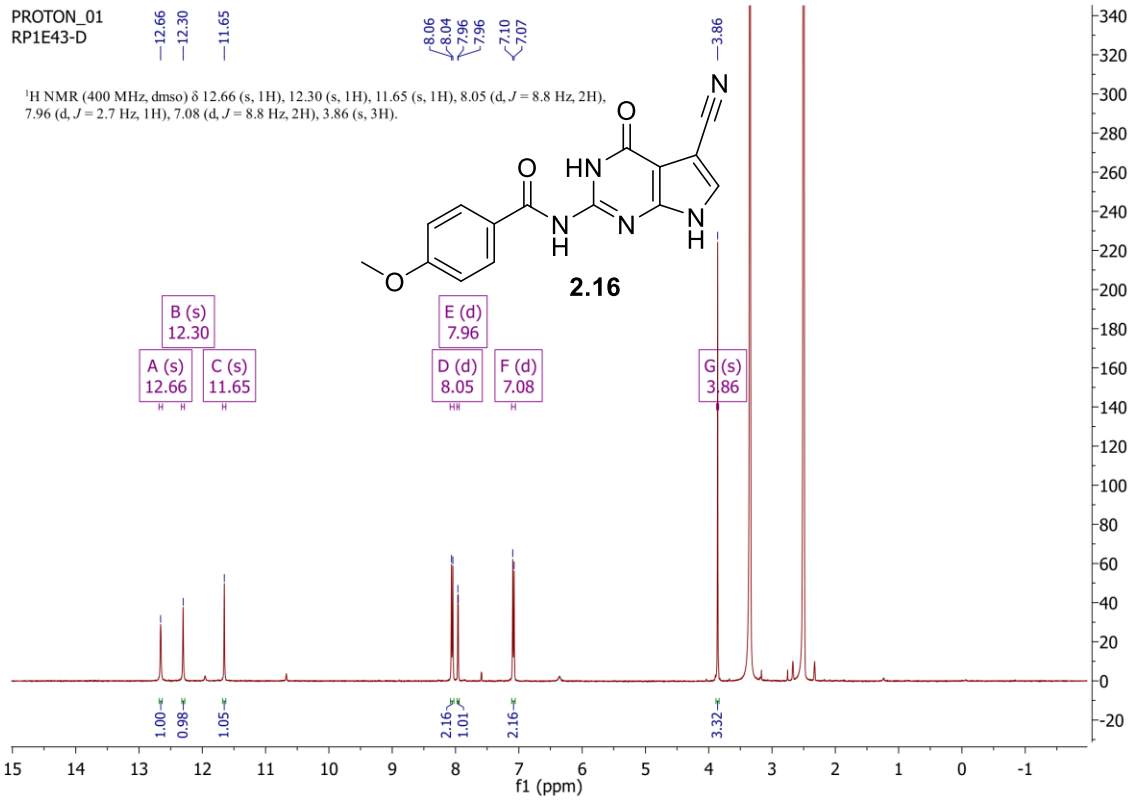
PROTON_01
RP1E43-D
12.66
12.30
11.65
8.06
8.04
7.96
7.96
7.10
7.07
3.86
[1]H NMR (400 MHz, dmso) δ 12.66 (s, 1H), 12.30 (s, 1H), 11.65 (s, 1H), 8.05 (d, J = 8.8 Hz, 2H), 7.96 (d, J = 2.7 Hz, 1H), 7.08 (d, J = 8.8 Hz, 2H), 3.86 (s, 3H).
2.16
B (s) 12.30
A (s) 12.66
C (s) 11.65
E (d) 7.96
D (d) 8.05
F (d) 7.08
G (s) 3.86
1.00
0.98
1.05
2.16
1.01
2.16
3.32
f1 (ppm)

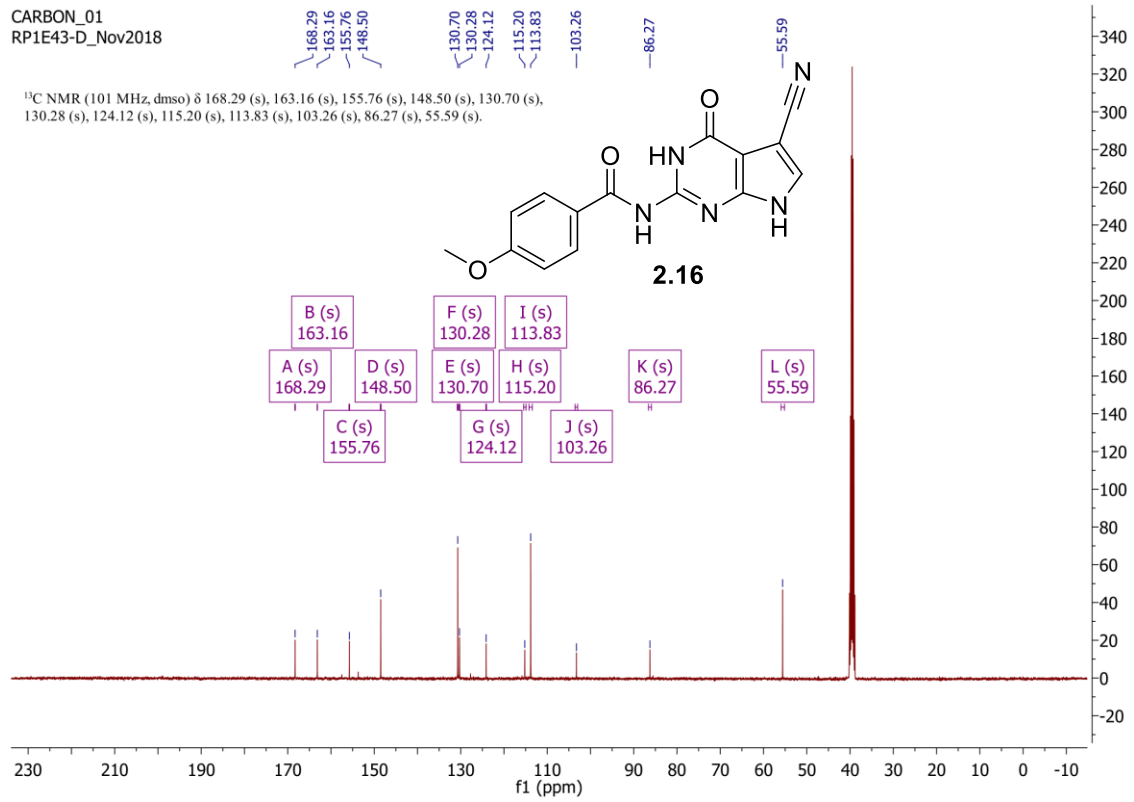
CARBON_01
RP1E43-D_Nov2018
168.29
163.16
155.76
148.50
130.70
130.28
124.12
115.20
113.83
103.26
86.27
55.59
[13]C NMR (101 MHz, dmso) δ 168.29 (s), 163.16 (s), 155.76 (s), 148.50 (s), 130.70 (s), 130.28 (s), 124.12 (s), 115.20 (s), 113.83 (s), 103.26 (s), 86.27 (s), 55.59 (s).
2.16
B (s) 163.16
F (s) 130.28
I (s) 113.83
A (s) 168.29
D (s) 148.50
E (s) 130.70
H (s) 115.20
K (s) 86.27
L (s) 55.59
C (s) 155.76
G (s) 124.12
J (s) 103.26
f1 (ppm)

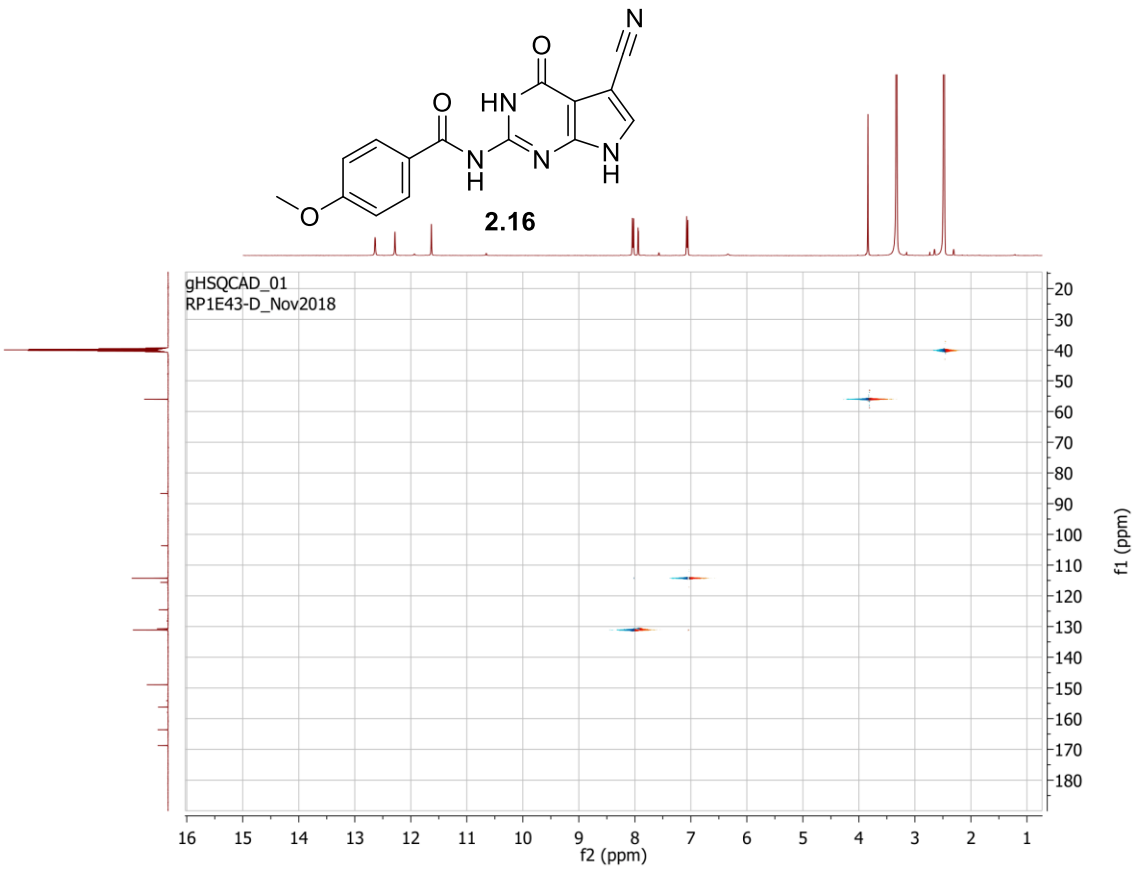

Trinity College Dublin

Bruker Open Access LC-MS - Formula Identification Report

Sample-ID		Station	
Submitter		Supervisor	
Analysis Name	RP1E43-D_RD3_01_18776.d	Acquisition Date	04/12/2018 16:54:11
Sample Description			

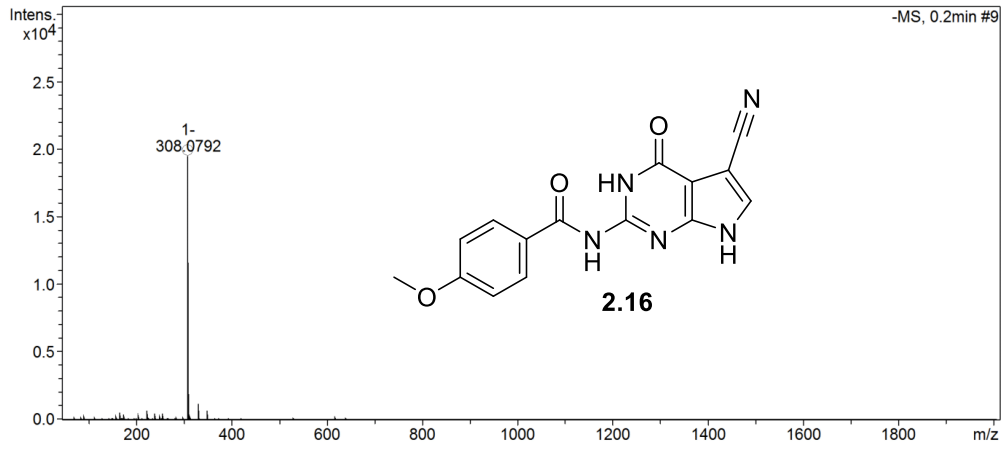

Meas. m/z	#	Ion Formula	m/z	err [mDa]	err [ppm]	rdb	N-Rule	e⁻ Conf	mSigma
308.079248	1	C15H10N5O3	308.078913	-0.3	-1.1	13.5	ok	even	57.2

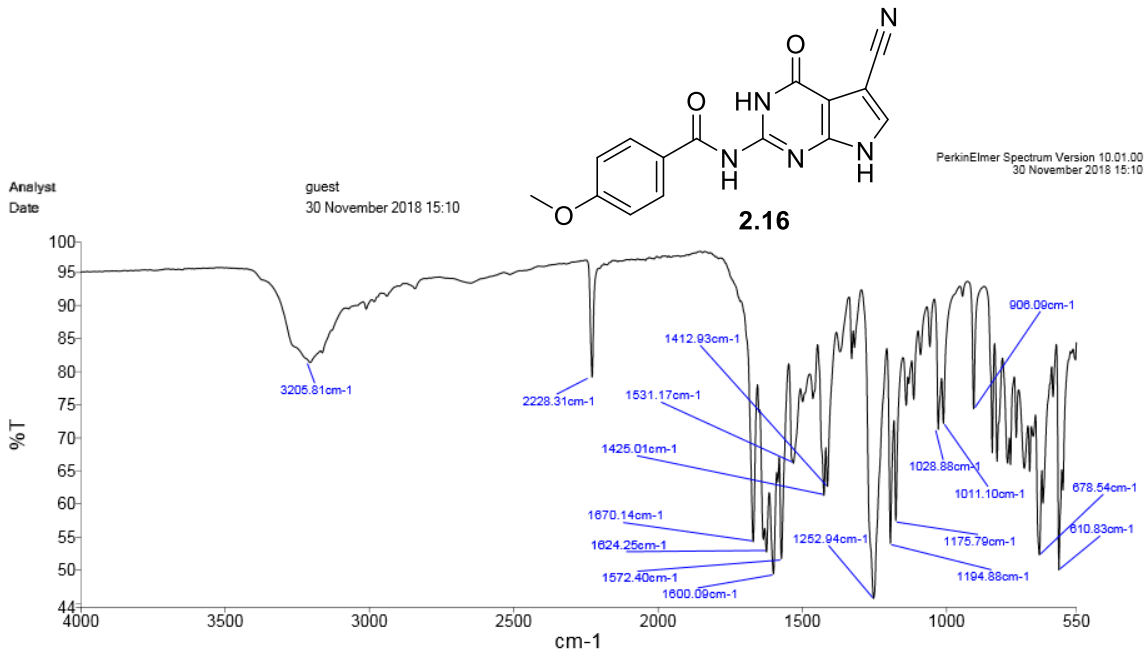

Sample Name	Description	Quality Checks
RPP09	Sample 009 By guest1 Date Friday, November 30 2018	The Quality Checks do not report any warnings for the sample.

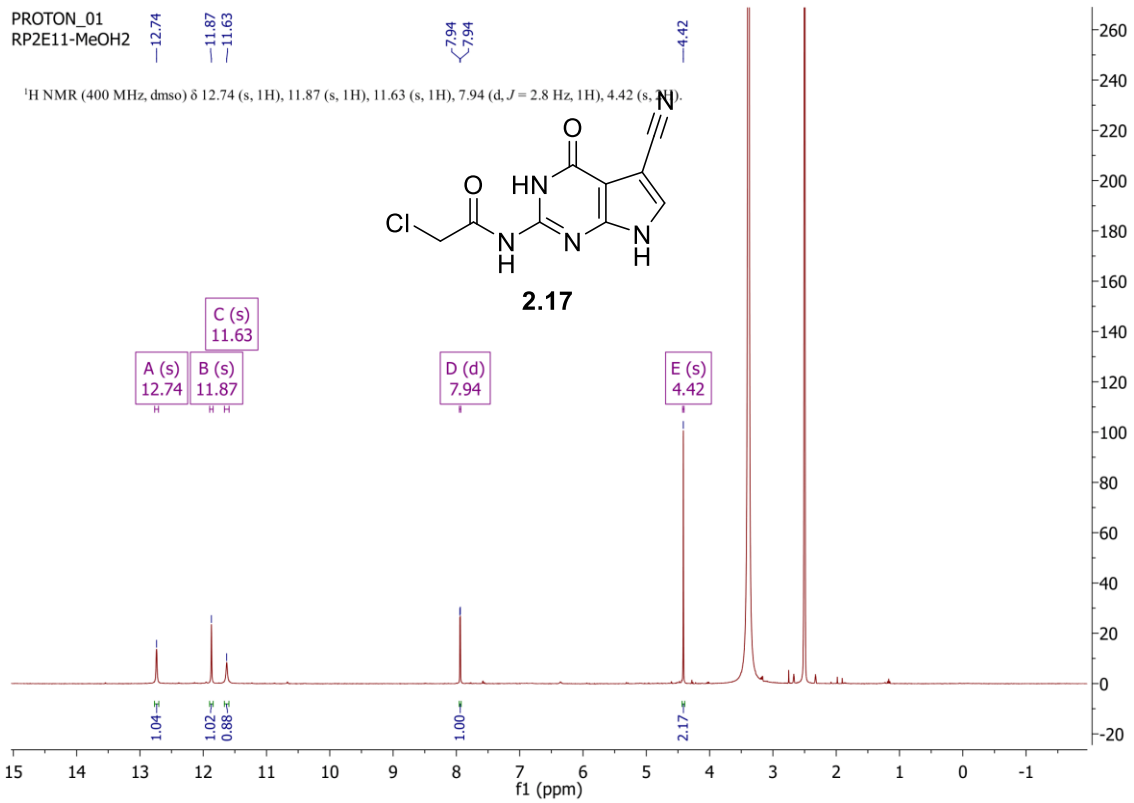

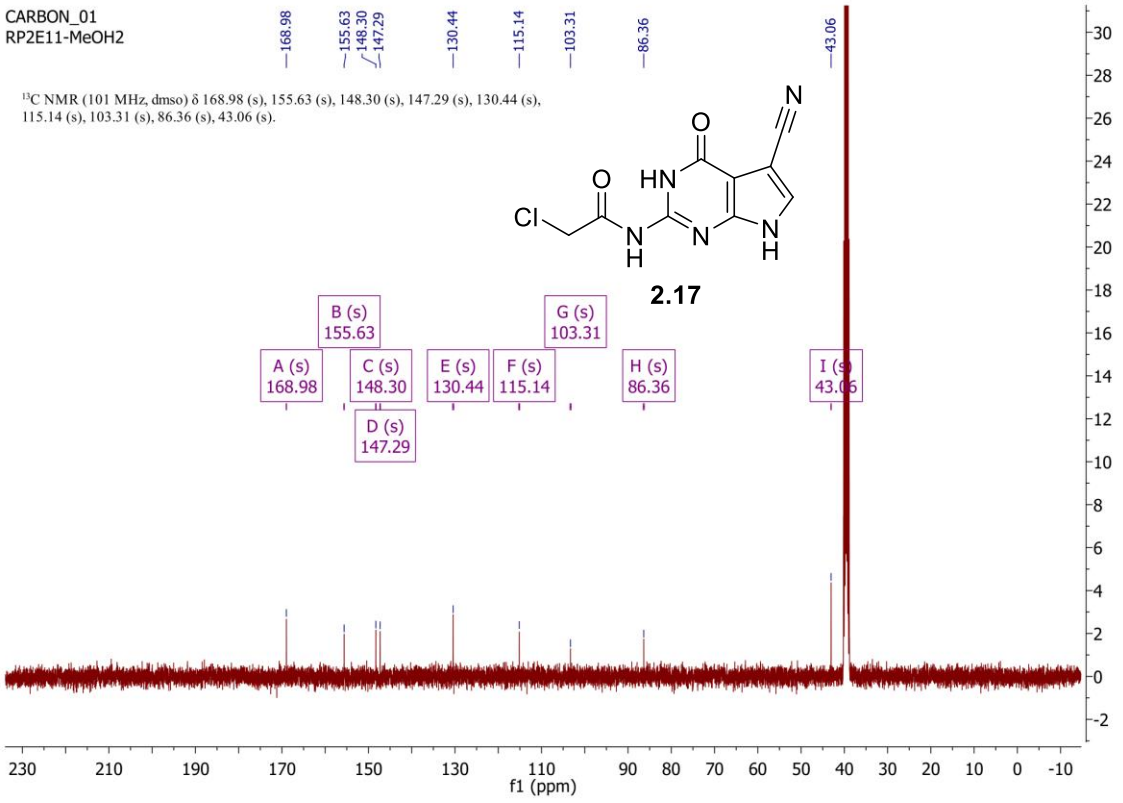
CARBON_01
RP2E11-MeOH2
168.98
155.63
148.30
147.29
130.44
115.14
103.31
86.36
43.06
13C NMR (101 MHz, dmso) δ 168.98 (s), 155.63 (s), 148.30 (s), 147.29 (s), 130.44 (s), 115.14 (s), 103.31 (s), 86.36 (s), 43.06 (s).
2.17
A (s) 168.98
B (s) 155.63
C (s) 148.30
D (s) 147.29
E (s) 130.44
F (s) 115.14
G (s) 103.31
H (s) 86.36
I (s) 43.06
f1 (ppm)

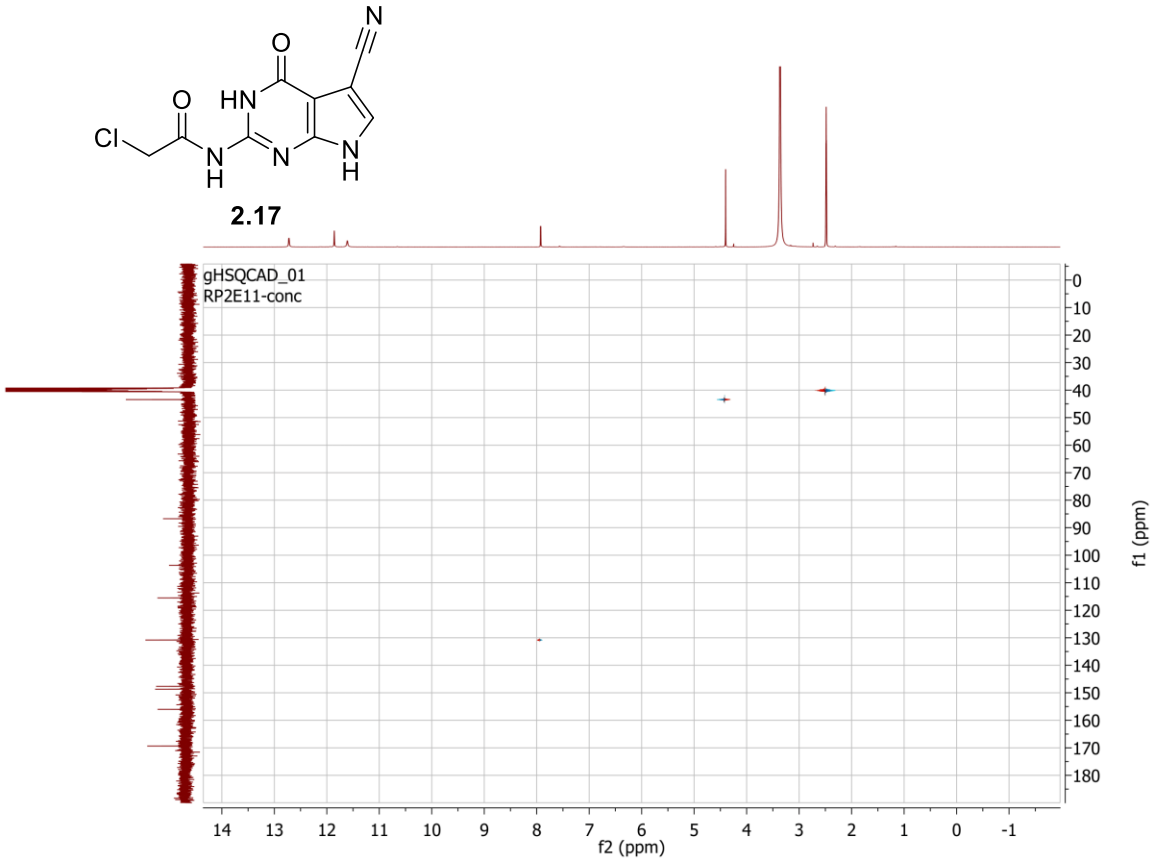
2.17
gHSQCAD_01
RP2E11-conc
f2 (ppm)
f1 (ppm)

Trinity College Dublin

Bruker Open Access LC-MS - Formula Identification Report

Sample-ID		Station	
Submitter		Supervisor	
Analysis Name	RPP14_RC2_01_20079.d	Acquisition Date	26/04/2019 11:10:27
Sample Description			

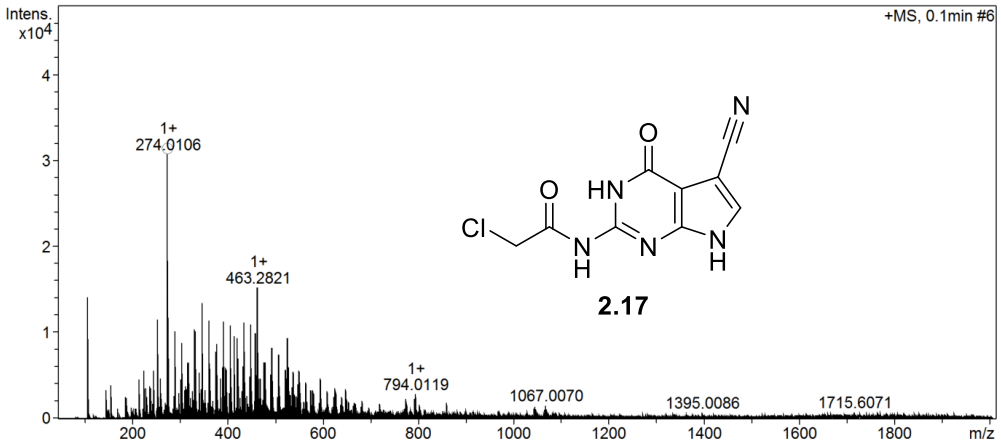

Meas. m/z	#	Ion Formula	m/z	err [mDa]	err [ppm]	rdb	N-Rule	e⁻ Conf	mSigma
274.010623	1	C9H6ClN5NaO2	274.010223	-0.4	-1.5	8.5	ok	even	26.7

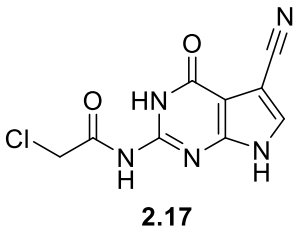

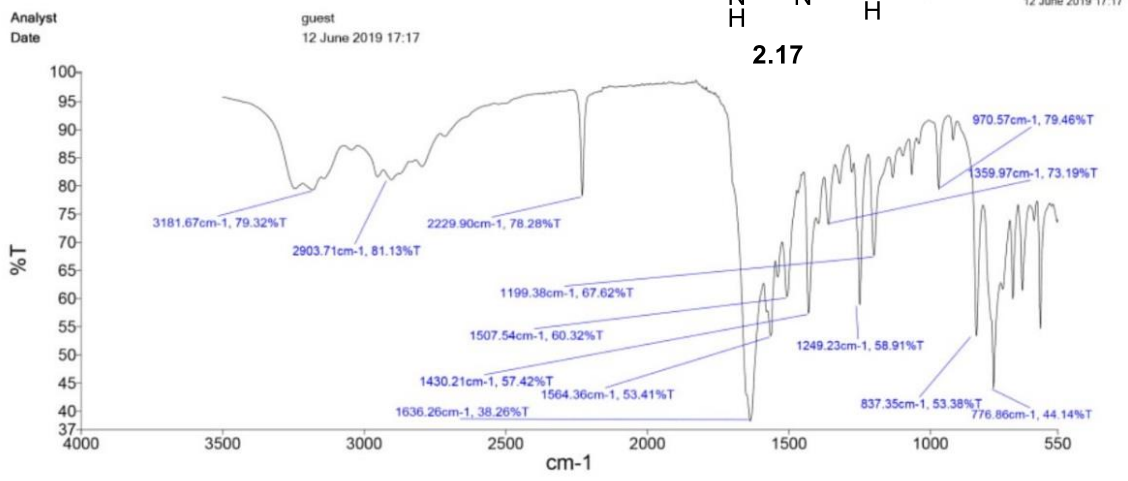

Sample Name	Description	Quality Checks
RP2E11	Sample 001 By guest1 Date Wednesday, June 12 2019	The Quality Checks do not report any warnings for the sample.

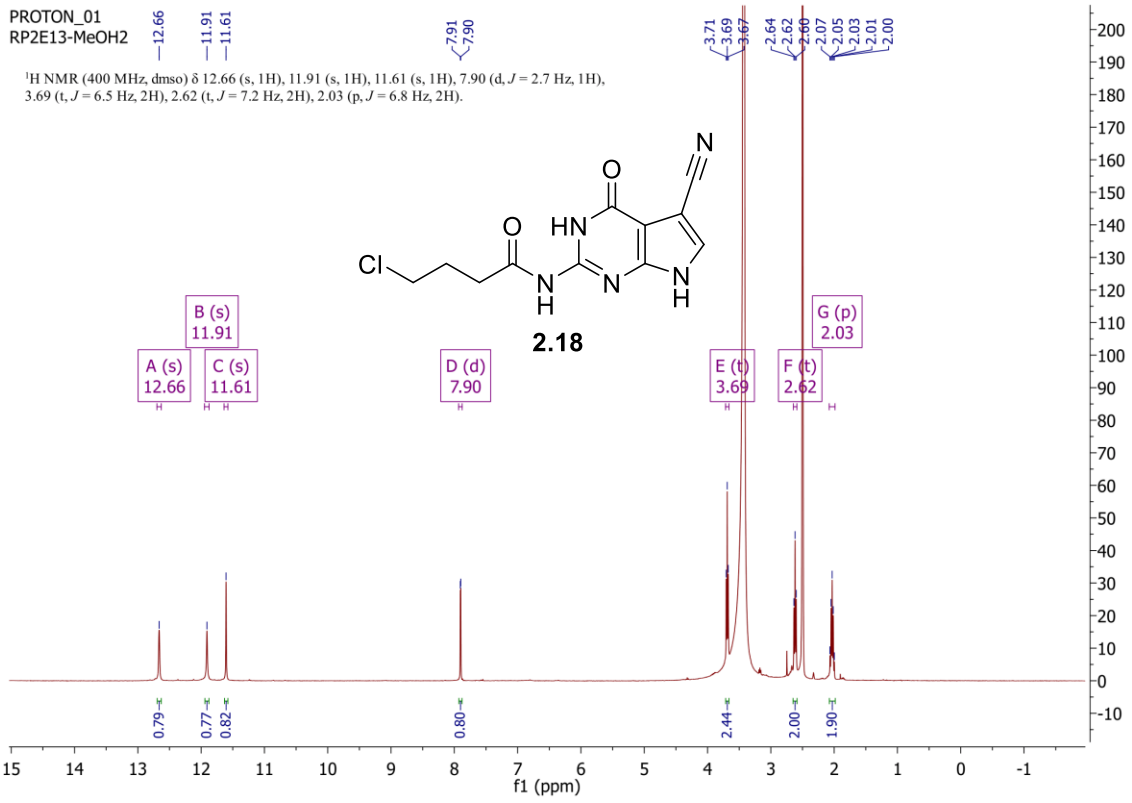
PROTON_01
RP2E13-MeOH2
12.66
11.91
11.61
7.91
7.90
3.71
3.69
3.67
2.64
2.62
2.60
2.07
2.05
2.03
2.01
2.00
^{1}H NMR (400 MHz, dmso) δ 12.66 (s, 1H), 11.91 (s, 1H), 11.61 (s, 1H), 7.90 (d, J = 2.7 Hz, 1H), 3.69 (t, J = 6.5 Hz, 2H), 2.62 (t, J = 7.2 Hz, 2H), 2.03 (p, J = 6.8 Hz, 2H).
2.18
B (s) 11.91
A (s) 12.66
C (s) 11.61
D (d) 7.90
E (t) 3.69
F (t) 2.62
G (p) 2.03
0.79
0.77
0.82
0.80
2.44
2.00
1.90
f1 (ppm)

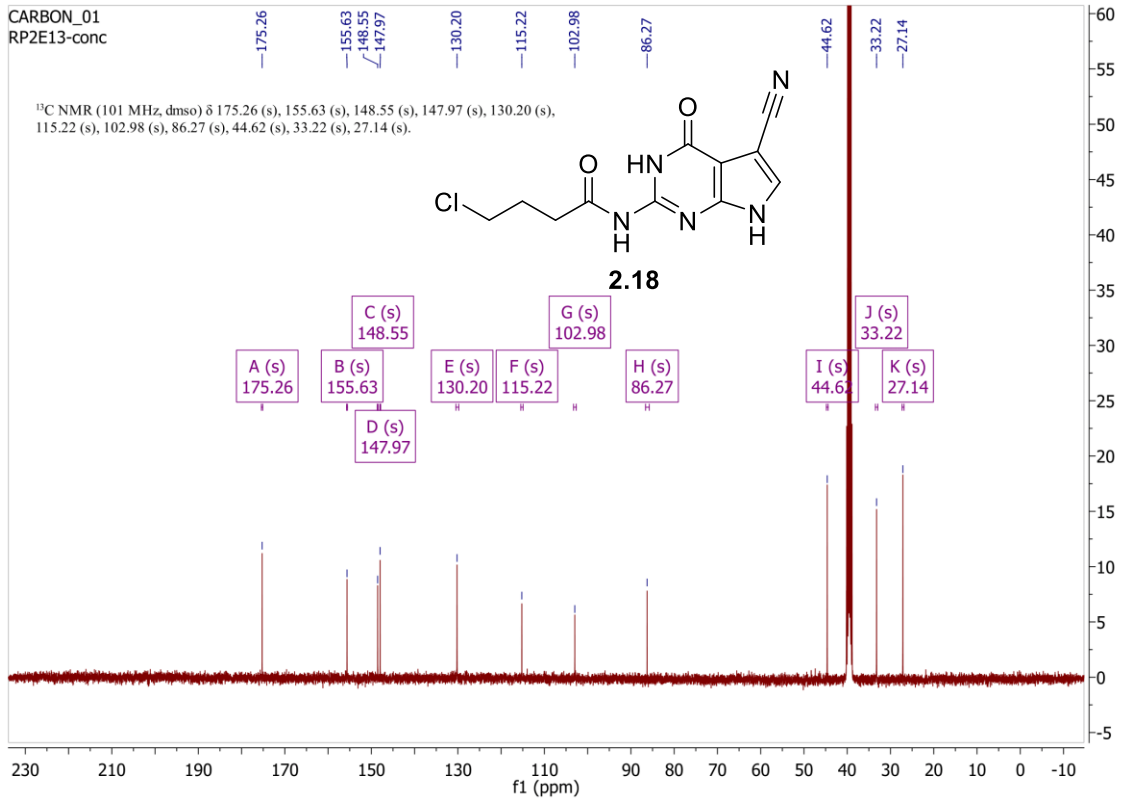
CARBON_01
RP2E13-conc
175.26
155.63
148.55
147.97
130.20
115.22
102.98
86.27
44.62
33.22
27.14
^{13}C NMR (101 MHz, dmso) δ 175.26 (s), 155.63 (s), 148.55 (s), 147.97 (s), 130.20 (s), 115.22 (s), 102.98 (s), 86.27 (s), 44.62 (s), 33.22 (s), 27.14 (s).
2.18
A (s) 175.26
B (s) 155.63
C (s) 148.55
D (s) 147.97
E (s) 130.20
F (s) 115.22
G (s) 102.98
H (s) 86.27
I (s) 44.62
J (s) 33.22
K (s) 27.14
f1 (ppm)

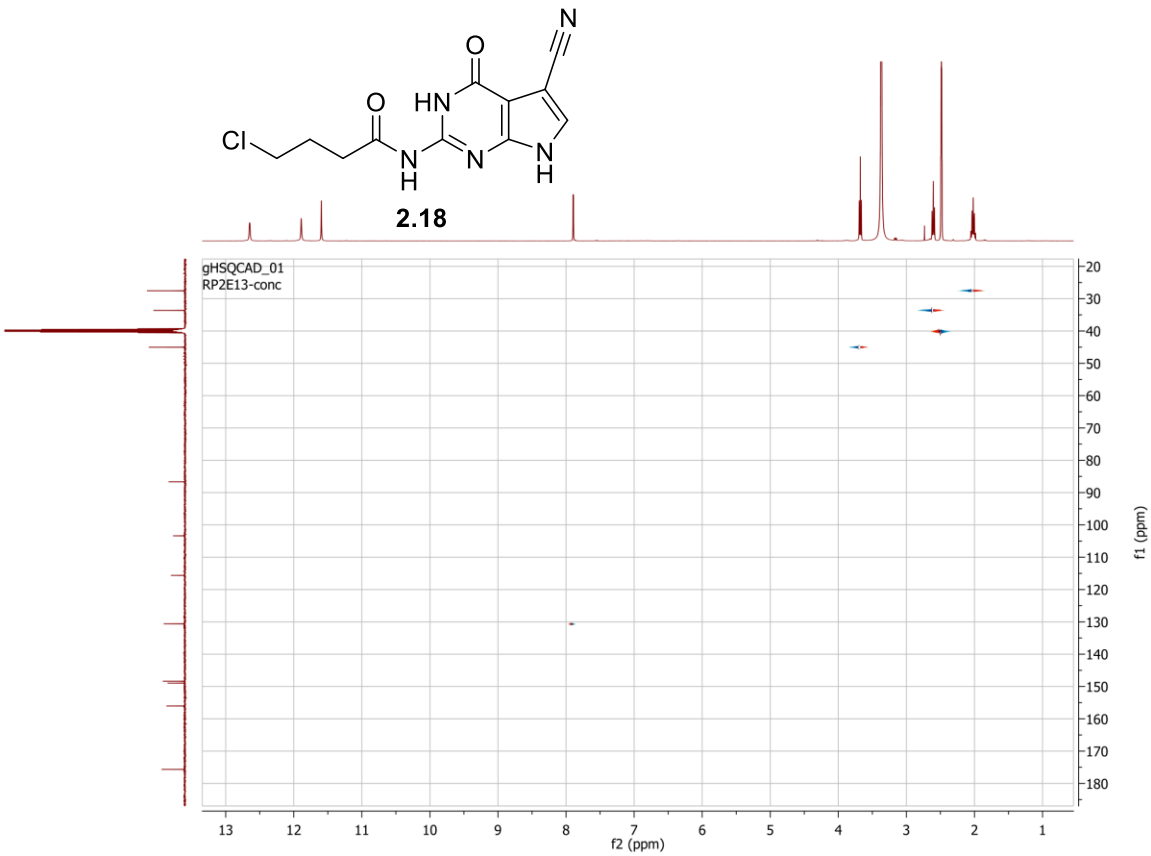

2.18

Trinity College Dublin

Bruker Open Access LC-MS - Formula Identification Report

Sample-ID		Station	
Submitter		Supervisor	
Analysis Name	RPP16_RC4_01_20081.d	Acquisition Date	26/04/2019 11:17:01
Sample Description			

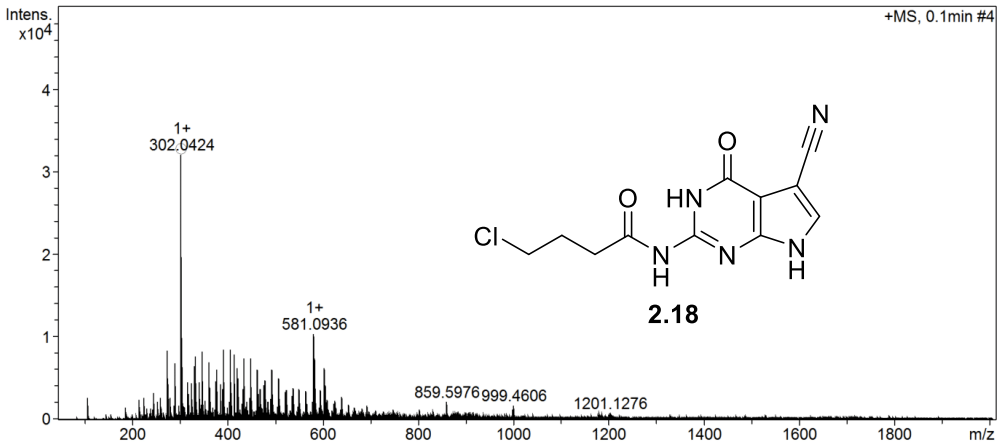

2.18

Meas. m/z	#	Ion Formula	m/z	err [mDa]	err [ppm]	rdb	N-Rule	e⁻ Conf	mSigma
302.042401	1	C11H10ClN5NaO2	302.041523	-0.9	-2.9	8.5	ok	even	22.4

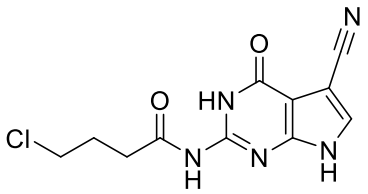

2.18

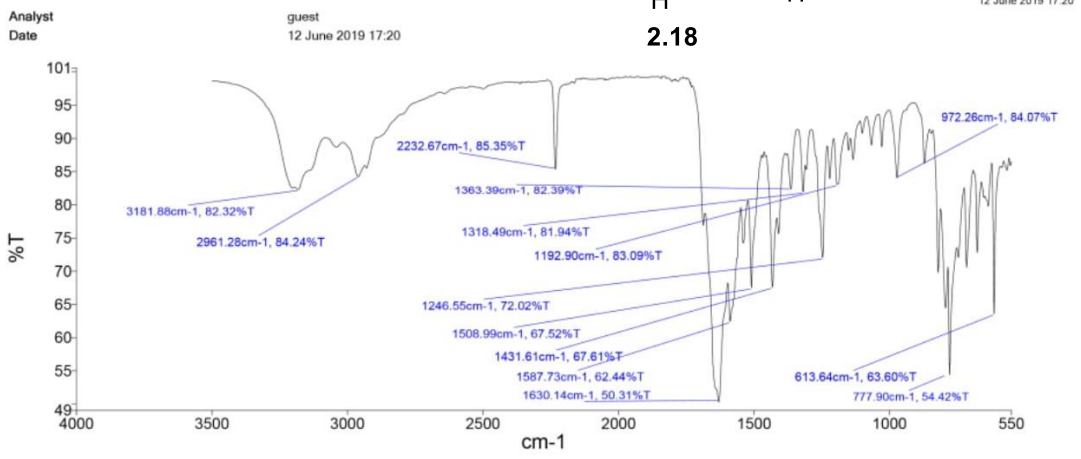

Sample Name	Description	Quality Checks
RP2E13	Sample 003 By guest1 Date Wednesday, June 12 2019	The Quality Checks do not report any warnings for the sample.

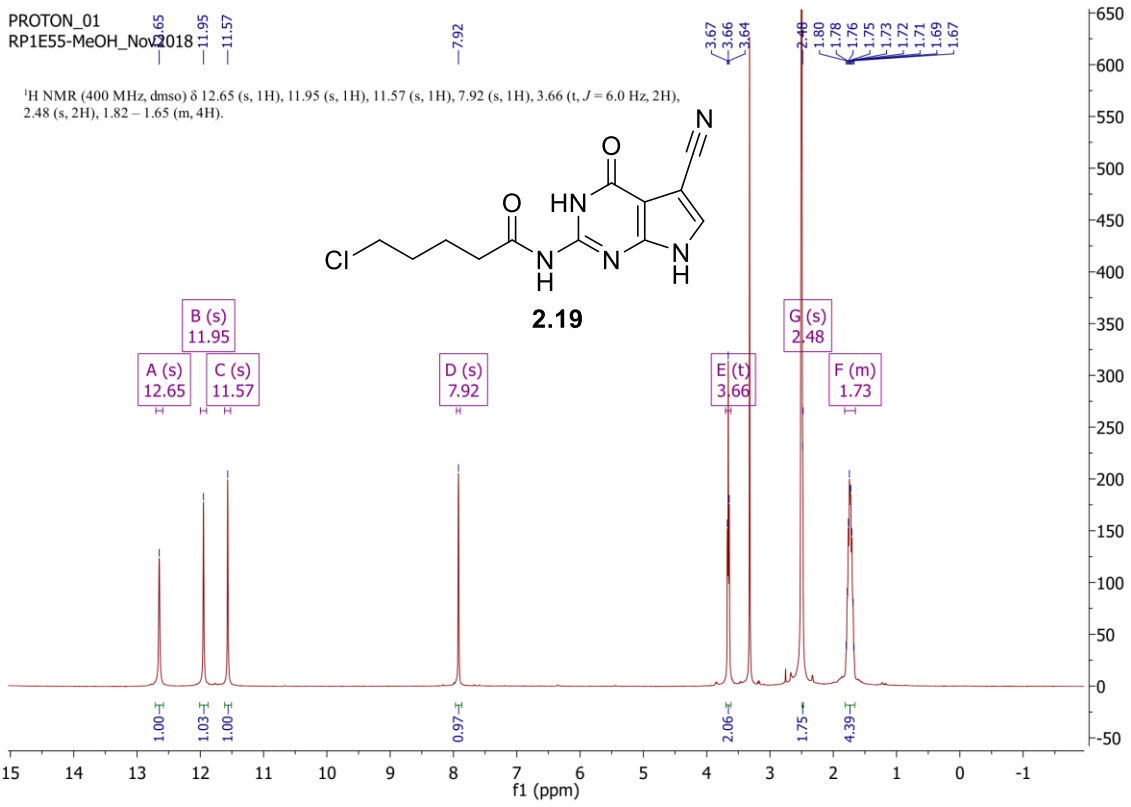

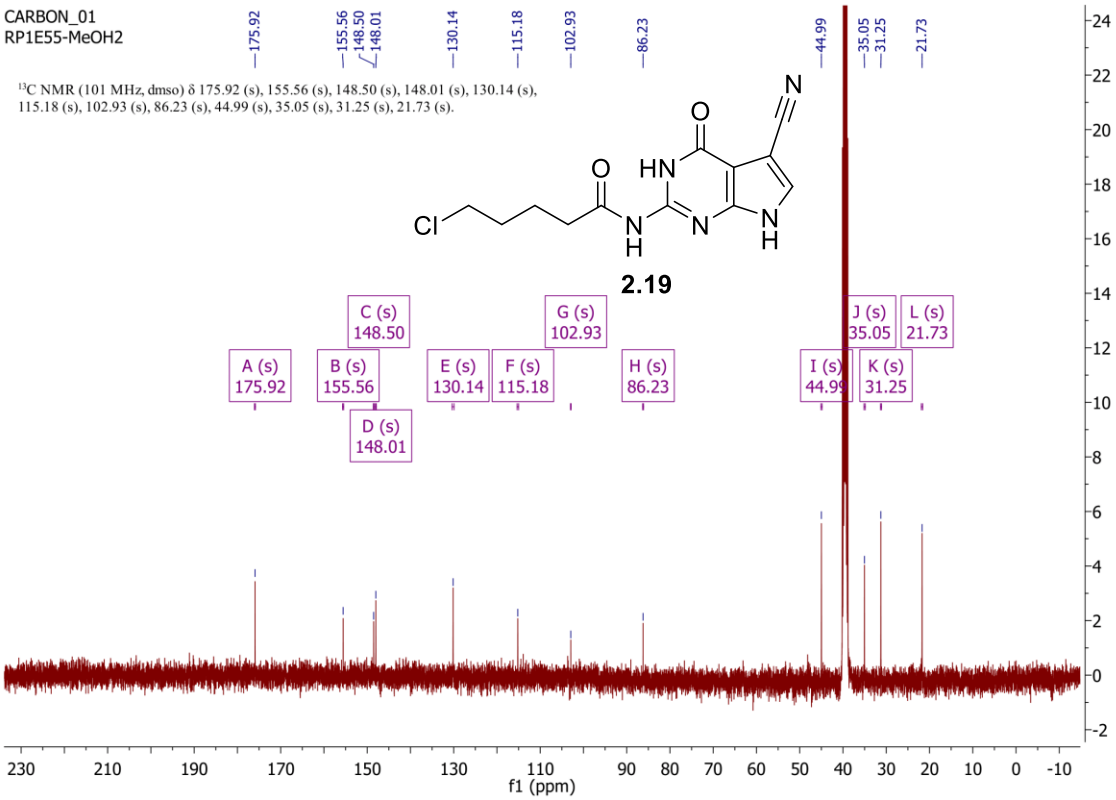
CARBON_01
RP1E55-MeOH2
175.92
155.56
148.50
148.01
130.14
115.18
102.93
86.23
44.99
35.05
31.25
21.73
13C NMR (101 MHz, dmso) δ 175.92 (s), 155.56 (s), 148.50 (s), 148.01 (s), 130.14 (s), 115.18 (s), 102.93 (s), 86.23 (s), 44.99 (s), 35.05 (s), 31.25 (s), 21.73 (s).
2.19
A (s) 175.92
B (s) 155.56
C (s) 148.50
D (s) 148.01
E (s) 130.14
F (s) 115.18
G (s) 102.93
H (s) 86.23
I (s) 44.99
J (s) 35.05
K (s) 31.25
L (s) 21.73
f1 (ppm)

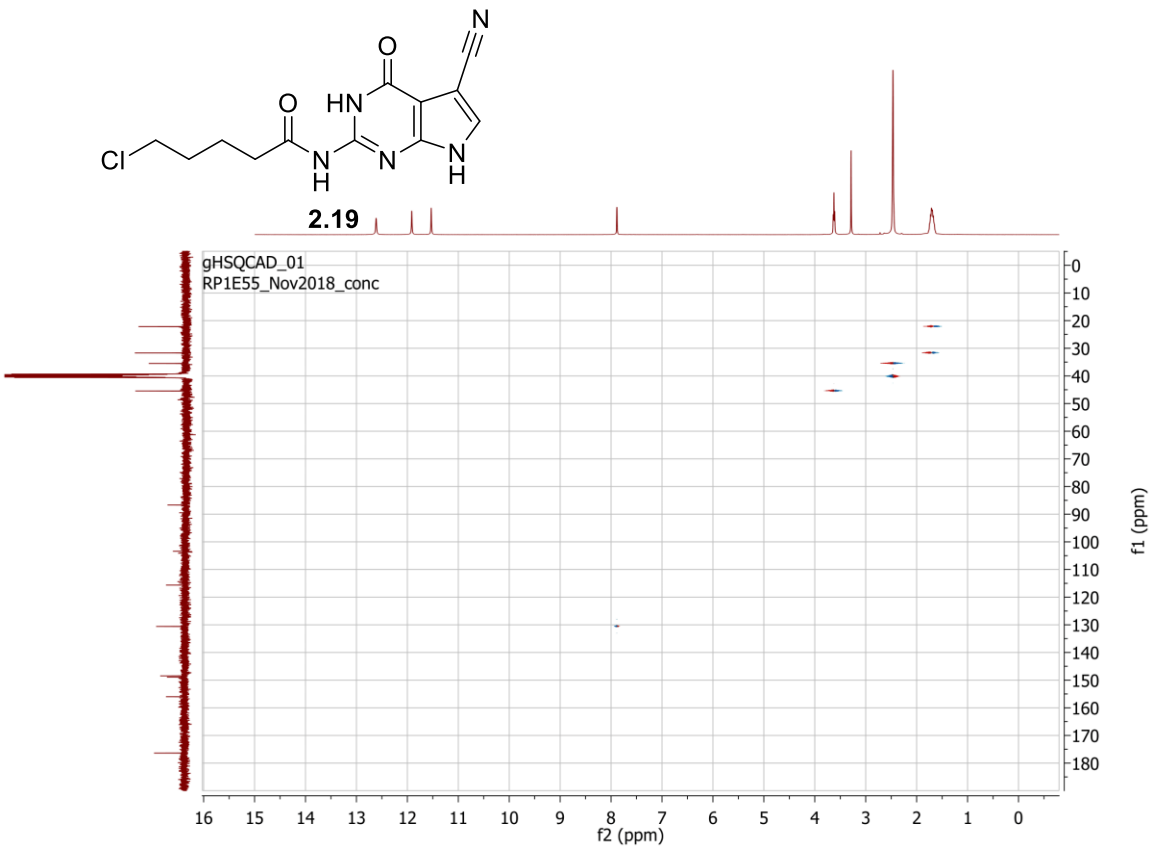
2.19
gHSQCAD_01
RP1E55_Nov2018_conc
f2 (ppm)
f1 (ppm)

Trinity College Dublin

Bruker Open Access LC-MS - Formula Identification Report

Sample-ID		Station	
Submitter		Supervisor	
Analysis Name	RP1E55_RD4_01_18777.d	Acquisition Date	04/12/2018 16:57:27
Sample Description			

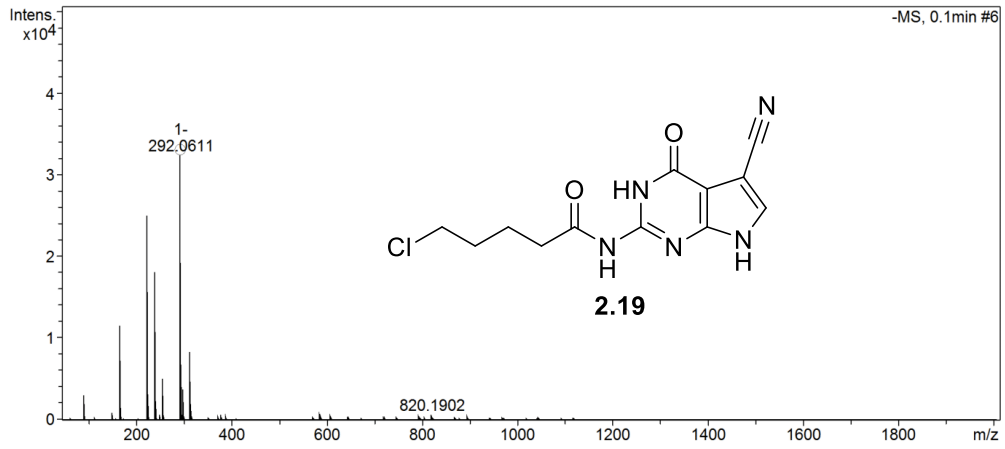

Meas. m/z	#	Ion Formula	m/z	err [mDa]	err [ppm]	rdb	N-Rule	e⁻ Conf	mSigma
292.061146	1	C12H11ClN5O2	292.060676	-0.5	-1.6	9.5	ok	even	70.8

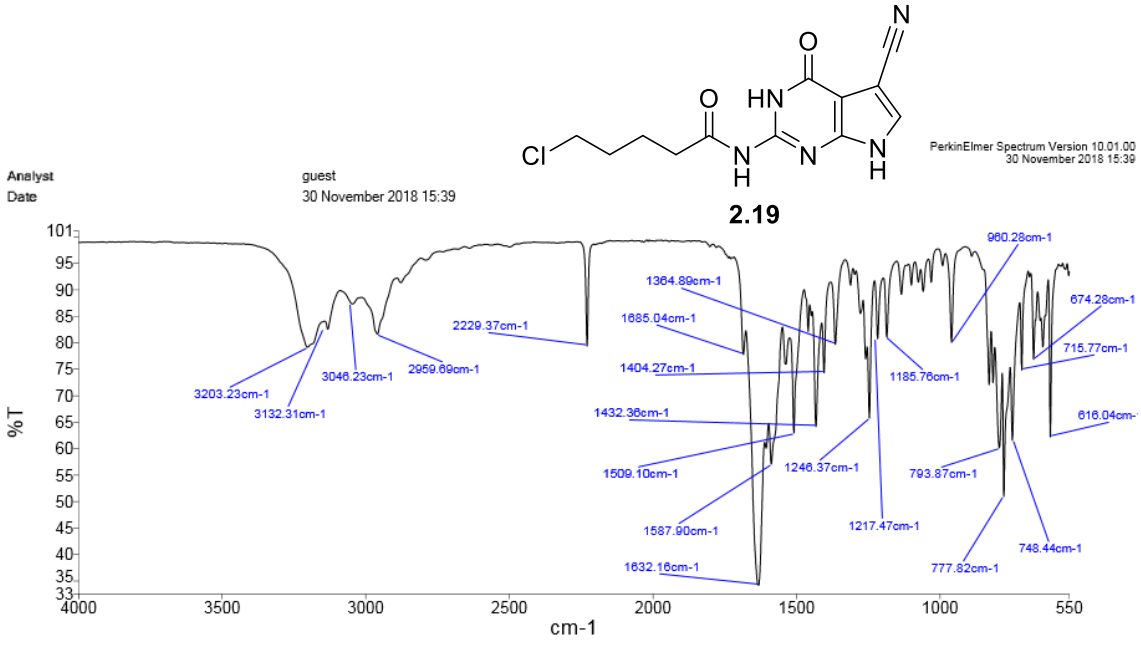

Sample Name	Description	Quality Checks
RPP13	Sample 012 By guest1 Date Friday, November 30 2018	The Quality Checks do not report any warnings for the sample.

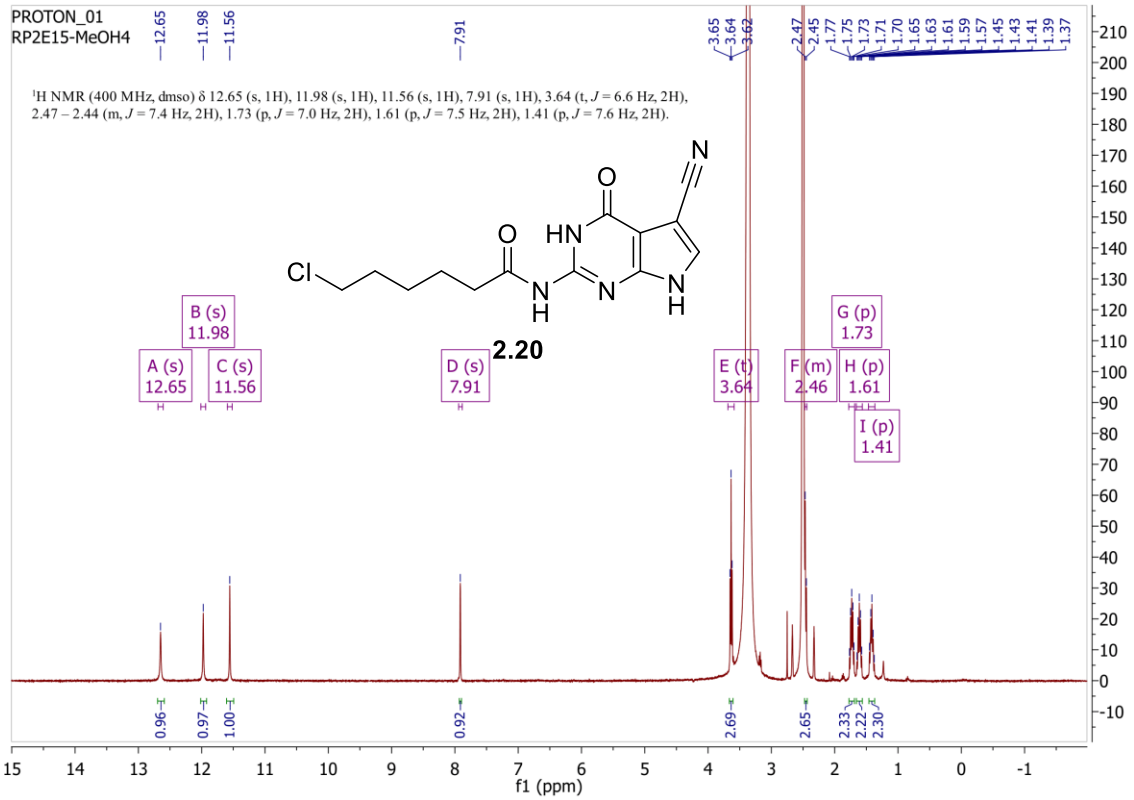
PROTON_01
RP2E15-MeOH4
12.65
11.98
11.56
7.91
3.65
3.64
3.62
2.47
2.45
1.77
1.75
1.73
1.71
1.70
1.65
1.63
1.61
1.59
1.57
1.45
1.43
1.41
1.39
1.37
¹H NMR (400 MHz, dmso) δ 12.65 (s, 1H), 11.98 (s, 1H), 11.56 (s, 1H), 7.91 (s, 1H), 3.64 (t, J = 6.6 Hz, 2H), 2.47 – 2.44 (m, J = 7.4 Hz, 2H), 1.73 (p, J = 7.0 Hz, 2H), 1.61 (p, J = 7.5 Hz, 2H), 1.41 (p, J = 7.6 Hz, 2H).
2.20
B (s) 11.98
A (s) 12.65
C (s) 11.56
D (s) 7.91
E (t) 3.64
F (m) 2.46
G (p) 1.73
H (p) 1.61
I (p) 1.41
0.96
0.97
1.00
0.92
2.69
2.65
2.33
2.22
2.30
f1 (ppm)

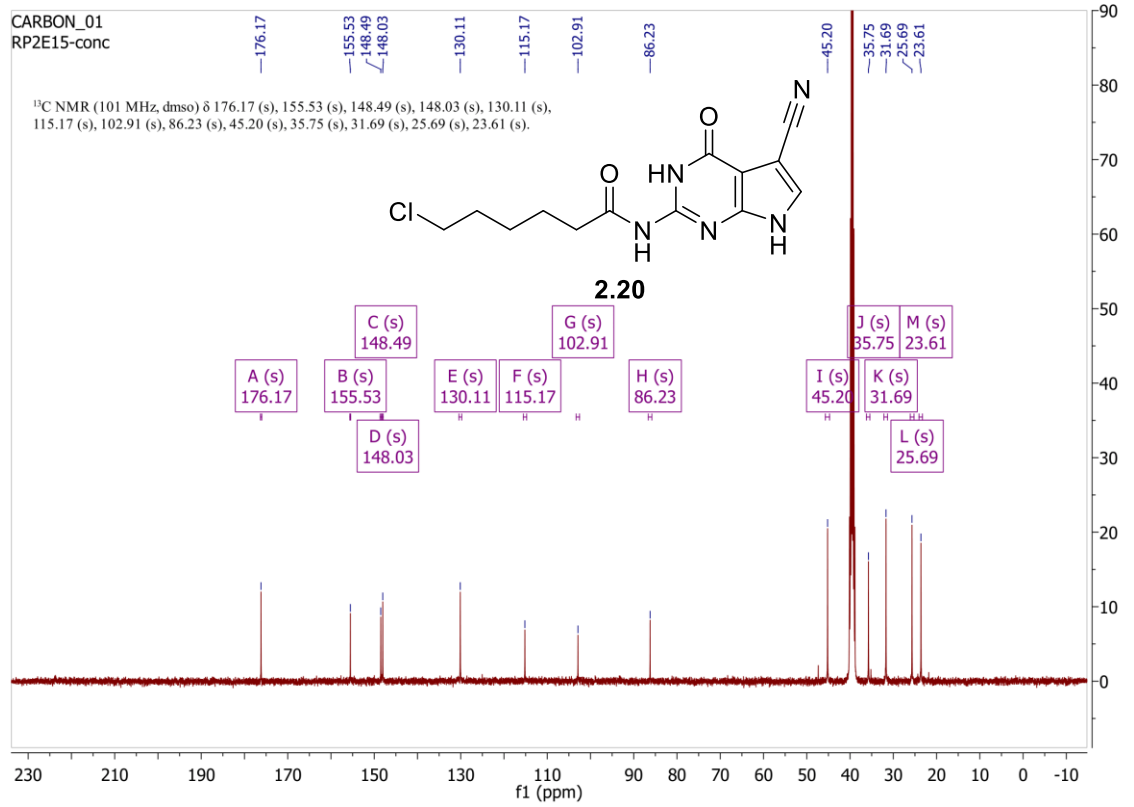
CARBON_01
RP2E15-conc
176.17
155.53
148.49
148.03
130.11
115.17
102.91
86.23
45.20
35.75
31.69
25.69
23.61
¹³C NMR (101 MHz, dmso) δ 176.17 (s), 155.53 (s), 148.49 (s), 148.03 (s), 130.11 (s), 115.17 (s), 102.91 (s), 86.23 (s), 45.20 (s), 35.75 (s), 31.69 (s), 25.69 (s), 23.61 (s).
2.20
A (s) 176.17
B (s) 155.53
C (s) 148.49
D (s) 148.03
E (s) 130.11
F (s) 115.17
G (s) 102.91
H (s) 86.23
I (s) 45.20
J (s) 35.75
K (s) 31.69
L (s) 25.69
M (s) 23.61
f1 (ppm)

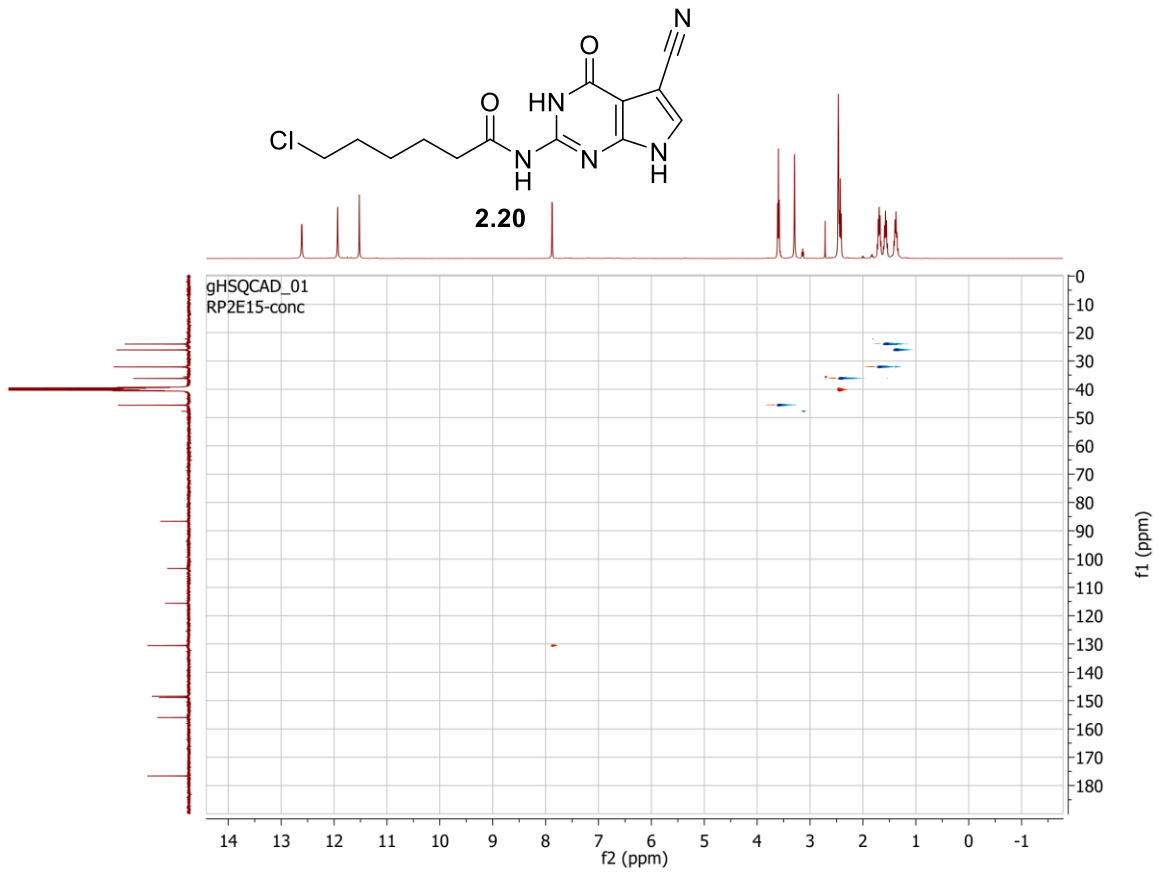

Trinity College Dublin

Bruker Open Access LC-MS - Formula Identification Report

Sample-ID		Station	
Submitter		Supervisor	
Analysis Name	RPP20_RC5_01_20082.d	Acquisition Date	26/04/2019 11:20:17
Sample Description			

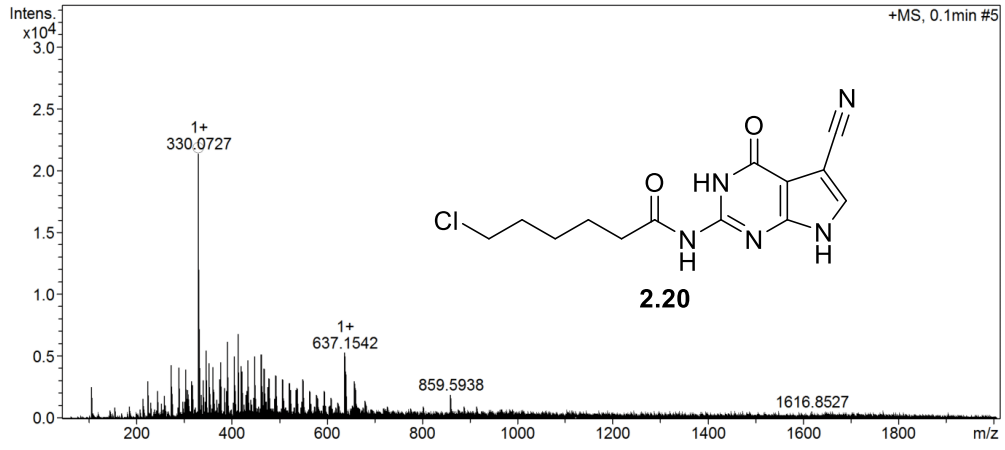

Meas. m/z	#	Ion Formula	m/z	err [mDa]	err [ppm]	rdb	N-Rule	e⁻ Conf	mSigma
330.072703	1	C13H14ClN5NaO2	330.072823	-0.1	-0.4	8.5	ok	even	25.5

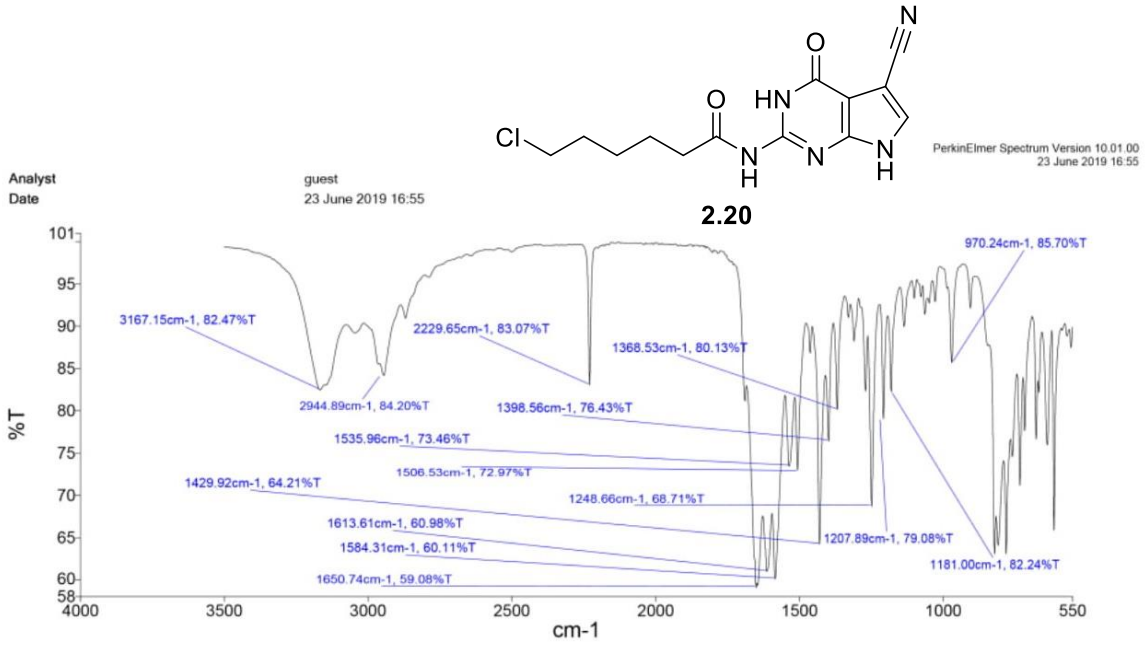

Sample Name	Description	Quality Checks
RP2E15	Sample 001 By guest1 Date Sunday, June 23 2019	The Quality Checks do not report any warnings for the sample.

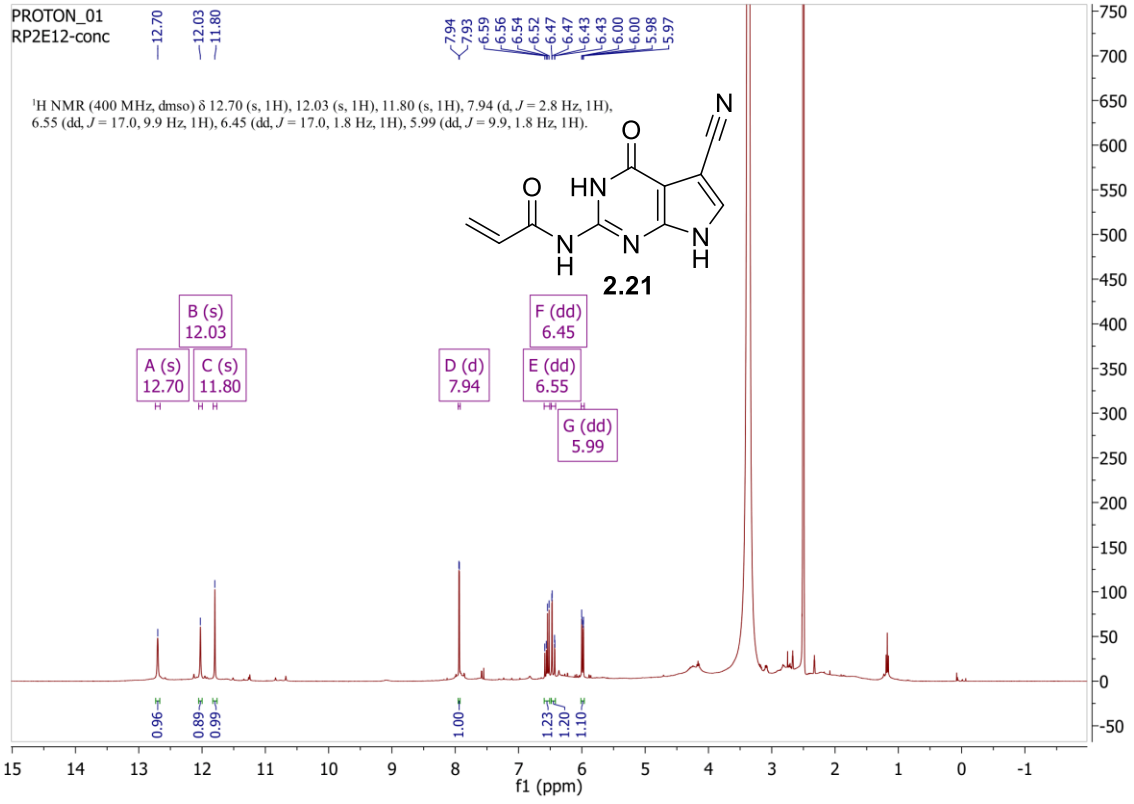

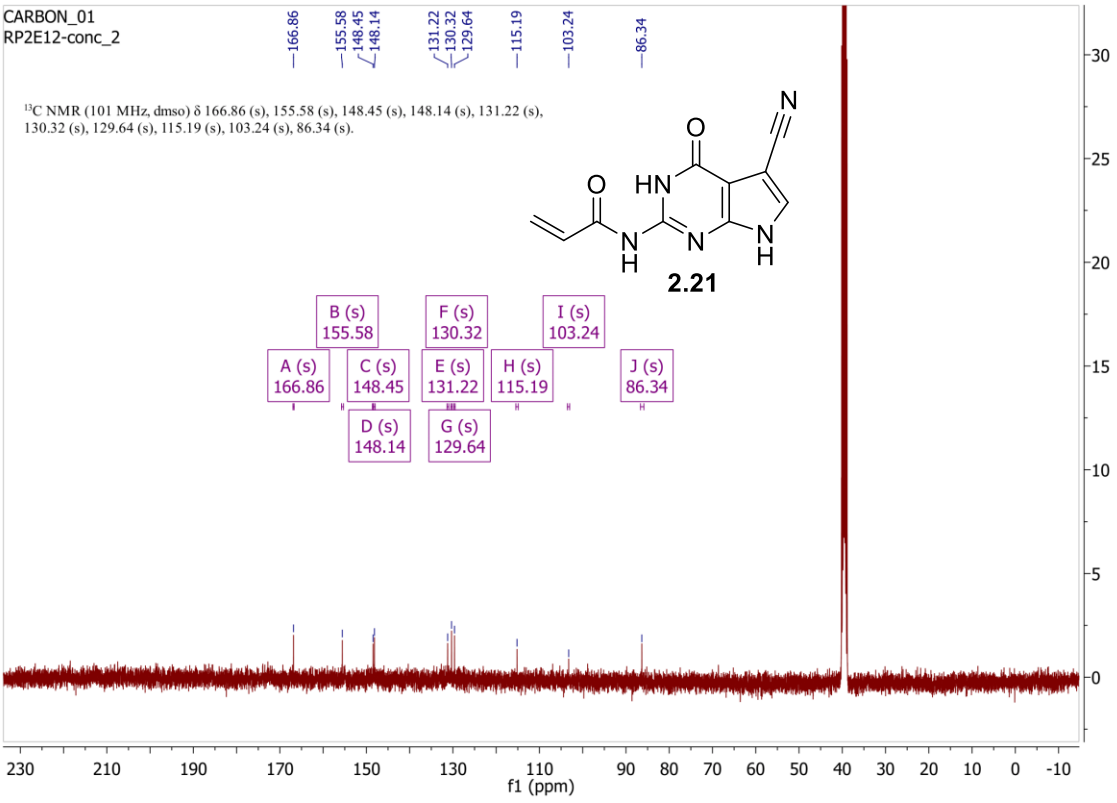
CARBON_01
RP2E12-conc_2
166.86
155.58
148.45
148.14
131.22
130.32
129.64
115.19
103.24
86.34
13C NMR (101 MHz, dmso) δ 166.86 (s), 155.58 (s), 148.45 (s), 148.14 (s), 131.22 (s), 130.32 (s), 129.64 (s), 115.19 (s), 103.24 (s), 86.34 (s).
2.21
B (s) 155.58
F (s) 130.32
I (s) 103.24
A (s) 166.86
C (s) 148.45
E (s) 131.22
H (s) 115.19
J (s) 86.34
D (s) 148.14
G (s) 129.64
f1 (ppm)

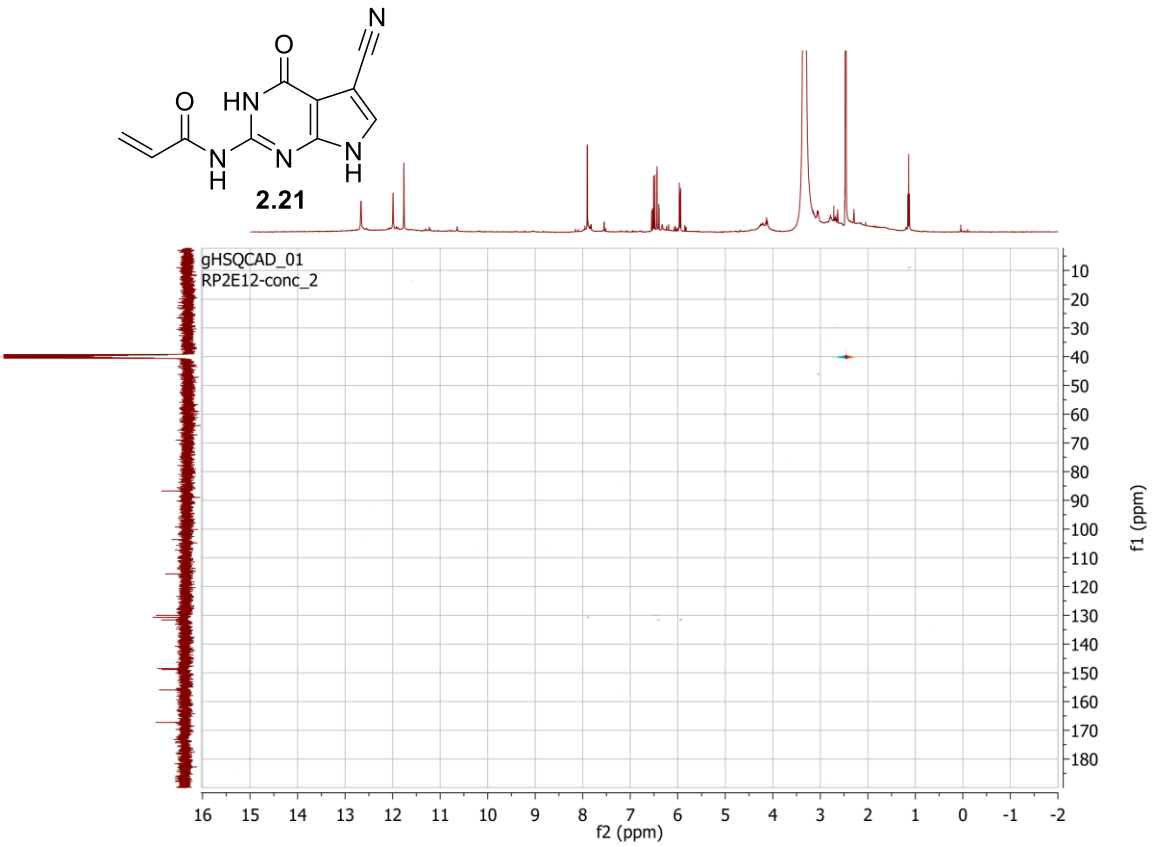
2.21
gHSQCAD_01
RP2E12-conc_2
f2 (ppm)
f1 (ppm)

Trinity College Dublin
Bruker Open Access LC-MS - Formula Identification Report

Sample-ID		Station	
Submitter		Supervisor	
Analysis Name	RPP12_RC1_01_20104.d	Acquisition Date	26/04/2019 12:33:02
Sample Description			

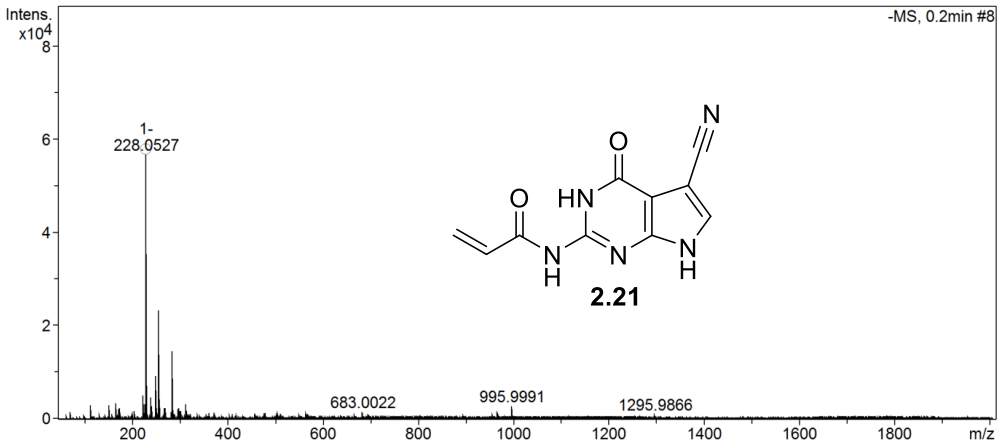

Meas. m/z	#	Ion Formula	m/z	err [mDa]	err [ppm]	rdb	N-Rule	e⁻ Conf	mSigma
228.052713	1	C10H6N5O2	228.052698	-0.0	-0.1	10.5	ok	even	7.1

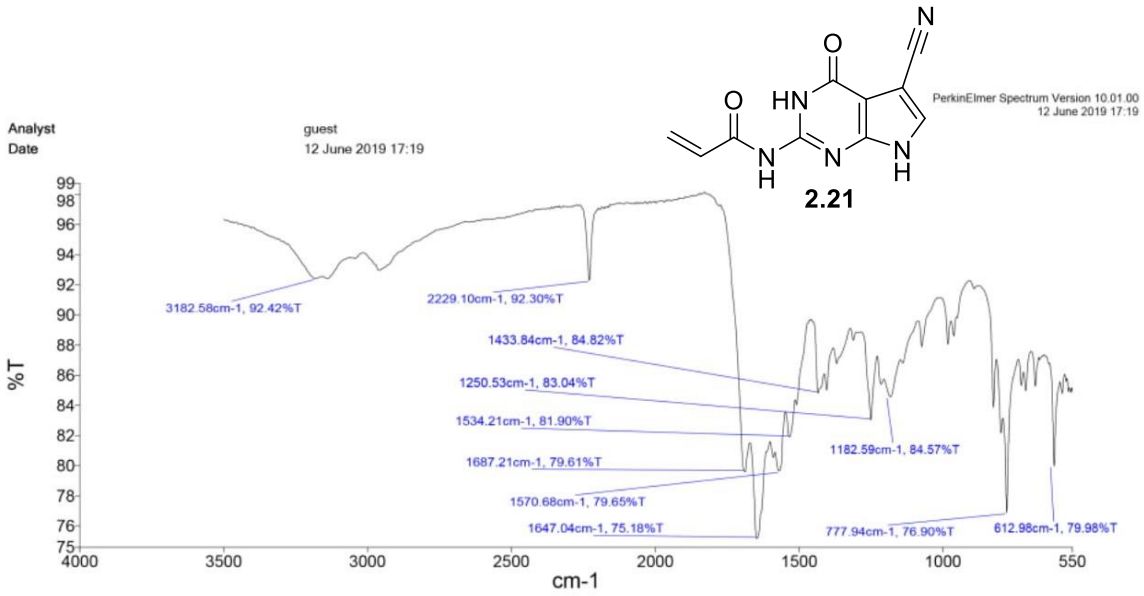

Sample Name	Description	Quality Checks
RP2E12	Sample 002 By guest1 Date Wednesday, June 12 2019	The Quality Checks do not report any warnings for the sample.

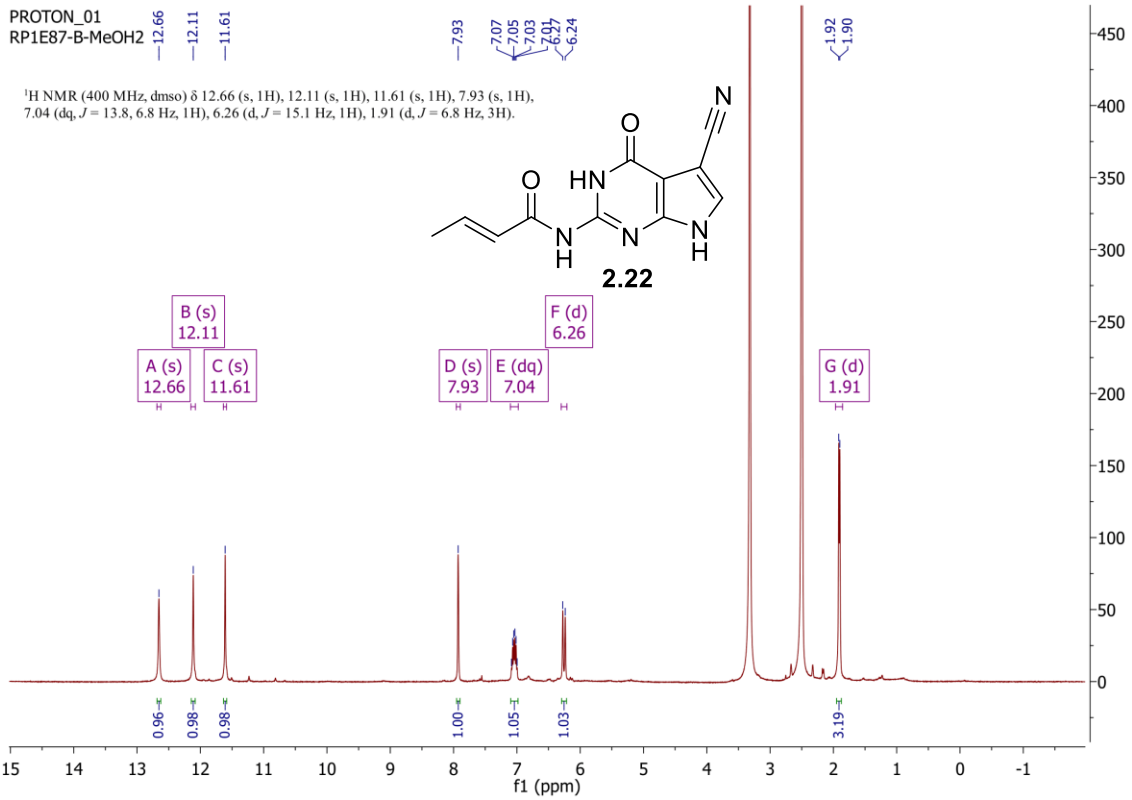
PROTON_01
RP1E87-B-MeOH2
12.66
12.11
11.61
7.93
7.07
7.05
7.03
7.01
6.27
6.24
1.92
1.90
^{1}H NMR (400 MHz, dmso) δ 12.66 (s, 1H), 12.11 (s, 1H), 11.61 (s, 1H), 7.93 (s, 1H), 7.04 (dq, J = 13.8, 6.8 Hz, 1H), 6.26 (d, J = 15.1 Hz, 1H), 1.91 (d, J = 6.8 Hz, 3H).
2.22
B (s) 12.11
A (s) 12.66
C (s) 11.61
F (d) 6.26
D (s) 7.93
E (dq) 7.04
G (d) 1.91
0.96
0.98
0.98
1.00
1.05
1.03
3.19
f1 (ppm)

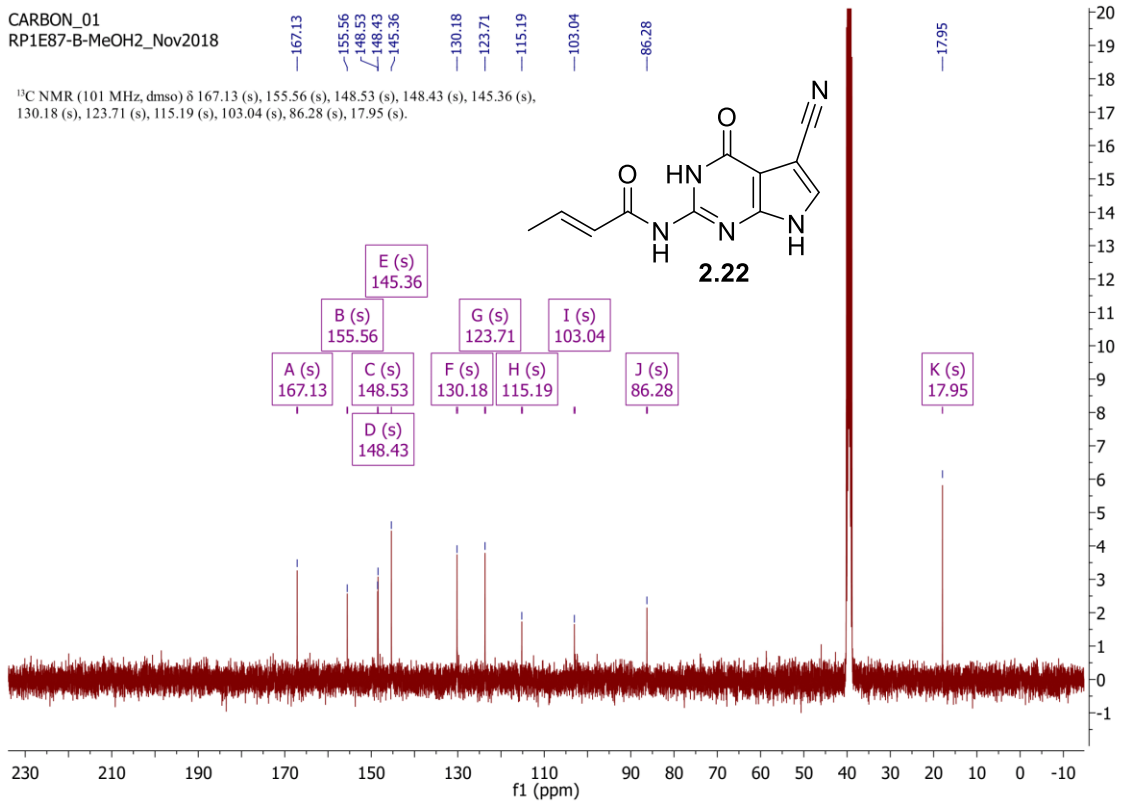
CARBON_01
RP1E87-B-MeOH2_Nov2018
167.13
155.56
148.53
148.43
145.36
130.18
123.71
115.19
103.04
86.28
17.95
^{13}C NMR (101 MHz, dmso) δ 167.13 (s), 155.56 (s), 148.53 (s), 148.43 (s), 145.36 (s), 130.18 (s), 123.71 (s), 115.19 (s), 103.04 (s), 86.28 (s), 17.95 (s).
2.22
E (s) 145.36
B (s) 155.56
G (s) 123.71
I (s) 103.04
A (s) 167.13
C (s) 148.53
F (s) 130.18
H (s) 115.19
J (s) 86.28
K (s) 17.95
D (s) 148.43
f1 (ppm)

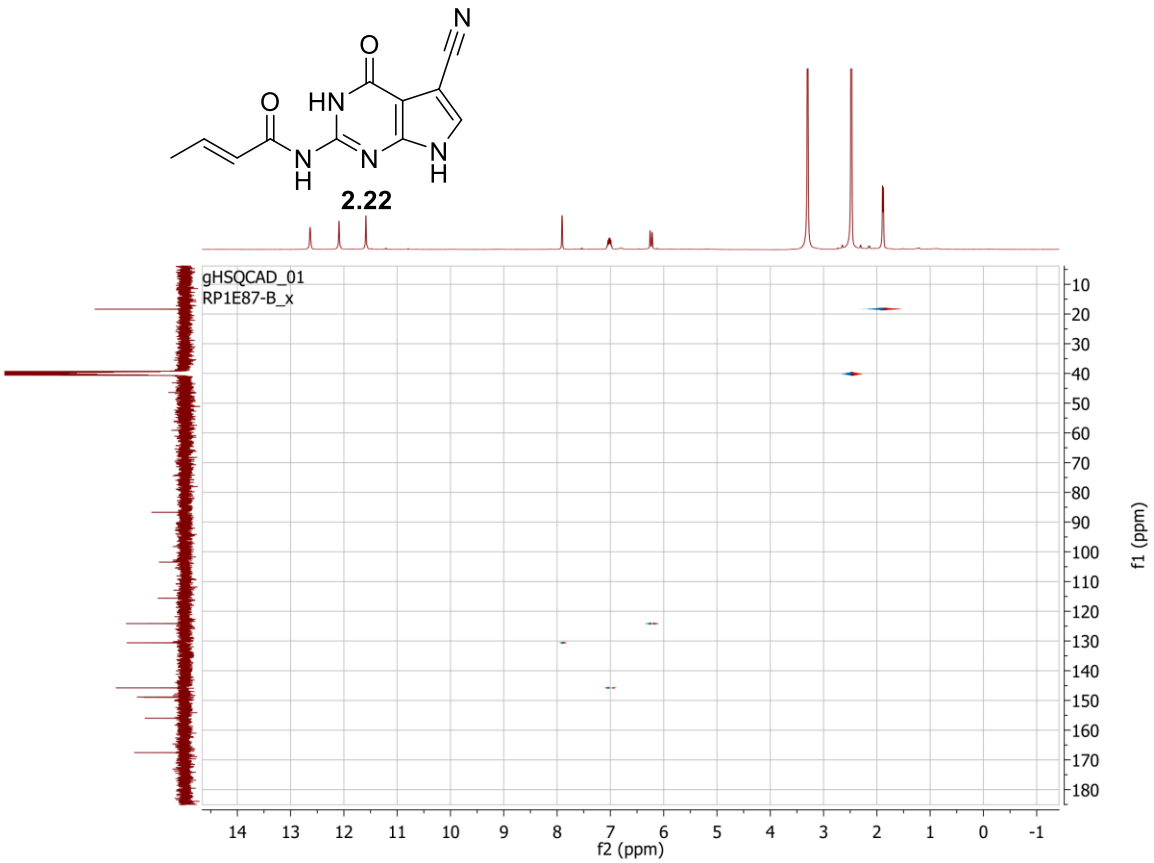

Trinity College Dublin

Bruker Open Access LC-MS - Formula Identification Report

Sample-ID		Station	
Submitter		Supervisor	
Analysis Name	RPP15_RC3_01_20080.d	Acquisition Date	26/04/2019 11:13:44
Sample Description			

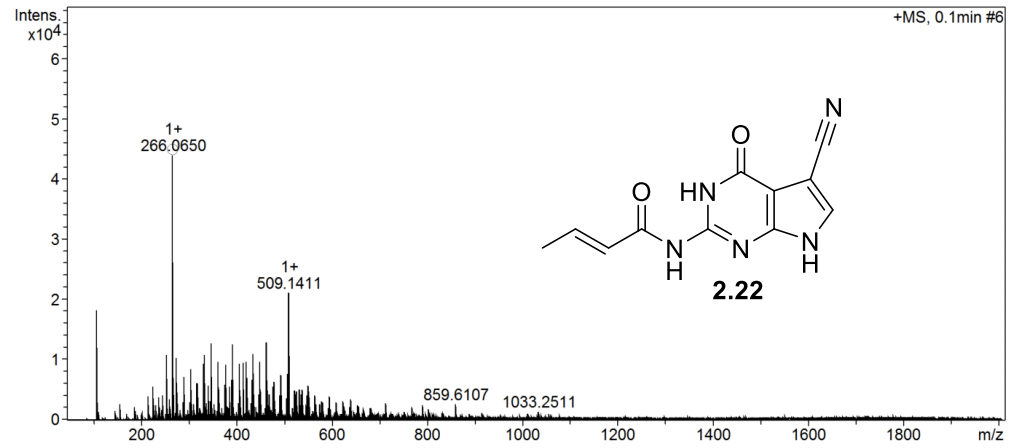

Meas. m/z	#	Ion Formula	m/z	err [mDa]	err [ppm]	rdb	N-Rule	e⁻ Conf	mSigma
266.065013	1	C11H9N5NaO2	266.064845	0.2	0.6	9.5	ok	even	12.6

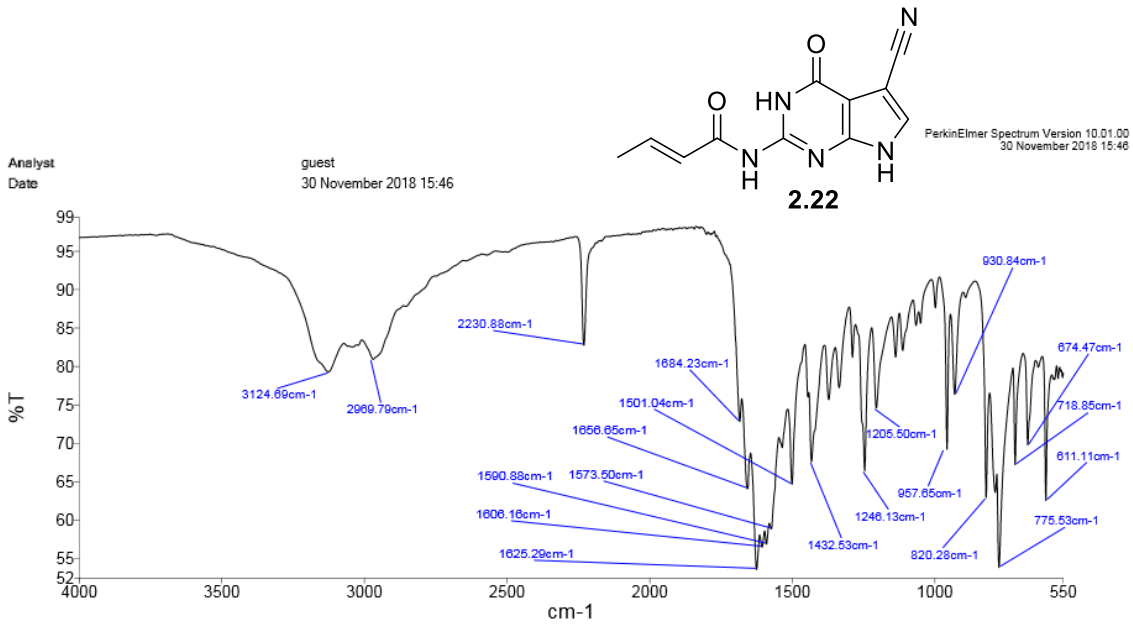

Sample Name	Description	Quality Checks
RPP15	Sample 013 By guest1 Date Friday, November 30 2018	The Quality Checks do not report any warnings for the sample.